THE MICRORNA-MEDIATED REGULATION OF PROTEINS IMPLICATED IN THE PATHOGENESIS OF ALZHEIMER'S DISEASE

Nipun Chopra

Submitted to the faculty of the University Graduate School
in partial fulfillment of the requirements
for the degree
Doctor of Philosophy
in the Medical Neuroscience Program,
Indiana University
April 2017

Accepted by the Graduate Faculty, Indiana University, in partial fulfillment of the requirements for the degree of Doctor of Philosophy.

Feng Zhou, Ph.D., Chair

Debomoy K. Lahiri, Ph.D.

Doctoral Committee

Eri Hashino, Ph.D.

November 29, 2016

Alexander Obukhov, Ph.D.

Acknowledgements

First and foremost, I'd like to thank my family for supporting me through this long journey, and for instilling in me the self-belief to make it through to the end. Secondly, I'd like to thank my mentor, Dr. Debomoy K. Lahiri for his patience, guidance and mentorship over the last six years. A debt of gratitude to my advisory committee for their critical advice that has got me to this moment.

Along the way, fellow graduate students and mentors in the Lahiri lab; Dr. Justin Long, Baindu Bayon, Dr. Jason Bailey and Dr. Balmiki Ray, have influenced my critical thinking skills and scientific prowess significantly. For that, and for allowing moments of levity, I would like to thank them.

Through their collaboration, I appreciate the guidance and materials provided by Dr. Hemachendra Reddy, Dr. Peter Nelson, Dr. Robert Vassar, Dr. Kumar Sambamurti, Dr. Alexander Niculescu and Dr. Kavita Shah. Additionally, Dr. Kwangsik Nho and Dr. Andrew Saykin for their valuable collaboration in the ADNI project.

Finally, to innumerable graduate students and friends made along the way – I thank each and every one of you for allowing me to bounce ideas off of you as well as discuss frustrations with you.

Nipun Chopra

THE MICRORNA-MEDIATED REGULATION OF PROTEINS IMPLICATED IN THE PATHOGENESIS OF ALZHEIMER'S DISEASE

Alzheimer's disease (AD) is a progressive neurodegenerative disorder characterized by the post-mortem deposition of amyloid-beta (Aβ) containing neuritic plaques and tau-loaded tangles. According to the amyloid hypothesis, the generation of Aβ via the cleavage of Aβ precursor protein (APP) by β-APP site-cleaving enzyme 1 (BACE1) is a causative step in the development of AD. Therefore, targeting the production and/or clearance of Aβ peptide (by Aβ-degrading enzymes such as Neprilysin) would help understand the disorder as well as serves as therapeutic potential to treat the disorder. MicroRNA are small, noncoding RNA capable of modulating protein expression by primarily targeting their 3'UTR. Therefore, identifying miRNA which target APP, BACE1 and Neprilysin (NEP) would elucidate the complicated regulatory mechanisms involved in protein turnover and provide novel drug targets. We identified miR-20b as a modulator of APP and soluble Aβ. We also identified the target site for miR-20b's binding on the APP 3'UTR. Further, miR-20b exerts influence on neuronal morphology, likely due to its APP reduction. We also identified miR-298 as a dual regulator of APP and BACE1 and confirmed miR-298's targeting of both 3'UTRs. We also showed that miR-298 overexpression reduced levels of both soluble Aβ40 and Aβ42 peptides. Additionally, we identified two SNPs in proximity to the MIR298 gene, which are associated with AD-related biomarkers. Based on these results, we showed miR-298 targets a specific isoform of tau by putatively binding a non-canonical target site on the MAPT 3'UTR. Finally, the insertion of the NEP 3'UTR into a reporter vector

increases reporter expression; suggesting regulatory elements targeting the 3'UTR. We subsequently identified miR-216 as reducing NEP 3'UTR-mediated luciferase activity. We also measured levels of NEP protein in various mammalian tissue – such as rodent and human fetal tissue, and subsequently showed measurable Aβ levels in correlation with NEP expression. Therefore, herein, we have identified miRNA involved in the regulation of proteins implicated in the pathogenesis of AD.

Feng Zhou, Ph.D., Chair

Table of Contents

Abbreviations

Aβ	Amyloid-β
ABCA7	ATP-binding cassette, sub family A member 7
AD	Alzheimer's disease
ADNI	Alzheimer's disease neuroimaging initiative
APLP1	APP like protein-1
APLP2	APP like protein-2
APP	Amyloid precursor protein
BACE1	β-amyloid cleaving enzyme-1
BBB	Blood brain barrier
BSA	Bovine serum albumin
CALLA	Common acute lymphoblastic leukemia antigen
CD10	Cluster of differentiation 10
CM	Conditioned media
CSF	Cerebrospinal fluid
CTF	C-terminal fragment
CTG	Cell Titer-Glo
ECL	Enhanced chemiluminescence
ELISA	Enzyme-linked immunosorbent assay
EOAD	Early onset AD
FAD	Familial AD
FBS	Fetal bovine serum
GWAS	Genome-wide association study
HFB	Human fetal brain
HRP	Horseradish peroxidase
HS	Horse serum
Hsa-	Prefix for human miRNA
LOAD	Late-onset AD
LTP	Long-term potentiation
MAPT	Microtubule associated protein tau
MiR/miRNA	MicroRNA
MME	Matrix metalloendopeptidase
Mmu-	Prefix for mouse miRNA
M-PER	Mammalian protein extraction reagent
NGF	Nerve growth factor
NEP	Neprilysin
PBS	Phosphate-buffered saline
PCR	Polymerase chain reaction
PICALM	Phosphatidyl binding clathrin assembly protein 1
PSEN1	Presenelin-1
PSEN2	Presenelin-2
PVDF	Polyvinylidene fluoride
qPCR	Quantative PCR
sAPP	Soluble APP
SORL1	Sortilin-related receptor-1

SNP	Single nucleotide polymorphism
TBS	Tris buffered saline
TBST	Tris buffered saline with tween-20
TREM2	Triggering receptor expressed on myeloid cells-2
UTR	Untranslated region

Chapter 1: Introduction

Alzheimer's disease (AD) is a progressive neurodegenerative condition affecting millions worldwide. AD is the most common form of dementia seen in the elderly population, comprising of about 70% of dementias in older adults, and is the 6th leading cause of death in the US [1,2]. According to the latest report from the Alzheimer's Association, currently 5.4 million Americans have AD, with 5.2 million of those being over the age of 65 (https://www.alz.org/documents_custom/2016-facts-and-figures.pdf). Notably, 1 out of 9 people over the age of 65, and 1 out of 3 people over the age of 85 have AD. By 2050, this number is expected to rise to 14 million people. The expected rise in incidence of AD would have a significant impact on the society at large. Current estimates predict that the number of neurologists in 2025 and 2050 will not be sufficient to handle the marked increase in AD incidence [3]. Along with the problems associated with AD itself, the disease is associated with other psychiatric problems in the elderly – such as depression [4,5], bipolar disorder [6], schizophrenia [7] and sleep alterations [8]. AD is also considered to be a moderate risk for suicidality [9]. Therefore, AD is expected to be a significant health and financial burden for the foreseeable future.

Interestingly, the incidence of the disorder varies greatly by geographical location [10]. The Asian-pacific populations have about a 3-5% prevalence of AD, with Japan being the highest in the region, at 11% [11-14]. Usually migrant populations living in the USA show an increased prevalence of AD compared to similar populations living in their home countries [15,16] - a possible effect of the complex interplay of genes, diet, environmental factors, etc. Interestingly, in terms of environmental factors, a meta-analysis suggested that early-life rural living may pose an increased risk for AD onset[17].

The disease was first described by Alois Alzheimer in a seminal paper which was translated into English [18]. Over the last 110 years, scientists have attempted to unravel the underlying mechanism of the disorder and to find a potential therapy to reverse the cognitive decline associated with the disorder. The progression of the disease was described in a seminal paper [19]. Pathology first manifests in the transentorhinal area and then migrates to the neocortex and hippocampal structure. In later stages of the disorder, pathology affects cortical structures globally [20]. Given the progression of the disease, it is not surprising that impaired cognitive and memory functions are hallmarks of the disease [20]. Unfortunately, there has not been much success in either elucidating the mechanism or finding a cure for AD.

Genetics of AD

Approximately 10% of AD patients have an early onset AD (EOAD), with diagnosis occurring between 45 and 60 years of age, whereas, the vast majority of AD diagnosis occurs after the age of 65 and is referred to as late-onset AD (LOAD)[21] . Mutations in the APP, Presenlin-1(PSEN1) and Presenelin-2 (PSEN2) genes are involved in the onset of EOAD [22-27] whereas APOE ε4 and TREM2 are widely accepted to be risk factors for LOAD [28-30], although GWAS studies have implicated loci on other genes such as phosphatidyl binding clathrin assembly protein (PICALM), sortilin-related receptor L (SORL1), ATP-binding cassette, sub family A member 7 (ABCA7) etc [31-35]. Of great interest has been the study of single nucleotide polymorphisms (SNP)s in aforementioned genes as well as examining GWAS for SNPs in previously unexplored AD-related genes. An asset in this field is the emergence of the AD neuroimaging initiative (ADNI) which

allows for GWAS-derived identification of novel genes, SNPs, as well as possible associations with CSF biomarkers [36,37].

The role of amyloid-beta precursor protein in AD

The amyloid-beta precursor protein (APP) plays a central role in the "amyloid cascade hypothesis" [38] as it is the parent molecular from which the potentially toxic amyloid- beta- fragment (Aβ) is generated. The hypothesis by Hardy and Higgins posits Aβ upstream of the pathological changes and cognitive decline associated with AD. Additionally, mutations in the APP gene are associated with EOAD, which is also known as familial AD (FAD) [39-42]. The APP gene is located on chromosome 21, which is why the inheritance of an extra copy of chromosome 21 (as seen in Down's syndrome) is associated with cognitive decline[43]. The gene comprises 19 exons and can be alternatively spliced into multiple forms [44,45], the form most commonly expressed in the neurons codes for 695 amino acids, whereas the larger forms (APP751/770) are expressed in glia [46-48]. APP is a single transmembrane protein implicated in a myriad of functions, [49] including cell adhesion[50], neurite outgrowth [51] , apoptosis [52] and cell signaling. APP can undergo both homodimerization and heterodimerization. APP is post-translationally modified by glycosylation, tyrosylation and phosphorylation [50,53]. While APP knockout mice are viable, they show aberrant long term potentiation (LTP), impaired locomotor activity and reduced brain weight[54-56] thereby confirming the important role of APP in normal brain development and function.

According to the Human Protein Atlas [57], a freely available database showing protein expression in various tissues and cell lines, APP expression is highest in the adult

human brain, but observable in most peripheral tissues. Very little APP expression was observed in lung or kidney tissues [57]. To our knowledge a tissue-wide expression profile of APP has not been conducted in human fetal tissue or rat tissue.

APP protein paralogs, APP-like protein 1 (APLP1) and APP- like protein 2 (APLP2) [58-60] have similar but not identical functional properties (Sambamurti et al., 2002). Crucial to our discussion on AD, these APLPs lack the Aβ domain, and therefore have different properties after being processed by enzymes like BACE1 [61]. APLPs are expressed in species such as worms and flies, while APP itself is first observed evolutionarily in amphibians [61,62].

The processing of APP is important to the generation of Aβ. APP can be processed in two major pathways: amyloidogenic and non-amyloidogenic s [63]. Under the non-amyloidogenic pathway, APP is cleaved by alpha-secretase (α-secretase) followed by the gamma-secretase (γ-secretase) complex (Figure1), liberating soluble APP α (sAPPα) [64] and a non-toxic 3 kDa protein (P3) fragment. SAPPα has been shown to involve in neurogenesis, potentially by binding to anchoring proteins in the extracellular matrix [65]as well as a regulator of neural stem cell proliferation [66]. SAPPα has also been implicated to protect against glutamate neurotoxicity in vitro [67,68].

In the non-amyloidogenic pathway during AD, due to a not yet understood reason, APP is preferentially cleaved by β-site APP cleaving enzyme-1 (BACE1) instead of α-secretase which liberates a soluble β-APP fragment (sAPPβ) and an APP-CTFβ fragment. sAPPβ is linked to potentially neurotoxic effects of its own, including a reduction in cell adhesion, and potentiating cell death by binding to the DR6 receptor [69,70]. The γ-secretase

complex then acts on the APP-CTFβ fragment to generate APP Intracellular domain (AICD) and the potentially toxic Aβ fragments.

The role of β-APP site-cleaving enzyme 1 in AD

Beta-Site APP-cleaving enzyme-1 (BACE1) or β-secretase is considered to be the rate-limiting enzyme in the generation of Aβ. BACE1 was discovered as the titular β-secretase independently by four different laboratories[71-74] and has been the focus of current AD therapeutics. BACE1 is first translated as a proenzyme but is significantly more active after removal of its prodomain and transport into early endosomes [75]. The mature BACE1 protein is 501 amino acid in length with a mass of ~70 kDa [71,74].

BACE1 is capable of cleaving multiple substrates including APP [71], Neuregulin-1 (NRG1) [76], beta-2 subunit of voltage-gated sodium channels [77], membrane-bound alpha-2,6-sialyltransferase (ST6Gal1) [78,79], and many other possible substrates [80]. Evidence suggests that BACE1's activity is strongest at an acidic pH [71,75], which is why it is believed to be active in early endosomes. However, it is important to note in subcellular terms, BACE1 is also detected on the plasma membrane, from where it can be endocytosed and recycled into endosomes [75], as well as evidence suggesting BACE1 localization in lipid rafts in the brain[81].

The protein has a homolog, BACE2, found on chromosome 21, with which is shares about 68% homology [82]. BACE2 is lowly expressed in the brain, but highly expressed in peripheral tissues such as colon, kidney and pancreas. [83] BACE2 cleaves APP within the Aβ domain and is considered to be non-amyloidogenic [84]. It was experimentally determined that BACE1 from branchiostoma was able to cleave APP at

the Aβ site, implicating a strong conservation of BACE1 from an evolutionary perspective [62]. However, it is important to note that BACE1 evolution far preceded the evolution of the Aβ domain, thereby implicating BACE1 in a variety of other roles independent of APP processing [62].

These functions include the cleavage of aforementioned substrates, as well as larger phenotypical roles, such as myelination in the CNS [85]; likely due to its cleavage of NRG1. Data from BACE1 knock out mice suggest that they are viable, but show impaired myelination and an increased seizure rate [85,86].

In terms of tissue-wide expression, BACE1 is found expressed at high levels in the human and rat brain [83]. The human protein atlas suggests that BACE1 is highly expressed in adult human kidney, gastrointestinal tissue and endocrine tissue [57]. Previous work has shown that BACE1 mRNA is increased in AD brain, as a function of Braak stage in the superior occipital gyrus, medial temporal gyrus and superior parietal gyrus [87]. Work in our lab confirms that BACE1 protein levels in the brain are increased when comparing AD vs. non-AD patients [88].

To our knowledge, expression patterns for BACE1 expression in human fetal tissues remains unexplored.

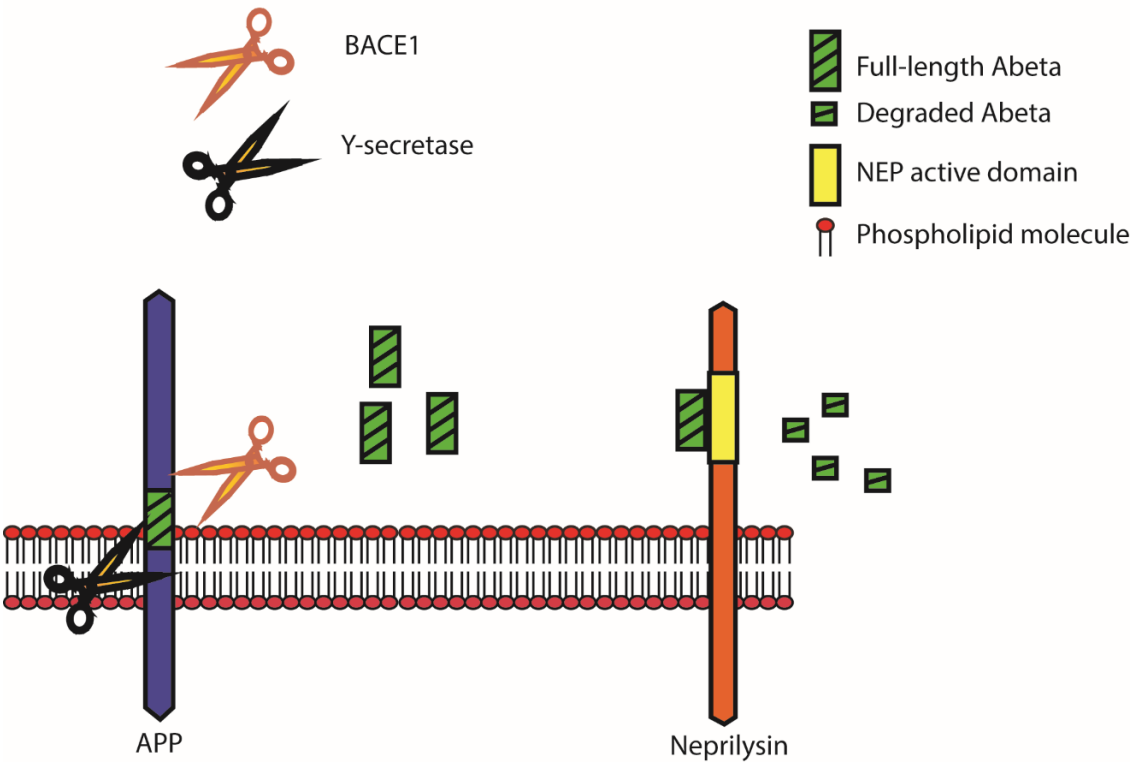

Figure 1: Diagrammatic representation of the cleavage of APP by BACE1 and γ-secretase resulting in the generation of Aβ. Also shown in the degradation of Aβ by NEP – one of many Aβ degrading enzymes.

Biogenesis and role of amyloid-beta peptides in neurodegeneration and AD

In accordance with the amyloid hypothesis, Aβ is the causative factor underlying the onset and progression of AD [38,89,90], although the validity of this hypothesis has been questioned recently (For a review [91]). Multiple lines of evidence link Aβ with AD and the onset of dementia. These include observations that Aβ is the major component of amyloid plaque in the brain [92-94] and the development of AD and increased Aβ deposition in patients with trisomy 21 [95].

The generation of Aβ (lying partly within the transmembrane domain and partly in the extracellular domain of APP [96]) is a consequence of a cleavage of APP by BACE1, producing the C99 fragment, and then a subsequent cleavage by the γ-secretase complex liberating the Aβ fragment [97] (Figure 1). The γ-secretase complex comprises at least four different proteases, such as presenilins, nicastrin, Aph-1 and Pen-2, and is responsible for a promiscuous cleavage of APP, producing Aβ of 40 or 42 amino acids in length [98,99]. Additional Aβ fragments have also been reported as a consequence of secondary cleavage by other secretases [100].

From a cellular standpoint, reports suggest that neurons, glia, fibroblasts as well as blood platelets are capable of releasing Aβ [101-103], which help in measuring levels of Aβ in the brain, CSF and blood/plasma.

The two Aβ fragments (Aβ40 and Aβ42) have different properties which are reportedly crucial to the onset of AD. Aβ42 tends to be more hydrophobic, amyloidogenic and toxic of the two species, and has the aggregative properties associated with neuritic plaque formation [104-108]. In familial AD, it is suggested that more so than the

levels of the two Aβ fragments, a higher Aβ42/ Aβ40 ratio that results in plaque deposition [109]. An interesting line of evidence suggests that Aβ40 may actually protect against AD onset and at low concentrations is involved in long-term potentiation (LTP) and normal memory processes [110-114].

While the mechanism underlying Aβ aggregation is still unclear, it is believed that as the concentration of Aβ40 and Aβ42 monomers increases, monomers change their conformation from an alpha-helical structure to beta-sheets, thereby increasing their aggregative properties [107,108]. The aggregation of these Aβ monomers results in the productions of dimers, trimers, oligomers, fibrils and eventually plaque [115], even though the exact processes remains unclear. Many have also speculated a prion-like mechanism underlying the formation of amyloid fibrils and plaque [116,117], but this too remains controversial [117-120].

The mechanism of Aβ neurotoxicity also remains under investigation. Correlatively, it has been shown that Aβ oligomers invoke neurotoxicity and are increased in the brain of AD patients and are also detected in CSF and plasma from AD patients [121,122]. Two potential mechanisms for this neurotoxicity are calcium toxicity and receptor-binding-mediated activation of intracellular cascades. Aβ is capable of forming cation permeable channels in the plasma membrane, thereby disrupting the well-regulated conductance properties which facilitate the electrochemical gradient [123-127]. It has also been shown that Aβ is able to bind various receptors such as lipoprotein-related peptide 1 (LRP1), SorLA, various acetyolcholinergic receptors and nerve growth factor (NGF) receptor [114,128,129]. While the signaling cascades propagating from binding of these receptors can vary, binding to the NGF receptor, in particular, can lead to neuronal death

[129,130]. Beyond its potential for toxicity, it has been shown that Aβ may set up a positive-feedback loop for its own production by binding to the promoter of APP and BACE1 [131,132] , thereby leading to the production of more Aβ and further toxicity.

Given the toxicity associated with Aβ and the multitude of evidence linking it's involvement in AD onset and progression, reducing Aβ levels is an important goal of AD therapies. We discuss the results of clinical trials attempting to reduce Aβ levels in a later section.

Role of neprilysin in AD

Perturbation of the homeostasis of Aβ-production and clearance can contribute to AD [133]. In vitro studies have shown that once Aβ has been generated, it can be cleaved by many enzymes [134,135] [136]. *In vivo* and *in vitro* results have focused on NEP and Endothelin converting enzymes-1 and 2 (ECE1 and ECE2) [137-139]. Given that NEP is associated with the extracellular surface of membranes [134], it is likely that it would be a major player in clearing amyloid beta plaques; both in the cytosol as well as in the extracellular domain.

NEP is also called neutral endopeptidase (NEP), cluster of differentiation 10 (CD10), common acute lymphoblastic leukemia antigen (CALLA), membrane metallo-endopeptidase (MME). NEP is an integral membrane glycoprotein and a zinc-containing metallopeptidase [140,141] that has been implicated in the clearance of Aβ [142-144], and AD [135,144-146]. It can be argued that a reduction in NEP expression/activity would result in an increase in Aβ load. In support of this idea, NEP gene-disrupted mice produced high levels of Aβ 40 and Aβ 42 [144,147]. Conversely, but consistently to NEP's predicted role, overexpression of NEP produced reduction in neuronal Aβ in cell culture models [148], in

drosophila [149], in mouse brains [150-152] and in neuronal human progenitor cells [153]. Moreover, Takaki et al. (2000) suggested that aging may cause a down-regulation of NEP in the brain [154]. Taken together, these results suggest that NEP has an important role in the clearance of Aβ required to prevent Aβ accumulation correlated with AD.

The NEP gene comprises 24 exons and produces three splice variants in rats and four splice variants in human [144,155-157]. NEP, which is a 750 amino acid protein (Figure 2), has two hydrophilic domains (extracellular and cytosolic), a single hydrophobic domain and a signal peptide, while the ATG start codon is situated on Exon 3 [140]. Within the region spanning the active site domain, are three sites to which Zn can bind (Figure 2). Also present are nine sulfide bonding sites and five glycosylation sites which contribute to the quaternary structure and post-translational modification of this protein respectively (Figure 2). The NEP gene cleaves Aβ at the Gly9-Tyr10 position and is capable of clearing both monomeric and oligomeric forms of AB [143,145,158]. The tissue distribution of NEP has also been studied using immunohistochemistry of mice brains. NEP levels are highest in the kidney, followed by lungs and brain [159]. Fukami et al. (2002) showed that mice overexpressing human-type APP reveal high NEP expression in regions such as substantia nigra and caudate putamen, a moderate expression in the hippocampus and neocortex and a low expression in the cerebellum [159]. Interestingly, cerebellar levels in 'steady-state' conditions reveal a different distribution – cerebellar NEP expression seems to be the highest, followed by cortical expression, and hippocampal expression [158]. To our knowledge, this disparity in results has not been studied further. At an ultrastructural level, NEP seems to be localized in the plasma membrane of axons, terminal boutons and possibly dendrites [145]. Moreover,

immunostaining suggests that in the hippocampus, NEP colocalizes with markers for glutamatergic neurons, but not with cholinergic or catecholaminergic neurons [159]. Since cholinergic neuronal loss is believed to be an early marker of AD, it is possible that the lack of NEP expression in cholinergic cells may contribute to an increased amyloid load and cell death of these cells.

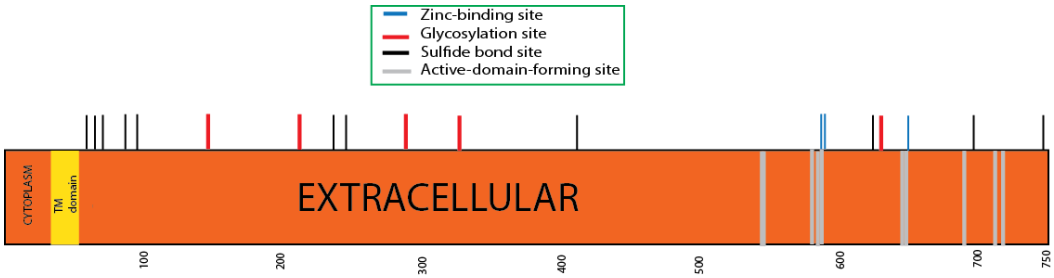

Figure 2: Structure of NEP protein. NEP is shown with the short cytoplasmic and transmembrane (TM) domain. Also shown are the zinc-binding site (blue), glycosylation sites (red), sulfide-binding sites (black) as well as the sites involved in the formation of the active site (silver). The numbers indicate the amino acid number at that site of the 750 AA protein.

Role of the microtubule associated protein tau in AD

Post-mortem AD brains consistently showed one of the hallmarks associated with AD – neurofibrillary tangles, and it was eventually observed that these tangles were a consequence of a dysregulation of the well-controlled process of microtubule assembly/disassembly [160-162]. The constituent of these filaments was found to be hyperphosphorylated tau protein [163]. Soon after, a mechanism of characterizing disease progression was devised by Heiko Braak [164]. In a seminal paper, Braak and Braak (1991) described worsening AD pathology and gave a quantitative description of stages 1-6 to a qualitatively determined increased amount of neurofibrillary tangles. This characterization is still used today to describe AD disease progression.

Microtubule associated protein tau (MAPT) is found on chromosome 17, comprises 16 exons and is 100kb in length [165]. The tau gene has 4 domains – an acidic N-terminal domain, a proline-rich domain, a tubulin-binding repeat domain and an acidic C-terminal domain [166]. In humans, the tau gene is alternatively spliced into 6 isoforms – due to a combinatorial splicing of one of exons 2, 3, 10 as well as its microtubule-binding domains [167]. The longest isoform is 441 amino acids in length [166].

Under normal conditions, tau interacts with tubulin and promotes microtubule assembly and stability. When tau is phosphorylated, it promotes disassembly and therefore, the phosphorylation of tau is crucial to maintain integrity of the cell [168] . However, during diseased states such as AD, and other tauopathies such as Pick disease, dementia pugilistica, etc., tau is heavily phosphorylated and the homeostasis between phosphorylation and dephosphorylation is lost [168,169]. In AD, all 6 tau isoforms are

hyperphosphorylated [170]. In AD brains, tau protein is 3 to 4 fold hyperphosphorylated compared to age-matched non-AD brains [171]. Therefore, reducing phosphorylated tau should be a suitable therapeutic target for AD.

Both in vivo and in vitro work affirm the neurotoxicity observed in response to experimental induction (or reduced neurotoxicity as a result of reduced) of hyperphosphorylation of tau [172-176]. As a proof-of-concept, the administration of human tau oligomers into mice resulted in impairment of LTP as well as reduced memory formation [177]. The measurement of phosphorylated tau and/or total tau in CSF has been studied as a possible biomarker for diagnosing AD onset/risk [178,179]. Several groups are looking at the ratio of phosphorylated tau to Aβ42 in the CSF as a more accurate biomarker for diagnosing early stage AD [180-182].

A review of AD treatment

In accordance with the prevalent *in vitro* and *in vivo* data, reduction of APP and BACE1 and/or an increase in NEP expression should result lowered Aβ levels and subsequently amyloid plaque. Congruently, a reduction in total tau and/or phosphorylated tau should result in a reduction in neurofibrillary tangle formation. Using these general hypotheses, many pre-clinical and clinical trials have been conducted to abrogate plaque and tangle formation and improve cognitive outcomes. Targeting either active (injection of Aβ antigen itself) or passive (injection of antibodies to Aβ) immunity, vaccines targeting monomeric or fibrillary forms of Aβ have gone to clinical trial [183,184].

CAD106 (Novartis) is an active vaccination against Aβ and successfully reduced plaque burden in transgenic mice [185] without the unwarranted T-cell responses seen with

earlier iterations of Aβ antibodies. CAD106 was well-tolerated in a vast majority of patients studied and has recently completed phase 2 clinical trials – although the results of their study are not yet available.

Targeting passive immunity, Solanezumab (Lilly) recently went to phase 3 trials. This antibody, which targeted monomeric Aβ, was well-tolerated but showed little cognitive improvement during the trial [186,187], although a sub-group of patients did show a reduction in cognitive decline. Bapineuzemab went through 2 clinical trials that showed no improvement in expected phenotypic outcomes, and consequently 2 other planned clinical trials with Bapineuzemab were terminated [188]. Gantenerumab, an antibody against fibrillary form of Aβ, was well-tolerated and is currently in phase 3 trial – both as a stand-alone drug, as well as in combination with a BACE1 inhibitor [189-191]. Finally, bimonthly subcutaneous injection of Crenezumab are being administered to AD patients with autosomal-dominant gene mutations; this study is in phase 2 and is scheduled to complete in 2020 [192].

BACE1 inhibition is an obvious theoretical target for reducing Aβ, as it is the rate-limiting enzyme in Aβ generation. MK-8931 (Merck) is a well-tolerated uncompetitive antagonist in phase 3 trial (clinical trial identifier: NCT01739348), but was recently discontinued [193]. Recently, a clinical trial with BACE1 inhibitor (LY-2886721) [194] was terminated due to liver toxicity (but see [195]). Inhibiting γ-secretase should also reduce Aβ levels and therefore semagecestat (Lilly) – a γ-secretase inhibitor – showed promising reduction of plasma Aβ levels in phase 1 and 2 clinical trials [196]. However, phase 3 trials with semagecestat were abandoned as some patients showed worsening of cognitive function as well as an increase in skin cancer rates [197,198].

To our knowledge, no clinical trials have been conducted with drugs increasing NEP expression/activity. Sacubitril (Novartis) is a NEP inhibitor that has been extensively studied as a means to control hypertension [199] (and see clinical trial identifier: NCT01692301). The ability of sacubitril to cross the blood-brain barrier (BBB), or its possible effect on Aβ levels and cognition, remains unexplored. While inhibiting NEP would not be desirable, it is worth exploring the effect of the same on brain Aβ levels, as it would elucidate whether NEP activity in the brain regulates levels of Aβ in vivo. There is currently one tau vaccine – AADvac1 – which showed preclinical promise in reducing tauopathies in rats [200].

It is important to note that the few drugs approved for AD therapy are not targeted at Aβ generation, clearance or tau at all. Cholinesterase inhibitors, such as donepezil, galantamine, and rivastigmine have success in retarding AD development, especially when administered early [201]. Unfortunately, there is great heterogeneity in the efficacy of these drugs as well [201], for example, galantamine was shown to modulate nicotinic receptors as well [202]. Memantine, an NMDA partial antagonist, is approved for moderate to severe AD treatment. This drug has previously shown benefit in cognitive outcomes, however, a recent study showed that memantine did not improve cognitive outcomes in mild to moderate AD [201,203].

Therefore, due to the limited success of AD therapies, a novel means to reduce Aβ levels is warranted.

MicroRNA

Overview

MicroRNA (miRNA) were initially discovered in *C. elegans* in the early 90's [204]. It was shown that LIN-14, a factor important to larval development was regulated by lin-4, which happened to be a 22 nt non-coding RNA. Additionally, it was observed that lin-4 was partially complementary to a sequence on the LIN-14 3' UTR [204]. Therefore, the idea that short non-coding RNA could influence protein expression by targeting the 3'UTR was generated. In 2000, in another seminal paper, let-7 was discovered [205] as a regulatory miRNA controlling processes involved in larval development and maturity. Since then, a multitude of discoveries of miRNA across various species has been made. Current estimates are approximately 30,000 mature miRNA across 206 species [206]. While estimated to be ~2400 in number, recent work has revealed the presence of 3707 novel miRNA in the human genome [207].

Nomenclature and biogenesis of miRNA

The nomenclature of miRNA can occasionally be confounding, but follows consistent principles. The first three letters indicate the species to which the particular miRNA is endogenous to – for example, hsa- and mmu- indicate human and mouse miRNA respectively. The miRNA numbers reflect the order in which they were discovered. For example, miR-20 was discovered before miR-298. If the mature sequence of two miRNA is very similar, they are often given the same number followed by a letter. For example, miR-20a and miR-20b are two miRNA that have similar mature sequences in their seed sequence, yet are derived from two different chromosomes. Occasionally, a

few miRNA are generated from close proximity within the same genomic region – such as the miR106a-363 family. This family comprises of miR-106a, miR-18b, miR-19b-2, miR-92a and miR-20b and miR-363, and are all derived from a ~1kb region on chromosome X [208].

The biogenesis of miRNA is a well-regulated and well-conserved process involving a variety of proteins and chaperones (For review, see [209]). MiRNA are transcribed by RNA Polymerase II as primary miRNA comprising a stem loop structure as well as the double-stranded RNA containing the mature miRNA sequence as well as a poly-A tail and a 5' overhang. These miRNA can have their own promoter elements and can often reside in intronic regions on the genome. For example, miR-298 and miR-20b reside in intronic regions on chromosome 20 and chromosome X, respectively. The primary miRNA is then acted upon by Drosha and DiGeorge syndrome critical region 8 (DGCR8) which generates the double-stranded stem-loop structure called the pre-miRNA. The pre-miRNA is then exported out of the nucleus to the cytosol by exportin-5. In the cytosol, Dicer and TAR RNA-binding protein (TRBP) act synergistically to excise out the stem-loop, generating the double-stranded RNA. The double-stranded miRNA is then loaded onto argonaute (AGO)-2 protein. Work by Schwarz (2003) explained an initially confounding question – which of the two strands becomes the mature, functional RNA. Schwarz and colleagues suggest that the strand with the less thermodynamically stable 5' end will become the mature strand, and that a single hydrogen bond can be the deciding factor discerning which of the two strands becomes the mature strand [210]; the argonaute-miRNA forming the RNA-induced silencing complex (RISC). This RISC then targets mRNA targets based on the sequence of the mature strand. It should be noted that

RISC-independent miRNA activity – based on secondary structure alone – has been reported [211].

In canonical miRNA binding, the mature miRNA targets a 7-8 nt complementary sequence usually on the 3'UTR mRNA, usually this involves a "seed" sequence beginning 2-6 nt from the 5' end of the miRNA [212]. However, non-canonical binding involving imperfect complementarity in the seed sequence and nucleation due to mismatched pairs have also been reported [213]. After the target has been loaded onto RISC, either the mRNA transcript is destabilized or translation is inhibited, subsequently affecting protein expression [214].

MiRNA in disease states and AD

As more miRNAs have been discovered, it has become apparent that they play a multitude of roles, and the perturbation of these miRNA can lead to disease states. In the early 2000s, a role for miRNA in human cancer was discovered [215]. MiR-15a and miR-16 were found to be important to processes in chronic lymphocytic leukemia [215,216]. Roles for miRNA in the onset of pancreatic cancer and lymphoma were soon elucidated as well [217,218]. While the miRNA involvement in cancer was gathering storm, it was also becoming apparent that miRNA could regulate other disease states as well. Huang et al. (2007) showed that miR-125, miR-223 and miR-382 can inhibit HIV replication [219]. In the CNS, miR-34a, miR-155 and miR-326 levels were found to be increased in multiple sclerosis (MS) and were found to be negative regulators of CD47, which lead to increased macrophage-mediated phagocytosis of myelin [220]

The involvement of miRNA in AD was first reported in the mid-2000s. Various miRNA have been found to be upregulated or downregulated in brain tissue derived from AD patients when compared to that derived from control patients. For example, miR-34 was found to be upregulated in the hippocampus [221], while miR-146a was found to be upregulated in the temporal cortex as well as in the hippocampus [222]. Meanwhile, miR-107, miR-181 and miR-106 were all found to be downregulated in the temporal cortex derived from AD patients [223-225], whereas miR-29 was found to be downregulated in both temporal cortex as well as the cerebellum of AD patients [226]. MiRNA can also be successfully detected and differentially expressed in biofluids such as urine, CSF and serum [224,226-230] thereby implicating their utility as possible biomarkers for diagnosing AD in a noninvasive manner.

A number of laboratories have identified miRNA that modulate the expression of proteins implicated in the pathogenesis of AD, such as APP, BACE1, NEP and MAPT. For example, Niwa et al (2008) showed that in *C. elegans*, APP-like-1 (apl-1) protein is regulated by the let-7 family of miRNA [231]. Since then, miR-101 [232,233], miR-16 [234,235], miR-153 [236,237], miR-384 [238], miR-193b [239] and miR-200b [240] have been found to regulate the expression of APP in vitro. Moreover, a number of SNPs were found on the APP 3'UTR in AD patients, suggesting further possible targets for miRNA [241].

Only few miRNA study involves NEP Thompson and colleagues (2011) showed that miR-155 indirectly regulates the expression of NEP – by targeting the PU.1 transcription factor [242]. Therefore, the possible regulation of NEP by miRNA remains largely unexplored.

Many groups have also shown repression of BACE1 expression by a variety of miRNA. These include miR-29a/b and miR-9 [226], miR-195 [243], miR-339-5p [88], miR-384 [238], miR-135a [240] and miR-135b [244]. In rodent models, miR-124, miR-298 and miR-328 were also shown to regulate BACE1 expression [245,246] .

Emerging work in the last few years has begun to elucidate the regulation of total tau expression as well as phosphorylated tau by miRNA. The first indication of this was the observation that Dicer knock out mice showed an increased expression of tau protein [247]. Given the role Dicer plays in miRNA processing, it was hypothesized that tau is under the regulatory control of unidentified miRNA. Notably, miR-16 and miR-132 are involved in the regulation of splicing exon 10 of tau as well as the phosphorylation of tau [247,248]. Work in a gut cell lines revealed that miR-34c-5p regulates tau protein as well [249]. Separate groups identified miR-138, miR- 125b, miR-922 and miR-125b regulating the phosphorylation of tau indirectly [250]. MiR-138 was shown to increase tau phosphorylation by targeting the 3'UTR of the Retinoic acid receptor alpha (RARA) [250]. RARA, in turn, increased the activity of glycogen synthase kinase 3β (GSK3β) – capable of phosphorylating tau. Similarly, Zhao et al (2014) showed that miR-922 promotes tau phosphorylation by targeting the 3'UTR of ubiquitin carboxy-terminal hydrolase L1 (UCHL1). The reduction in UCHL1 then contributed to increased phosphorylation of tau as well as tangle formation [251,252]. MiR-125b was shown to increase tau phosphorylation by simultaneously increasing kinase and inhibiting phosphate expression [253]. Finally, recent work showed miR-219 levels were reduced in AD autopsy brains and miR-219 was shown to regulate total tau expression by binding directly to the tau 3'UTR [254]. A Table of miRNA regulating tau would be useful

Free-floating, unbound miRNA are degraded by a variety of exonucleases, but 3' methylation and sequestration by exosomes helps maintain miRNA integrity from exonucleases [255-257]. In fact, emerging literature posits exosomes as an important means of miRNA transport between cells and in biofluids [258]. Exosomes were discovered in the 1980s and are nanovesicles (~30-100nm in size) that are capable of shuttling proteins, lipids and miRNA [258-260]. Exosomes are released from a variety of cell types, including neurons, by budding from the plasma membrane [261,262]. Various groups have successfully detected exosomes in biofluids such as blood, urine and CSF [263-265]. While the isolation of exosomes can be tricky [258,266], several groups have profiled miRNA signatures from exosomes as a means to identifying miRNA differentially expressed in AD [265,267-269]. Gui et al. (2015) showed that exosome-derived long non-coding RNA can be differentially expressed in patients with AD [265]. Similarly, in a small cohort of AD and control patients, CSF-exosomal profiling identified 75 miRNA upregulated miRNA and 74 downregulated miRNA [269]. Of these, miR-146a, miR-11 and miR-1274 were identified as strongest candidates after statistical correction [269]. The Exocarta website (www.exocarta.org) identified ~2400 exosomal miRNA across various multiple organs; therefore, it is likely that many more candidates will be identified, as the field matures. Finally, using deep-sequencing, miRNA from exosomes were also successfully detected from CSF-derived exosomes [268].

Environment, epigenetics and miRNA

In accordance with models posed elsewhere [270], Alzheimer's disease onset may be a consequence of the complex interplay of genetics, environment and epigenetics [271]. In order to show a role for miRNA in this model, one to show that miRNA can modulate

epigenetic factors, and itself be modulated by environmental factors. The modulation of various epigenetic markers has been shown in Arabidopsis [272], mouse models [273] and human clinical samples [274]. Further, miRNA-mediated methylation [272,275-277], acetylation [273] and ribosylation [278] have been reported; primarily related to tumorigenesis. Interestingly, miRNA themselves can be under the influence of epigenetic modification of their gene promoters [279-281]. Therefore, there seems to be a complex, bidirectional interplay between miRNA and epigenetic modification [282]. Moreover, it has been shown that environmental factors such as cigarette smoke [283], physical activity [284], metal exposure [285] and infection [286] can regulate miRNA levels.

Predicting miRNA binding

There are many commonly used bioinformatics tools to identify putative miRNA binding sites within the 3'UTR mRNAs that target expression of proteins in AD. TargetScan searches perfect complementarity in the seed region of the miRNA and then filters out complementarity outside the seed sequence [287]. TargetScan also favors well-conserved putative binding sites on UTRs [287]. The MiRanda algorithm favors binding at the 5' end more than at the 3' end, and then also ranks predictors based on the free energy calculation of binding [288]. The PicTar algorithm relies on conservation of the 3'UTR and the thermodynamic stability of binding, and is therefore less biased by the seed sequence [289]. Similarly, DIANA-MICROT looks beyond the 3'UTR – to the coding region and only considers the free energy of binding sites [290]. The PITA algorithm is unique that it considers the secondary structure of the transcript along with the complementarity in the seed sequence [291]. Finally, RNA-hybrid looks only at binding efficiency, not conservation or canonical seed-sequence binding [292].

MiRNA in clinical trials

While delivering miRNA to the brain is problematic, microRNA and their inhibitors are now being used in clinical trials. An University of Iowa trial (Clinical trial #NCT02579187) will evaluate the effect of miRNA delivery on bone development and inflammatory markers after oral surgery. An earlier clinical trial attempting intravenous liposomal injection of miR-34 to treat liver cancer (Clinical trial #NCT01829971) or melanoma (Clinical trial #BCT02862145) were terminated due to immune-related side effects. Meanwhile, multiple clinical trials (NCT01612871, NCT02009852, NCT01207531, NCT02247453, NCT03059524, NCT02466113, etc) are examining the diagnostic potential for miRNA in various human disease states. In Alzheimer's disease, a recently completed trial (NCT02129452) measured miR-206 from the olfactory neuroepithelia of AD patients. The results of this study are not available. Similarly, the levels of miR-107 as a function of gemfibrozil intake in AD patients (NCT02045056) or as a clinical diagnosis of BACE1 expression in the CSF (NCT01819545) are ongoing.

Chapter 2: Overall Rationale

AD is a complex disorder involving multiple proteins with their own respective regulatory mechanisms. Non-coding miRNA species are an important subsystem of this larger regulation of proteins. Therefore, identifying miRNA that regulate the proteins involved in AD would further elucidate the mechanism of the disease as well its progression. Given the importance of APP, BACE1 and NEP to the amyloid hypothesis, we focused on identifying miRNAs which target these proteins and confirming that specific interaction via well-designed experiments using human epithelial, neuronal and glial cell lines, as well as human primary mixed brain cultures. Notably, use of well-characterized autopsied human brain tissue specimens from control and Ad subjects is another major strength of the work presented herein. In addition to understand the biochemical cascade of the disease, we believe that miRNA may be used as novel, clinically relevant therapeutic agents in the treatment of AD. Finally, the identification of SNPs within proximity to the genomic regions of these miRNAs may further confirm the importance of these miRNA to disease state and/or highlight genomic signatures of the disease itself. Our overall experimental workflow is shown in Figure 3.

We hypothesized that identified miRNA would each reduce respective targets, APP, BACE1 and NEP respectively and subsequently alter levels of soluble Aβ.

Chapter 3: Specific Aims

Our overall aim was to functionally validate miRNA that target proteins implicated in the generation and clearance of beta-amyloid. Understanding novel function(s) of the proposed miRNAs, such as miR-20b and miR-298, is important irrespective of their role in the "amyloid hypothesis". In particular, we were interested in identifying miRNA that may target both APP, BACE1 and NEP and subsequently modulate levels of soluble beta-amyloid. Having identified miR-20b as a putative modulator of APP, and miR-298 as a putative modulator of both APP and BACE1, our specific aims were –

Specific Aim 1: To show that miR-20b modulates endogenous APP levels and subsequently levels of beta-amyloid.

-SA 1a: To show that miR-20b targets the APP mRNA 3'UTR and modulates endogenous APP levels in different mammalian cells and human primary mixed brain cultures.

-SA 1b: To show that miR-20b modulates levels of soluble Aβ.

Specific Aim 2: To show that miR-298 modulates both endogenous APP and BACE1 levels and subsequently levels of beta-amyloid.

-SA 2a: To show that miR-298 targets both the APP mRNA and BACE1 mRNA 3'UTRs and modulates expression of both proteins in different mammalian cells and human primary mixed brain cultures.

-SA 2b: To show that miR-298 modulates levels of soluble Aβ.

Specific Aim 3: To study levels of NEP protein in various cell types and tissues and identify putative miRNA that target NEP mRNA 3'UTR.

-SA 3a: To successfully detect NEP protein in mammalian cell cultures and human fetal brain, lungs and kidney tissues.

-SA 3b: To identify putative miRNA that target the NEP mRNA 3'UTR.

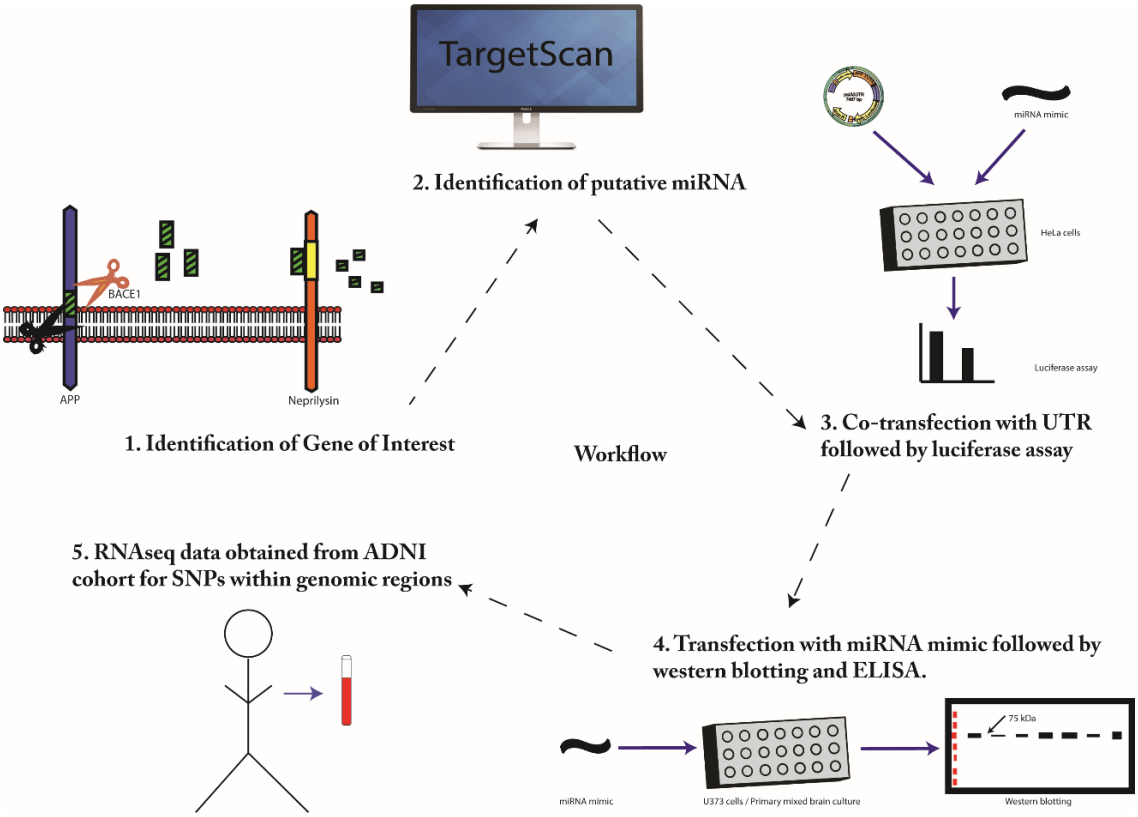

Figure 3: **Workflow diagram showing steps involved in identifying miRNA implicated in the modulation of proteins implicated in AD.** This methodology was followed for the work herein and starts from bioinformatics tools, through validation of miRNA and subsequent identification of SNPs in proximity to the miRNA gene.

Chapter 4: Materials and Methods

Cell Culture

All cell lines were procured from ATCC, except LNCaP cells, which were a generous gift from Dr. Kavita Shah (Purdue University). Cervical cancer cell (HeLa), human glioblastoma-astrocytoma (U373) and neuroblastoma (NB) (SK-N-SH) cells were grown in Minimum Essential Medium (MEM, Life Tech) enriched with 10% fetal bovine serum (FBS, Roche) and 1x antibiotic-antimycotic. Human prostate cancer cells (LNCaP) were grown in Roswell Park Memorial Institute (RPMI) media enriched with 10% FBS and 1x antibiotic-antimycotic. Rat pheochromocytoma cells (PC12) were grown on collagen (Roche)-coated plates and were cultured in RPMI with 10% horse serum (HS), 5% FBS and 1x antibiotic-antimycotic. In order to differentiate NB and PC12 cells, the media was switched to low serum (1%) and were treated with 10μM all-trans retinoic acid (ATRA, Roche) or 50ng/ml nerve growth factor (NGF, Sigma) for 7-10 days. All cells were grown in 100mm dishes until 70% confluent and either lysed (as described below) or split into the appropriate format (Table 1). All cell lines were grown in a 5% CO2 incubator.

Human fetal brain culture

Human fetal brain (HFB) culture was grown as described previously [293]. Briefly, tissue was received in Dissection media (Hibernate-E (Gibco)) media enriched with 1x Glutamax (Gibco), 1x Antibiotic-antimycotic, Normocin and B27 (Gibco)) and the blood vessels were removed. The tissue was then sliced into small sections using a sterile scalpel, and placed into 5mL of Trypsin-EDTA and placed on a shaker for 10-15 minutes. The trypsin was then inactivated using 1mL of HS and the suspension is centrifuged to

remove the trypsin. The pellet was resuspended in 5 ml of fresh dissection media, and then using a wide-bore Pasteur pipette, the tissue is triturated further. This step was repeated one more time. The viability of the cells was determined using the trypan-blue exclusion method [294] and the cells were plated at the appropriate density, in accordance with the format of the experiment (Table 1). After counting and plating, the cells were placed in a 37 °C with 5% CO2 and 9% O2.

Plating of cells

To count the cells, the 100mm plate was washed once with sterile phosphate-buffered saline (PBS) and 3 mL of Trypsin-EDTA was applied to the cells to dislodge them from the plate. 10mL of serum-containing media was added to inactivate the trypsin, followed by centrifugation and removal of the trypsin-containing media. The cell pellet was resuspended in fresh media and 30µL of the suspension was dissolved in trypan blue and mounted onto a hemocytometer. In accordance to the count obtained, cells were seeded onto 24-well, 48-well or 96-well (Table 1).

Preparation of "cell lysate" and protein estimation

Cell culture media was removed and stored at -80°C. The adherent cells were washed with cold PBS. After removal of PBS, appropriate amount of mammalian protein extraction reagent (M-PER, ThermoFisher) was added to lyse the cells (Table 1). The plate was then placed on a shaker at 4°C for 10 minutes, after which the lysate was collected into an autoclaved 1.5 mL tube (Eppendorf) and centrifuged. The supernatant was stored and used for western blotting and enzyme linked immunosorbent assay

(ELISA) as described below. For 96-well plates, lysates were transferred to opaque-bottom plates for CTG/luciferase assay (see below).

Format	**Number of cells per well**	**Amount of M-Per buffer used to lyse**
96-well	75,000	50uL
24-well	150,000	100-120uL
6-well	500,000	300uL

Table 1: Various cell-culture formats used for the in vitro study of miRNA effects on AD-implicated proteins.

Target	Source/Vendor	Clone #	Catalog #	Host	Dilution Which buffer?
Alpha-tubulin	Sigma		T9026	Mouse	1:1,000,000
APP	Millipore	22C11	MAB348	Mouse	1:1000
BACE1	Cell signaling	D10E5	5606	Rabbit	1:1000
BACE1	Abcam		Ab2077	Rabbit	1:1000
Beta-Actin	Sigma		A5441	Mouse	1:1,000,000
Neprilysin	Abcam		Ab951	Mouse	1:1000
Neprilysin	Fabgennix	101AP	101AP	Rabbit	1:150
Neprilysin	Fabgennix	112AP	112AP	Rabbit	1:150
Neprilysin	Fabgennix	131AP	131AP	Rabbit	1:150
Neprilysin	Fabgennix	141AP	141AP	Rabbit	1:150
Neprilysin	Fabgennix	151AP	151AP	Rabbit	1:150
Neprilysin	Fabgennix	161AP	161AP	Rabbit	1:150
Neprilysin	GeneTex		GTX53381	Rat	1:500
Neprilysin	GeneTex		GTX111680	Rabbit	1:1000
Neprilysin	Millipore		AB5458	Rabbit	1:1000
Neprilysin	RnD		MAB1126	Rat	1:500
Neprilysin	RnD		AF1182	Goat	1:500
Neprilysin	Santa Cruz		SC-46656	Mouse	1:1000
Tau	Abcam		Ab80579	Mouse	1:1000

Table 2: List of antibodies used for western blotting and immunocytochemistry.

Secondary antibody	Company	Catalog #	Dilution
Goat anti-mouse	Rockland	610-1319	1:3000
Goat anti-rabbit	Rockland	611-1322	1:3000
Donkey anti-goat	Jackson	705-035-003	1:3000
Goat anti-rat	Rockland	212-1302	1:3000

Table 3: List of horseradish peroxidase-conjugated secondary antibodies used for western blotting.

DNA transfection

Using the NanoDrop spectrophotometer, the concentration of the appropriate DNA plasmid (Table 4) was measured. The previous day, approximately ~75,000 cells/well were seeded onto a 96-well plate. On the day of the transfection, 300ng/well of DNA and 0.3ul/well of Transfectin (BioRad) reagent were suspended in 20µl/well Opti-MEM (Gibco) media, mixed and incubated at room temperature for 20 minutes. 80uL of fresh media devoid of antibiotics as well as the transfection complex was added to each well and left undisturbed in a 5% CO2 incubator for 48 hours. For miRNA reporter assays, the same procedure was used, except 50nM of miRNA mimic was added to the DNA-transfectin-Opti-MEM complex.

MiRNA transfection

5 nmol of mature miRNA or siRNA mimic (ThermoFisher) was resuspended in 1000µL of nuclease-free water to obtain a final concentration of 5uM. Transfections were performed one day post-seeding, in the case of HeLa and U373, and at DIV 17 of the HFN culture. Lipofectamine RNAiMax was used as a transfection reagent and all miRNA-RNAiMax complexes were suspended in Opti-MEM media and brought up to a volume of 100uL. For cell line experiments, 20nM of siRNA, 50nM of miRNA and 2ul/well of RNAiMax were used, whereas, For HFN transfections, 50nM of siRNA, 75nM of miRNA and 3ul/well of RNAiMax were used. Plates were left undisturbed in the incubator until time of harvest – 72 hours later. For the time course experiment, wells were lysed at intervals of 24 hours.

Plasmid name	Company/modification	Plasmid size (kb)
PsiCheck2	Promega/none	6.3
APP 3' UTR	Promega/APP 3'UTR insert (1.2 kb)	7.5
MiR-298 mutant-1	Promega/APP 3'UTR with miR-298 site-1 mutagenized	7.5
MiR-298 mutant-2	Promega/APP 3'UTR with miR-298 site-2 mutagenized	7.5
MiR-20b mutant	Promega/APP 3'UTR with 20b site mutagenized	7.5
NEP 3'UTR	Promega/NEP 3'UTR insert (3.3 kb)	9.5
BACE1 3'UTR	Promega/BACE1 3'UTR insert (3.9 kb)	10.2

Table 4: List of DNA plasmids used.

Western blotting

In accordance with our data showing linearity for well-expressed proteins such as APP and BACE1 (See Figure 4), between 3ug-9ug of protein was loaded onto each well per gel, whereas for lowly expressed NEP, between 10-150ug of protein was loaded and run on either 10-lane, 15-lane or 26-lane pre-cast gels (BioRad). The gels were run for 1 hour at 200V and transferred onto PVDF-membrane using the iBlot system (Invitrogen). After transferring proteins, membranes were briefly immersed in methanol, acetic acid and then stained with Ponceau S (Sigma). After confirmation of transfer via Ponceau-S stain, membrane was blocked for 1 hour in 5% milk in Tris-buffer saline with Tween-20 (TBST).

After blocking, the blots were probed with the appropriate primary antibody (see Table 2 and Figure 2) for either 3 hours at room temperature or overnight at 4°C. The membrane was subsequently washed in TBS (3x 5 min each) and then probed with the appropriate horseradish peroxidase (HRP) conjugated-secondary antibody (see Table 3) for 1 hour, followed by washing in TBST. Finally, the bands were visualized using the enhanced chemiluminescence (ECL) method. Antibodies used in the work herein were studied for linearity of their western blot signal (Figure 4).

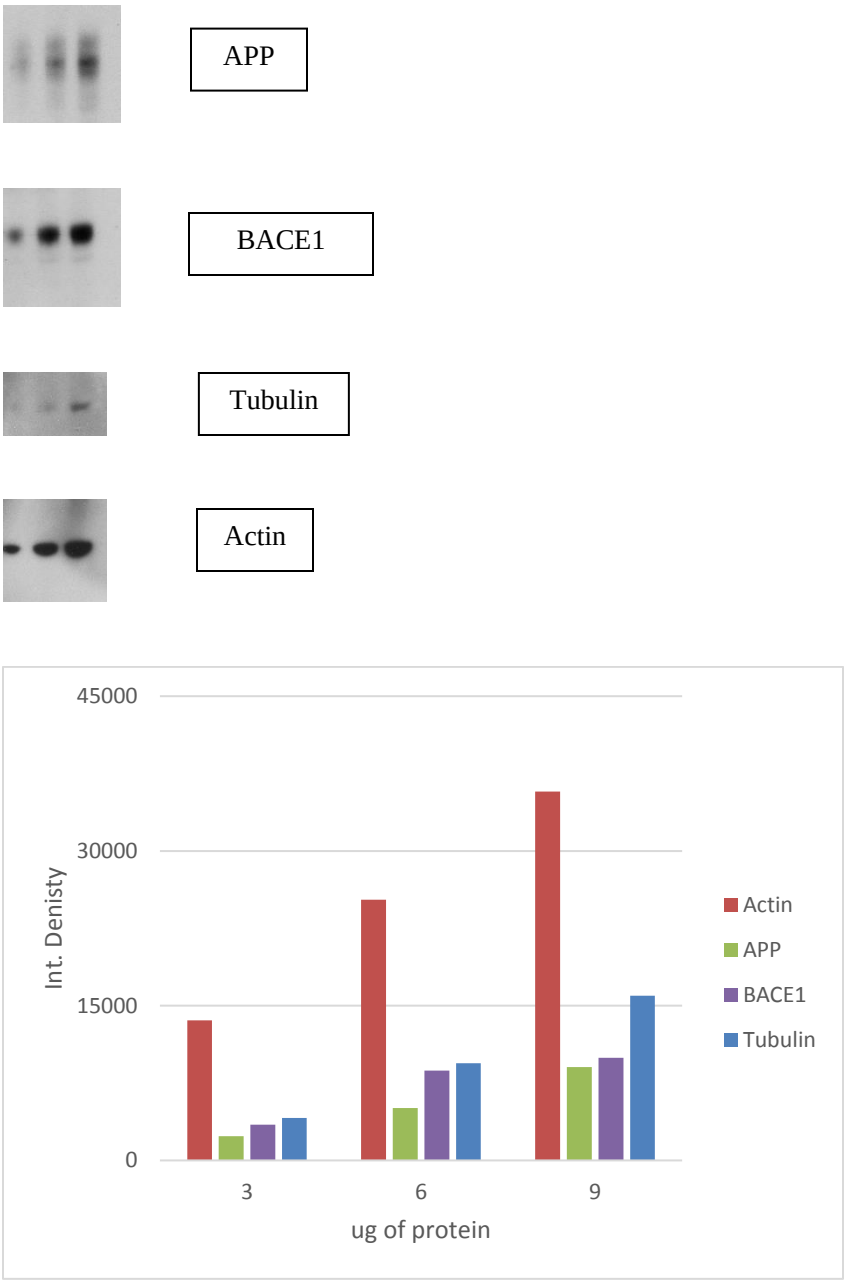

Figure 4: Linearity of protein detection in Western blot. Lanes loaded with pooled sample of autopsied AD brain tissue extracts with 3ug, 6ug and 9ug of protein and probed with 4 key antibodies used in this work. Non-normalized densitometry is also shown to confirm linearity of detection.

Immunocytochemistry (ICC)

Human neuronally differentiated (NB+RA) cells were grown as previously described (see Methods). Cells were fixed using 4% paraformaldehyde and permeabilized using 0.1% Triton-x 100. Wells were blocked for 20 minutes with 10% HS in phosphate-buffered saline (PBS). Primary antibody (1:100, Figure 2) was dissolved in 1% HS and applied to the wells and left overnight at 4°C. After rinsing 3 times with PBS, cy3-conjugated goat anti-rabbit antibody was applied to the cells for 1 hour and kept in the dark to avoid bleaching of the fluorophore. The wells were visualized using a fluorescent microscope (Leica) using the red-filter. For a control, one well was treated with 1% HS in PBS, devoid of primary antibody, followed by secondary antibody application. This well served to visualize the immunoreactivity of the secondary antibody itself.

ELISA of different proteins and peptides

Two independent, specific and sandwich ELISA protocols were used to measure levels of different Aβ peptides as briefly described below. For the Aβ (1-40) and Aβ (1-42) ELISA, the conditioned medium (CM) samples were used to measure levels of soluble Aβ peptides as per the manufacturer's protocols (IBL America). Briefly, 5 µL (for Aβ 40) or 25µL of CM (for Aβ 42) was brought up to 100µL with EIA buffer and applied to wells pre-coated with a monoclonal antibody targeting the specific Aβ peptide overnight. The following day, HRP-conjugated polyclonal detection antibody was applied after washing, and TMB-substrate was used to measure optical density (OD) at 450nm. The actual Aβ peptide content was calculated by comparing ODs against those

generated by a standard curve generated using known amounts of recombinant Aβ peptides (See Figure 6 for examples of standard curves).

NEP ELISA (RnD) procedure was performed in accordance with the protocol with the following modification. Briefly, plates were coated with a capture antibody targeting NEP. After a blocking step, sequential addition of lysate, detection antibody and HRP-conjugated to biotin-streptavidin steps for visualization were performed. Based on experience with previous ELISAs, we observed that the OD) measurements in ELISA were a consequence of cross-reactivity of the amplification step. To eliminate the possibility of a non-specific result, we tested each sample both with and without the addition of the detection antibody. The ODs were then calculated as $OD_{\text{with detection antibody}} - OD_{\text{without detection antibody.}}$ The resultant OD values were normalized to the mean of the control values and exhibited as shown.

NEP enzyme assay

Commercially available NEP substrate (RnD), which is tagged to a fluorophore (mca) and a quencher (dnp), was added onto each well of a 96-well plate in assay buffer (100mM Tris-HCL pH 7.5, 50mM NaCl, and 10 µM $ZnCl_2$). Both the NEP inhibitor (Thiorphan, 10µM) and ACE inhibitor (Captopril, 0.1µM) were added to appropriate wells. Recombinant NEP (RnD) was serially diluted to generate a standard curve to normalize unknown samples. All volumes were brought up to 100µl of assay buffer and placed at 37 C for 1 hour in the dark. Readings were taken for 90 minutes, every 2 minutes with excitation at 320nm and emission at 405 nm.

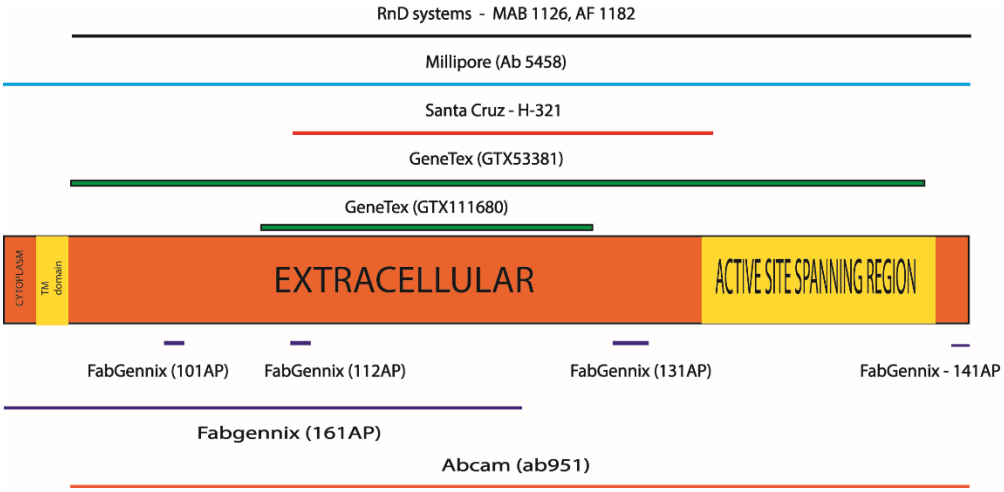

Figure 5: The immunogens used to generate various commercially available antibodies. The information provided by various vendors regarding the immunogens for their respective antibodies is indicated here. As shown above, the regions targeted by various antibodies are short (FabGennix) to medium length (Santa Cruz) to full length (Millipore). Additionally, regions involved in various domains are also covered by the multitude of immunogens. FabGennix 151AP was generated by injecting three epitopes – FabGennix 101AP, 112AP and 131AP, and is therefore not shown on this diagram.

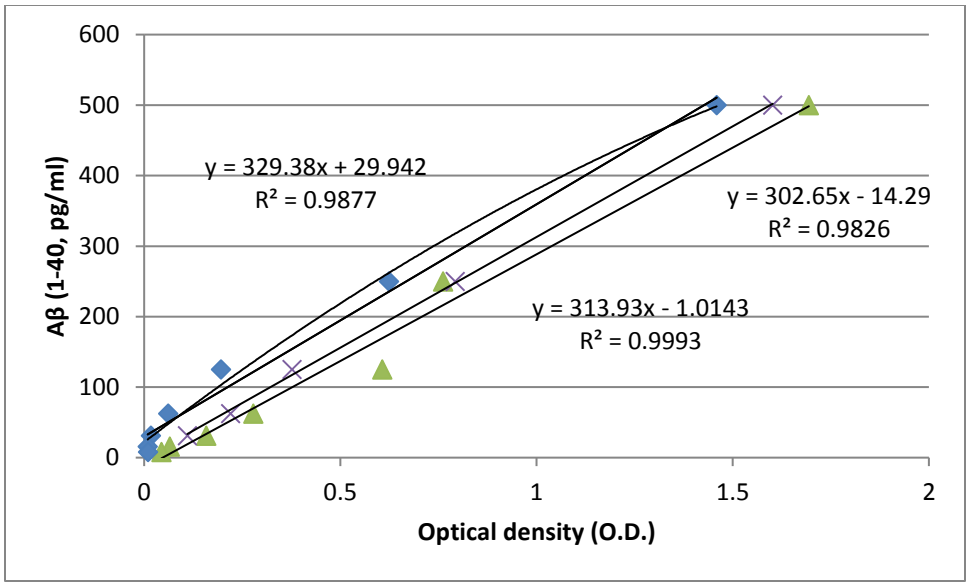

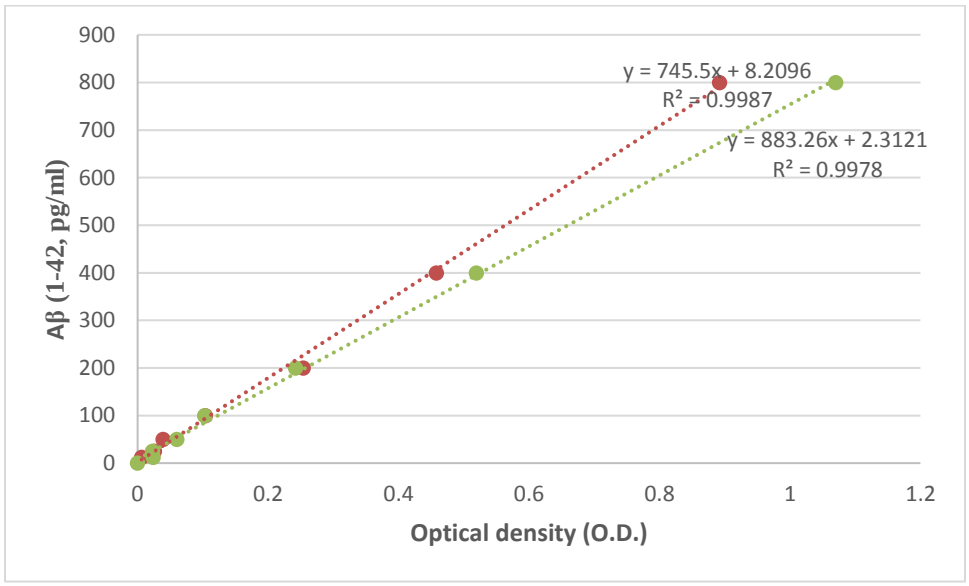

Figure 6: Standard curves generated for IBL Aβ (1-40) and Aβ (1-42) ELISAs.

Known quantity of each peptide was serially diluted as per the manufacturer's instructions. Each color represents standard curve generated in a separate ELISA experiment to ensure consistency of each ELISA protocol.

Site-directed mutagenesis

The target sites of miR-298 and miR-20b on the APP 3'UTR were identified using Targetscan. The two sites were mutated independently using the QuikChange Lightning kit (Agilent). Briefly, primers generated with regions overlapping the 7 nucleotide target sites were used in the mutagenesis step. The previously mentioned APP mRNA 3'UTR was denatured and the mutagenic primers were extended with the *PfuTurbo* DNA Polymerase enzyme provided by the kit. Parental DNA was digested by Dpn I restriction enzyme, and transformation into competent cells was completed with the digest. To confirm mutagenesis, plasmids were run on a DNA gel, showing the introduction of a novel enzyme site – replacing the miR-298 target site.

Luciferase assay

30µL of lysates were transferred to an opaque-bottom 96-well plate. Protocol was run on a GloMax system according to the manufacturer's instructions. First, 30uL of substrate for firefly luciferase activity was added to each well, and luciferase activity was recorded. After a quenching step, substrate for Renilla luciferase was added to each well and luciferase activity was recorded. The ratio of Renilla/firefly luciferase was calculated and plotted.

Cell-titer Glo (CTG) assay

30uL of lysates were added to an opaque-bottom 96-well plate. To each well, 30uL of CTG buffer (Promega) was added, and the subsequent ATP-dependent release of light was measured and plotted.

Rat tissue processing

Two female 74 day old Wistar rats were humanely sacrificed by decapitation and their liver, lung, kidney, cortex and hippocampus were removed and placed in ice-cold PBS as per the IACUC protocol. These tissues were homogenized in Polytron and centrifuged at approx. 10,000g for 10 minutes, and their supernatant was stored and used in subsequent western blotting and ELISA experiments.

Fetal tissue processing

Fetal brain, kidney, spleen/pancreas, heart, lung and adrenal cortex were received in Hibernate-E media. Each tissue was rinsed with PBS and the blood vessels were removed using forceps. The tissue was suspended in 300µL of M-Per buffer and dissociated in the polytron until a homogenous suspension was visible. These samples were centrifuged at ~10,000 g for 10 minutes and the supernatants were used for western blotting and ELISA experiments.

Reverse transcription quantitative PCR (RT-qPCR)

Post-mortem tissues were homogenized and RNA extracted as previously described [236]. RNA was first converted to cDNA using the Taqman miRNA RT kit (Life Sciences). The assay was run in accordance with the manufacturer's protocol. Briefly, RNA, oligoprimers, dNTPs and reverse transcriptase were brought up to a volume of 20uL per reaction and incubated on a thermocycler. The settings used were: 16°C for 30 minutes, 42°C for 30 minutes and 85°C for 5 minutes. The cDNA was then combined with the universal PCR master mix and the fluorescent-probe-containing miRNA assay

(specific for either miR-298 or miR-20b) and analyzed on a 7300 RT-PCR instrument (Applied Biosystems).

Samples were quantified by comparison to a pre-generated standard of known amounts of RNA, which comprised a HPLC-purified synthetic miR-298 or miR-20b (Sigma) reconstituted to a stock of 10uM and serially diluted.

Imaging and neurite measures

Transfected plates were placed in the Incucyte Zoom (Essen Bioscience) and imaged once a day to obtain 4 time points: 24, 48, 72 and 96 hours. In a separate experiment, APP siRNA harvested plate was imaged at 72 hour only. Using the 'neurotrack' analyzer, masking of cells and neurites were performed to ensure inclusion of cell bodies and neurites. Specifically, minimum cell body clusters were set to 50 μm^2, Segmentation adjustment was set to 1.2, minimum cell width to 5μm, neurite filtering to 'best', neurite sensitivity to 0.35 and the neurite width was set to 1 μm. Importantly, the same parameters were used for all the conditions analyzed. The neurite lengths and branch points obtained were normalized to the cell body clusters (a measure of cell number within a field of view).

Chapter 5: Specific Aim 1 – To show that miR-20b modulates endogenous APP levels and subsequently levels of beta-amyloid

Rationale

The amyloid hypothesis implicates that APP plays a central role in the generation of potentially toxic amyloid-beta peptides. Therefore, understanding regulatory mechanisms governing the expression of APP would identify the biochemical cascade of pathway of AD leading to potentially novel AD drug targets. APP has previously been shown to be modulated by miRNA expression, such as miR-101 and miR-153 [233,236] (. Our goal was to identify a miRNA that modulates APP as well as regulates levels of soluble Aβ peptide. Finally, having identified a miRNA which modifies this AD-related proteins/peptides, we were interested in the possible regulation of the genomic region of the miRNA itself.

Based on the bioinformatic prediction tools, we hypothesized that miR-20b would target the APP mRNA 3'UTR and reduce levels of both APP protein as well as soluble Aβ peptide.

Results

MiR-20b targets the APPmRNA 3'UTR and is a negative regulator of APP expression

Using at least 3 different predictive algorithms, we found that miR-20b was predicted to target the APP mRNA 3'UTR (Table 5). The TargetScan context ++ score of 76 suggests that 76% of sites for this miRNA have less favorable scores than this site. The PhastCon score suggests that the target site for miR-20b on the APP mRNA 3'UTR is well conserved. The highly negative ΔΔG score from PITA suggests that the miRNA has high predicted binding affinity at that site. The predicted 7-mer-m8 target site on the APP mRNA 3'UTR is located at the 710-716 positions on the UTR (Figure 7). There is perfect complementarity between the seed sequence of mature miR-20b and this 7-mer target mRNA sequence, underlying the highly negative ΔΔG score. No sites were predicted for miR-20b binding in the coding region or the short of APP mRNA 5' UTR.

Confirmation of the miR-20b target site on the APP 3'UTR.

Dr. Justin Long from our lab successfully inserted the full-length APP 3'UTR into a dual-luciferase reporter vector [233], thereby allowing us to test whether miR-20b targets the APP3'UTR. Using a lipid-based transfection system, we co-transfected HeLa cells with the luciferase reporter with three different miRNAs: miR-20b, miR-101 (positive control) and a negative control miRNA (NCM), which is not predicted to target the APP mRNA 3'UTR. We found that that the co-transfection of the reporter vector with miR-101 and miR-20b reduced luciferase-mediated activity by 40% and 30% respectively (Figure 8A). Co-transfection with the negative control mimic had no effect on luciferase

activity. Together these results suggest that miR-20b targets the APP mRNA 3'UTR (Figure 8A).

To confirm the validity of the predicted target site, we mutated the 7 nucleotide target site of miR-20b using the site-directed mutagenesis protocol (Figure 8B and 8C). We validated the mutagenesis by DNA restriction digestion (data not shown). Co-transfection of the mutagenized APP 3'UTR with miR-20b revealed no reduction of luciferase activity (Figure 8C). In the same plate, wild-type APPmRNA 3'UTR co-transfected with miR-20b showed a reduction of luciferase as previously shown (Figure 8B). Together, these results confirm that the miR-20b targets specific sequences on the APP 3'UTR, which is the 710-716 site, as predicted.

Prediction algorithm	APP score
TargetScanHuman 7.1	76[a]
PicTar	2.34[b]
DIANA-microT version	0.515[c]
microRNA.org	0.6663[d]
PITA	-12.70[e]
rna22	-18.6[f]

[a] context ++ score percentile; a quantitative prediction of how highly ranked a particular miRNA is compared to other miRNA predicted to target a sequence
[b] This is a PicTar score for miR-20, not miR-20b in particular is not available in the PicTar algorithm.
[c] miTG score; Prediction score. Threshold of miRNA discovery was set to 0.2
[d] PhastCon scores; Provides scores based on conservation of the target site using a hidden Markov model
[e] ddg score; based on hybridization energgy and site accessiblity
[f] Folding energy (kcal/mol); with allowance for single G:U bulge

Table 5 – Identification of miR-20b as a putative modulator of APP. Six separate bioinformatics algorithms predict that miR-20b targets the APP mRNA 3'UTR. An explanation for each score is also included herein. Crucially, each miRNA predictive tool has its own specific parameters for predicting putative miRNA. Some of these parameters overlap between algorithms and some are unique.

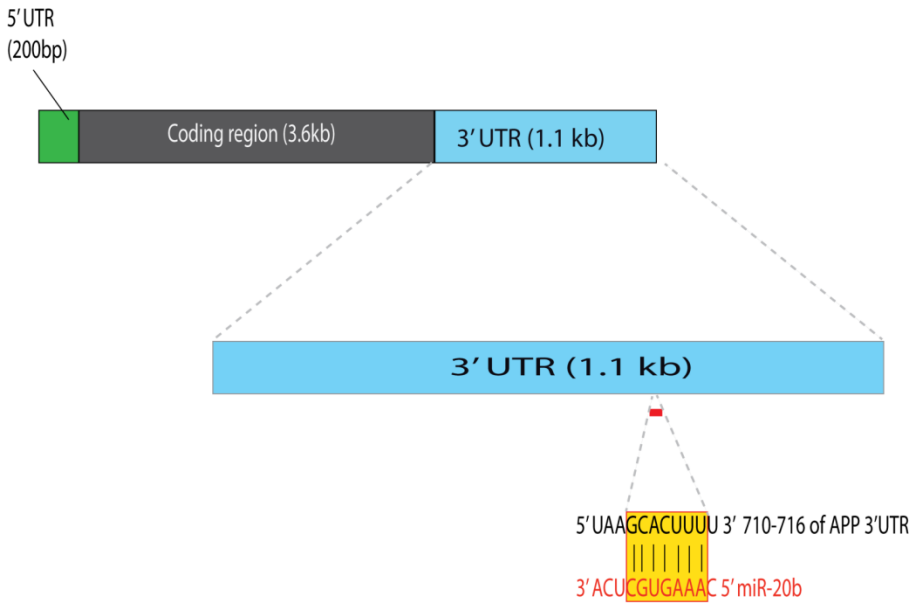

Figure 7: Predicted target site of miR-20b on the APP 3'UTR. Scaled figure showing 7-mer binding site for miR-20b on the APP 3'UTR. Also shown are the short 5' UTR, 3.6 kb coding region drawn to scale.

A

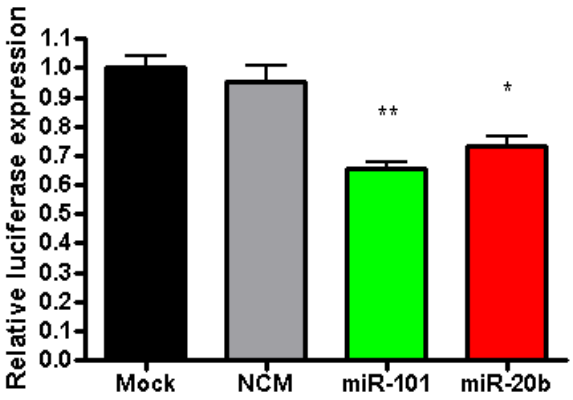

	+	+	+	+
Neg. control miRNA		+		
miR-101			+	
miR-20b				+

B

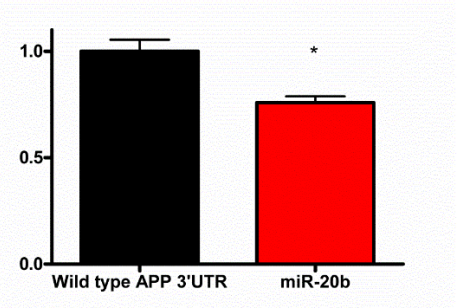

C

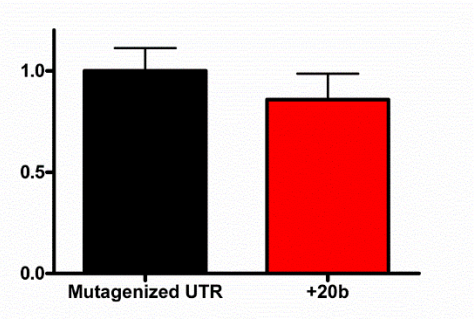

Figure 8: miR-20b reduces APP 3'UTR-mediated luciferase expression. A) Co-transfection of miR-20b with the full-length APP mRNA 3'UTR results in a reduction of APP 3'UTR-mediated luciferase activity, compared to a negative control miRNA ($p<0.05$). B) and C) Mutagenesis of the seed-sequence reverses the 20b-mediated reduction of the APP 3'UTR-mediated luciferase activity .

MiR-20b reduces APP protein expression in HeLa cells

Having validated the miR-20b targeting of the APP mRNA 3'UTR, we investigated the effect of miR-20b on APP *protein* expression. Using HeLa cells – a consistently transfectable human cell line that expresses APP – we tested the effects of four miRNAs – miR-520c-3p, miR-20b, miR-144 and NCM (Figure 9). We also used APP siRNA as a positive control to confirm transfection efficiency and experimental outcomes. We found that APP siRNA, miR-520c-3p and miR-20b reduced APP levels by 90%, 60% and 60%, respectively (after normalization to β-actin) compared to Mock- and NCM-transfected cells (Figure 9). MiR-144 and NCM did not reduce APP levels in a statistical significant manner. Therefore, we found that miR-20b reduces human APP levels in mammalian cells of the epithelial type.

MiR-20b reduces APP levels in a mixed primary human neuronal cell culture

After confirming the modulation of miR-20b in HeLa cells, we tested thes effect of miR-20b in a human mixed neuronal primary cell culture model. Using a previously validated model developed in our lab [293] we found that APP siRNA reduces APP expression by 50% (Figure 10). MiR-298 reduces APP expression by about 25% compared to mock-transfected cells. Co-transfection of an antagomir to miR-20b (inhibitor) could reverse the miR-20b-mediated reduction of APP (Figure 10). Although the co-transfection of the inhibitor produced a slight increase in APP expression compared to mock, this was not statistically significant ($p>0.05$). Similarly, the slight increases observed on transfection with the antagomir alone and with NCM were not statistically significant ($p>0.05$).

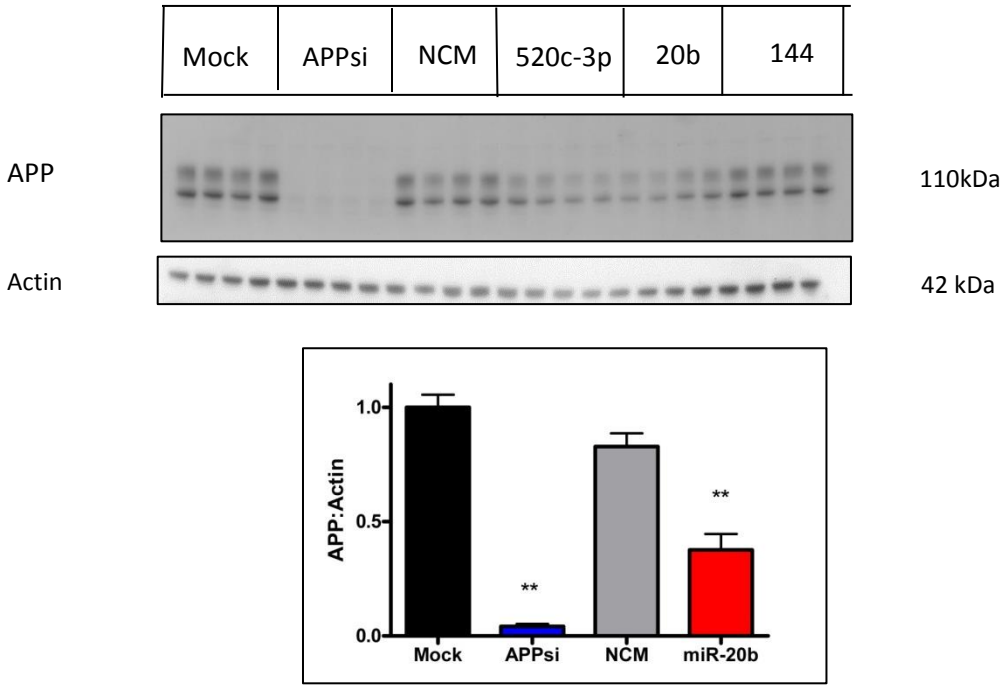

Figure 9: Transfection of miR-20b results in the reduction of APP expression in HeLa cells. APP bands were normalized to β-actin bands using densitometry. N=4, $p<0.05$. Cells were transfected for 72 hours using RNAiMax, cell were lysed, proteins were boiled and separated using sodium dodecyl sulfate polyacrylamide gel electrophoresis (SDS-PAGE). Antibodies against APP (clone 22C11) and β-actin were used for detection of the protein. APP siRNA was used as positive control, while NCM (negative control miRNA) was used to test for non-specific effects associated with introducing exogenous miRNA into the cell culture system.

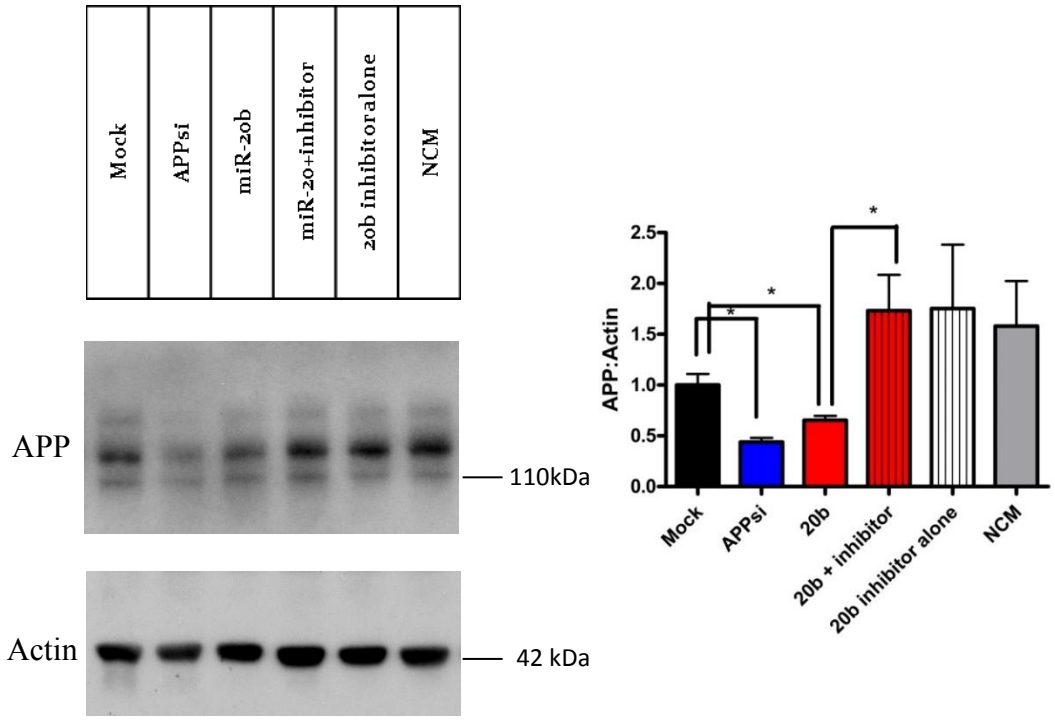

Figure 10: miR-20b reduces APP levels, and its inhibitor reverses miR-20b-mediated reduction of APP. In a primary human cell culture model, the co-transfection of an antagomir to mature miR-20b reduced the miR-20b-mediated reduction of APP expression. (n=4, $p<0.05$). The set included here is a representative set of n=4. APP siRNA reduces APP expression by approximately 50%, while miR-20b reduced expression by ~40% compared to mock- or NCM-transfected cells. ANOVA was used to compare different groups.

MiR-20b and APP siRNA modulate synaptic connectivity

We tested whether transfection of miR-20b could modulate, directly or indirectly, the synaptic connectivity in the primary human mixed neuronal culture tested. Notably, both neurite length and neurite branch points were reduced in a time-dependent manner (Figure 11A and 11B) compared to mock- transfected cells. In a separate experiment, we tested whether transfection of APP siRNA, had a similar effect at 72 hours post-transfection. APP siRNA transfection did not reduce neurite branch points or neurite length compared to mock transfected cells (Figure 11C and 11D). To test whether this change in neuritic length and branch points could result a loss in synaptic activity, we tested the effect of miR-20b on the calcium influx of the same human cell culture using Fura-2 imaging. We found that miR-20b did not change KCl-induced influx of calcium (data not shown).

MiR-20b reduces soluble Aβ (1-40) levels in cell culture supernatants

In human primary mixed cells, we tested the effect of miR-20b overexpression on levels of soluble Aβ (1-40) peptide. Using a well-validated sensitive ELISA (IBL), we observed that miR-20b reduced levels of soluble Aβ (1-40) by about 25% (Figure 12). To compensate for individual differences in cell density in different wells, we normalized each replicate to the metabolic activity measured from the cell lysate obtained from that well (CTG).

MiR-20b expression is unchanged in post-mortem human brains

Total RNA was extracted from brain samples and levels of miR-20b were measured in these samples. We found that miR-20b expression was not significantly

changed across Braak stages of AD (Figure 13). While we did see a slight reduction in miR-20b expression between Braak stages III/IV and V/VI, this was not statistically significant (p=0.06) (Figure 9).

When combining all AD groups, we found no difference between miR-20b levels in control samples (n=5) vs control (n=20) (Figure 13).

A

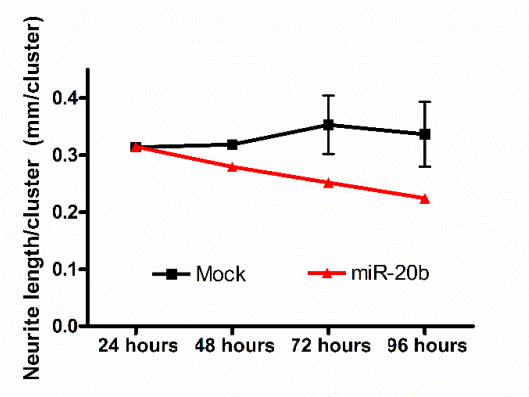
Neurite length/cluster (mm/cluster)
0.4
0.3
0.2
0.1
0.0
Mock
miR-20b
24 hours
48 hours
72 hours
96 hours

B

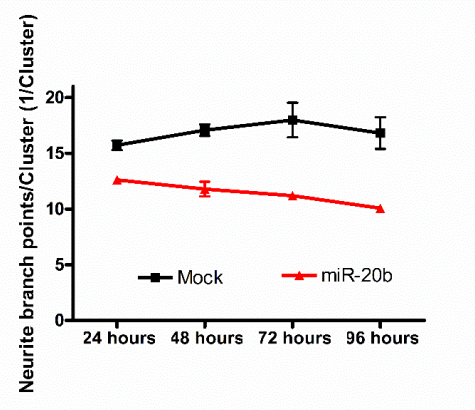
Neurite branch points/Cluster (1/Cluster)
20
15
10
5
0
Mock
miR-20b
24 hours
48 hours
72 hours
96 hours

C

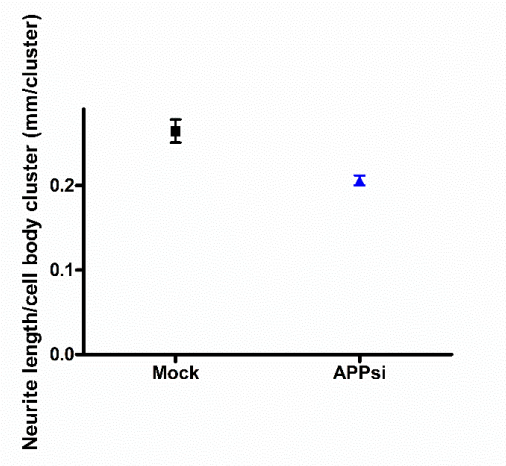
Neurite length/cell body cluster (mm/cluster)
0.2
0.1
0.0
Mock
APPsi

D

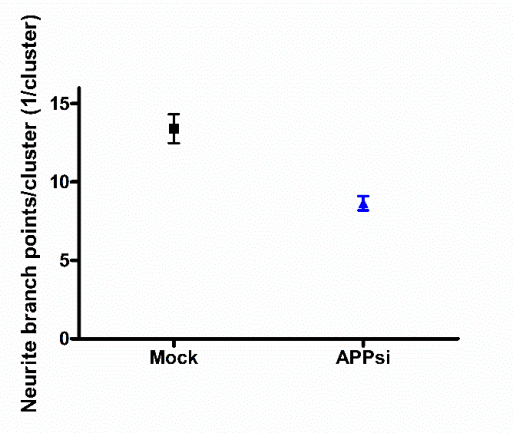
Neurite branch points/cluster (1/cluster)
15
10
5
0
Mock
APPsi

E **F**

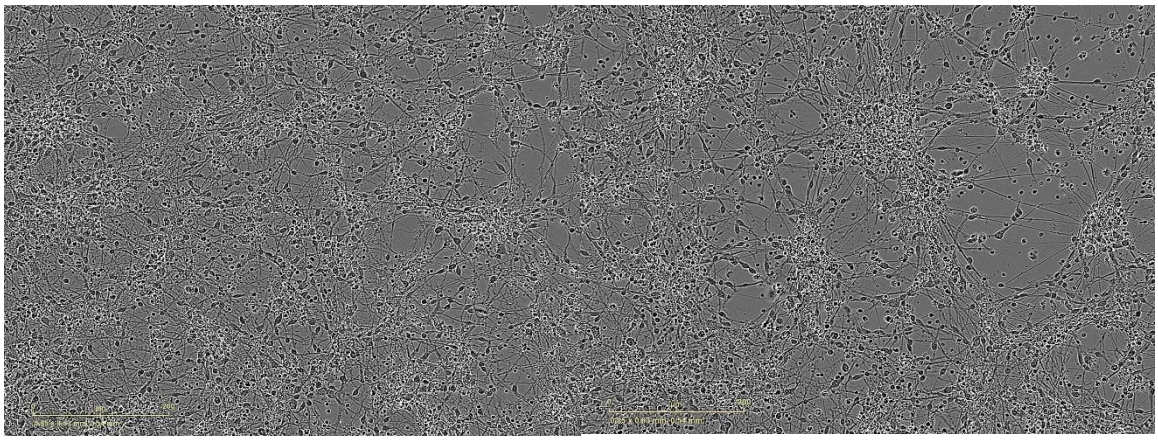

Figure 11: Transfection of miR-20b changes synaptic connectivity of neuronal culture. Transfection of miR-20b reduces neurite branch points/cluster (A, F) and neurite length/cluster (B, F) over a period of four days in vitro, compared to Mock-transfected (E). In a separate experiment, APP siRNA also reduces branch points (C) and neurite length/cluster (D) at 72 hours.

A B

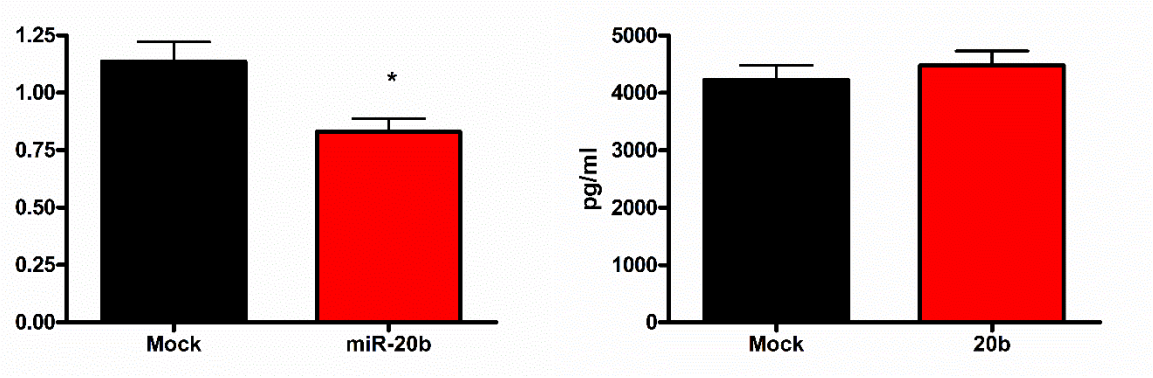

Figure 12: miR-20b reduces levels of soluble Aβ (1-40). Using cell culture supernatants from the primary human mixed brain culture, we showed overexpression of miR-20b results in a reduction of Aβ (1-40, A), but not soluble Aβ (1-42) peptide, B) production. The optical density values were normalized to the metabolic activity (ATP production) of the cells in panel A, whereas in panel B, we were able to calculate absolute values of the peptide ($n=4$, $p<0.05$).

A B

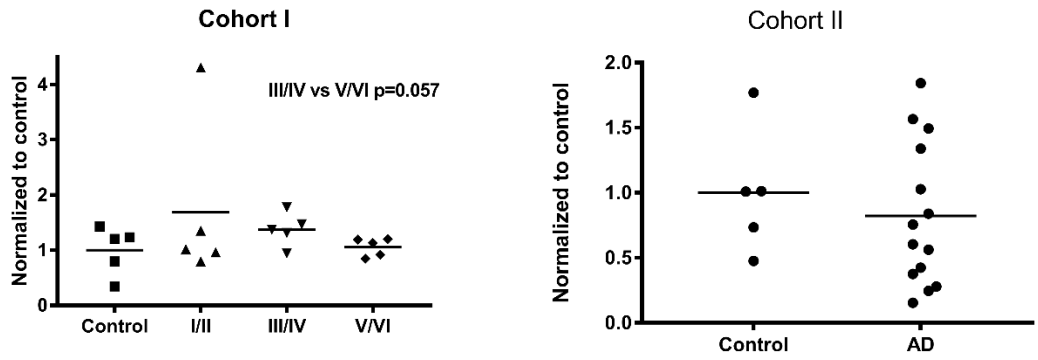

Figure 13: Using RNA extracted from post-mortem adult brains, we measured levels of miR-20b from these samples. We found no statistically different effects across various Braak stages (A), or when comparing AD against control samples (B). In both experiments, equal RNA was used to determine differences in miR-20b levels across groups.

Discussion

MiR-20b reduces expression of APP and soluble beta-amyloid (1-40)

The regulation of APP by various miRNA has been shown by various laboratories, including our own [232-234,236,238,295]. In searching the bioinformatics predictors further, we came across miR-20b as a putative modulator of APP expression. Using site-directed mutagenesis, we confirmed that miR-20b targets the predicted 7-mer site on the APPmRNA 3'UTR. We noticed that co-transfecting the mutagenized APP 3'UTR-containing plasmid along with miR-20b did not return luciferase activity to baseline. This is unlikely to be an anamoly due to lower transfection efficiency – as the output of Renilla to firefly luciferase should circumvent any problems related to transfection efficiency. It is possible that we introduced a new binding site on which endogenous miRNA acted to produce a slight (non-significant) reduction in luciferase activity.

We showed that miR-20b reduced levels of endogenous APP protein in two different tissue culture models. Each cell culture has its own advantages: HeLa cells are consistent and reliable in growth and transfection of miRNA, and express APP at a high level. The primary human mixed brain culture used herein is another important primary culture model for studying neurodegeneration as it contains neurons, glia and neuroprogenitor cells. It is important to note that the magnitude of APP reduction by miR-20b differs in the two cell lines. This can be due to two major factors: The transfection efficiency of the two cell culture models, and the differential endogenous miR-20b levels within each cell culture model. The fact that we did not directly test the latter (i.e., miRNA measurements) is a general limitation of the work herein. Speculatively, the former factor may play a role. This can be seen by observing that APP

siRNA,which provides an idea of the maximal level of transfection efficiency, knocks down APP more strongly in HeLa cells than it does in the primary human mixed brain cultures. We observed a small, not-statistically significant increase in miR-20b and miR-20b-inhibitor co-transfected wells. We believe that the antagomir inhibited exo added miR-20b, but did not sufficiently buffer endogenous miR-20b levels. In order to test this, future experiments should study the effect of miR-20b inhibitor *de facto* on the expression of APP in the cell culture. Our observation that miR-20b does not modulate KCl-induced calcium influx may be interpeted in many ways. It's possible that APP is not involved in the calcium response, or, miR-20b does not target voltage-gated calcium channels or their specific subtypes.

We found that miR-20b did not change in the post-mortem brains of a small cohort of age-matched controls vs increasing braak stages. It is important to note that our sample size was small (each group had an n=5), and that one needs to repeat the experiments with larger samples, at least for the Braak stages I/II and III/IV. Additionally, obtaining post-mortem brain samples proves to be a very difficult proposition, therefore increasing sample size is a non-trivial issue. The absolute value of miR-20b in these samples could not be measured as the miR-20b oligonucleotide standards obtained commercially (Sigma) did not show linearity during qPCR assay. On visually observing the original vial, it was apparent that a gel-like residue had precipitated into the vial, likely due to the PAGE-purification process.

It would be interesting to study the level of miR-20b in CSF and serum samples from AD patients. Previous work has shown a number of miRNAs that are differentially expressed in AD patients. A study that looked at miRNAs in serum of AD, MCI, vascular

dementia (VD) and non-AD controls found that 4 miRNA were downregulated in AD patients – miR-31, miR-93, miR-146a and miR-143 [296]. MiR-93 is of particular interest because it is in the same miR-17 microRNA precursor family to which miR-20b belongs to. However, this report did not reveal changes in miR-20b levels or other miR-17 precursor family members. In another study, miR-181c was downregulated in AD patients, while miR-9 was upregulated in serum samples from AD patients vs Controls [296,297].

While we have shown that miR-20b can reduce APP and soluble Aβ (1-40) levels in mammalian cell cultures, the ability of the miRNA to modulate Aβ (1-40) levels in animals remains unknown. Two obvious considerations for a discussion of miR-20b as a putative drug therapy involve 1. miR-20b's myriad other targets, and 2. The difficulty of delivering miRNA to the brain. MiR-20b has been previously shown to negatively regulate Endothelial PAS domain 1 [298], vascular endothelial growth factor in the lung [299], ephrin B2 and B4 in human placental tissue [300], proteinase-activated receptor-1[301], phosphatase and tensin homolog[302], signal transducer and activator of transcription 3 [303], IL-1 receptor-associated kinase 4 [304], hypoxia-inducible factor 1-alpha [305] and protein kinase B [306].

These proteins are involved in a variety of functions including neuronal development and maintenance, depending on the cell type, tissues and organs. Therefore, the off-target effects of miR-20b warrant serious consideration if it is to be a serious candidate as a therapy for reducing APP and Aβ in the brain. One possibility is that miR-20b targets APP with a greater propensity than it does other proteins, thereby, the effect of overexpressing miR-20b would be more significant on APP than the other

aforementioned proteins, again which depends on the tissue types. However, to our knowledge, there is no comparative study showing miR-20b having a higher binding efficiency to APP (or any protein).

The next problem is how to increase miR-20b levels in the brain. Three known compounds have been reported to increase miR-20b levels. First, 3, 3'-Diindolylmethane (DIM) was shown to increase levels of miR-20b in liver mononuclear cells [304]. DIM is found at appreciable levels in vegetables such as broccoli, and seems to be well tolerated, although it's ability to cross the BBB remains unknown. Second, one year intake of Natalizumab increased levels of miR-20b in the blood of patients with multiple sclerosis (MS) [307]. As a corollary, the same authors deleted the miRNA-106a~363 gene (including the miR-20b locus) and found that it severely enhanced experimental autoimmune encephalitis – a mouse model for MS – in mice compared to wild-type mice [307]. Natalizumab is well-tolerated and is capable of crossing the BBB. Finally, prednisone acetate was shown to increase miR-20b levels in the serum from patients suffering from myasthenia gravis [308].

While miR-20b is capable of being modulated by the three aforementioned drugs, systemic administration of any of those drugs would cause miR-20b modulation of other targets in various organs. For this same reason, systemic increase in miR-20b would not be advisable. Therefore, a more selective, targeted increase of miR-20b is warranted.

Chapter 6: Specific Aim 2 - To show that miR-298 modulates both endogenous APP and BACE1 levels and subsequently levels of beta-amyloid

Rationale

Along with APP, the regulation of BACE1 protein is crucial to the generation of potentially toxic amyloid peptides. Therefore, identifying miRNA that target both proteins would elucidate an important regulatory element modulating two pivotal proteins implicated in Aβ production. Additionally, this miRNA would serve to be a potentially powerful miRNA drug target for future AD therapy.

Our goal was to identify a miRNA that modulates both APP and BACE1 and subsequently reduces levels of soluble amyloid-beta peptide(s). The ability to modify more than one protein involved in the amyloid pathway would make a miRNA a potentially strong candidate for selection for drug trials. Finally, having identified a miRNA which modifies these AD-related proteins/peptides, we were interested in the possible regulation of the genomic region of the miRNA itself.

Based on recent bioinformatics prediction tools, we hypothesized that putative dual target miR-298 would bind the APP mRNA 3'UTR and BACE1 mRNA 3'UTR and reduce levels of both APP and BACE1 proteins as well as soluble Aβ peptides.

Results

MiR-298 is predicted to target both APP- and BACE1 mRNA 3'UTRs.

Using three different bioinformatics tools, we found that miR-298 was predicted to target both the APP mRNA 3'UTR and BACE1 3'UTR (Table 6). Both target sequences on both the UTRs are well conserved across mammalian species (Figure 14) as shown by a high context ++ score percentile score. The highly negative binding ΔΔG score suggests that the binding efficiency between the mature miRNA and the mRNA UTRs is strong as well. There are two predicted miR-298 targets on the APP mRNA 3'UTR - a 7-mer-m8 target sequence from 549-555 nucleotides and a 7-mer-A1 target sequence from 781-787 nucleotides on the APP mRNA 3' UTR (Figure 14). There is one predicted target sequence for miR-298 on the BACE1 mRNA 3'UTR; a 7-mer-A1 site on 4225-4331 nucleotide positions on the 4.4 kb UTR. There are no predicted target sites for miR-298 in either of the coding regions or APP mRNA 5'UTR and BACE1 mRNA 5'UTR.

Name of prediction algorithm	APP score	BACE1 score
TargetScanHuman 7.1	83[a]	79[a]
PicTar	N/A[b]	N/A[b]
DIANA-microT version	0.871[c]	0.644[c]
microRNA.org	0.7359[d]	0.6359[d]
PITA	-14.24[e]	-13.22[e]
rna22	-20.9[f]	-12.1[f]

[a] context ++ score percentile; a quantitative prediction of how highly ranked a particular miRNA is compared to other miRNA predicted to target a sequence
[b] miR-298 is not available in the PicTar algorithm as it is not conserved across various mammalian species
[c] miTG score; Prediction score. Threshold of miRNA discovery was set to 0.2
[d] PhastCon scores; Provides scores based on conservation of the target site using a hidden Markov model
[e] ddg score; based on hybridization energgy and site accessiblity
[f] Folding energy (kcal/mol); with allowance for single G:U bulge

Table 6: MiR-298 is predicted to target both APP 3'UTR and BACE1 3'UTR. Six separate bioinformatics algorithms predict that miR-298 targets the 3'UTR of APP and BACE1. An explanation for each score is also included herein. Crucially, each miRNA predictive tool has its own specific parameters for predicting putative miRNA. Some of these parameters overlap between algorithms and some are unique.

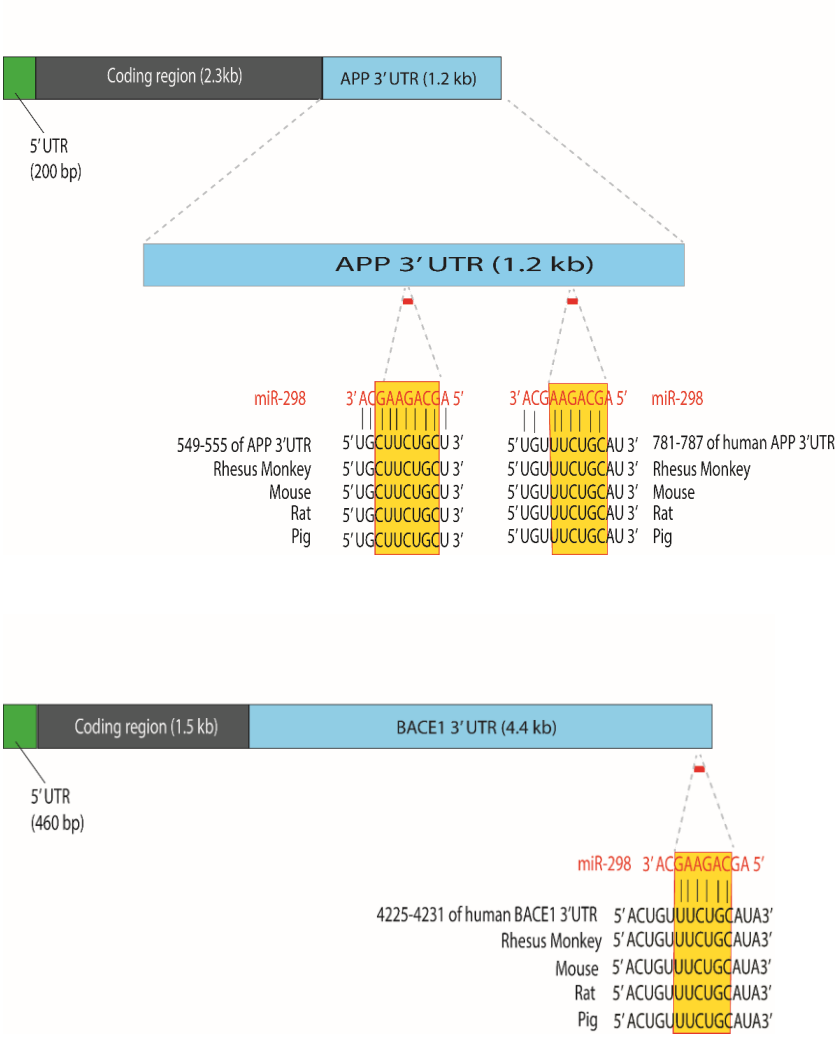

Figure 14: Predicted binding sites for miR-298 on the APP- and BACE1 3'UTRs. MiR-298 is predicted to have two possible binding sites on the APP 3'UTR and one predicted site on the BACE1 3'UTR. Also shown are the short 5' UTRs and coding regions for both APP and BACE1.

MiR-298 targets the APP mRNA 3'UTR

Using the same reporter vector described previously, we tested whether miR-298 targets the APP mRNA 3'UTR. We found that co-transfection of miR-298 along with the dual-luciferase vector reduces luciferase activity by 25% compared to both mock-transfected and a NCM-transfected cells (Figure 15A). MiR-101, a previously validated modulator of APP expression was used as a positive control and reduced luciferase expression by 30% (Figure 15A).

To confirm which of the two target sites was functional, we used site-directed mutagenesis procedure to mutate each site separately. We confirmed the mutagenized site using the specific DNA restriction digestion followed by gel electrophoresis (data not shown). We found that co-transfection of miR-298 with an APP 3'UTR containing the mutagenized site-1 showed a reduction in luciferase activity similar to wild-type APP co-transfected with miR-298 (Figure 15B). On the other hand, co-transfection of miR-298 with the reporter vector containing the mutagenized site-2 showed no difference in luciferase expression (Figure 15C).

Together, these results show that miR-298 targets the APP mRNA 3'UTR at the predicted site-2.

A

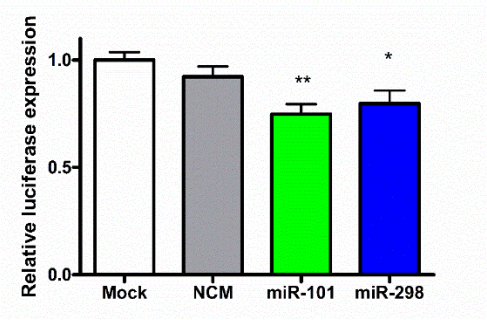

B

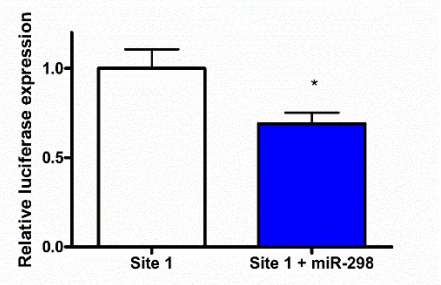

C

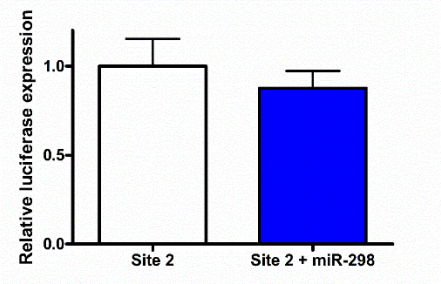

Figure 15: miR-298 targets the APP 3'UTR. Transfection of miR-298 in HeLa cells reduces APP 3'UTR-mediated luciferase expression (A), and mutation of target site-1 does not reverse this effect (B), but mutation of site-2 does (C). The entire seed-site of interaction was mutagenized using the Lightning mutagenesis kit (see Methods) and the seed-site was initially confirmed by separation on a DNA agarose gel. In all three experiments, cells were transfected in a 96-well format for 48 hours and subsequently lysed. The ratio of Renilla to Firefly luciferase was calculated and the values obtained from the mock condition was set at '1'.

MiR-298 targets the BACE1 mRNA 3'UTR

Previously, in our lab, Dr. Justin Long successfully inserted the full-length BACE1mRNA 3'UTR into a dual-luciferase reporter vector [88]. We co-transfected this reporter vector with mature miR-298 to address whether miR-298 targets the BACE1 3'UTR into HeLa cells. We found that miR-298 reduced relative luciferase expression by 30% compared to the reporter alone and a NCM (Figure 16). The slight reduction observed when comparing mock to NCM is non-significant (Figure 16).

We were unsuccessful in mutagenizing the predicted target site for miR-298 on the BACE1 3'UTR (data not shown).

Human miR-298 reduces APP and BACE1 expression, but mouse-miR-298 does not

The sequence of miR-298 itself is not conserved between human and mouse genomes. One of the mismatched nucleotides is within the seed-sequence itself – at the 6th position within the sequence from the 5' end (Fig 17). In order to address whether this lack of conservation would manifest itself in an inability to regulate APP and BACE1 protein expression, we transfected separately the mature human-miR-298 (hsa-miR-298) and mature mouse-miR-298 (mmu-miR-298) into a human glioblastoma cell line that expresses both APP and BACE1.

We found that hsa-miR-298 reduced expression of APP and BACE1 by 40% and 75% respectively, whereas mmu-miR-298 did not reduce levels of either protein (Figure 17). The slight increase observed in mmu-298 expression for both proteins was not statistically significant when compared to mock-transfected cells. BACE1 siRNA was used as a positive control and reduced BACE1 expression by 80% while having no effect

on APP expression compared to mock-transfected cells (Figure 17), as expected. Levels of non-target β-actin served as a loading control and remained consistent across conditions.

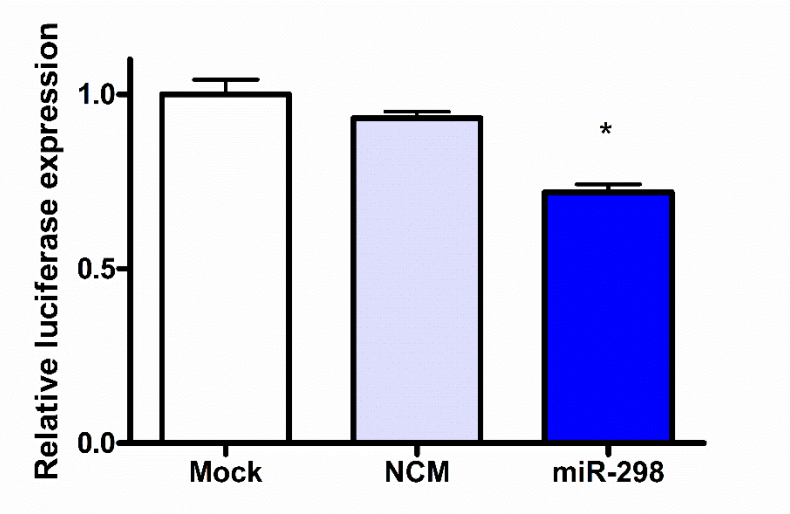

Figure 16: miR-298 targets the BACE1 mRNA 3'UTR. Transfection of miR-298 in HeLa cells reduced BACE1 3'UTR-mediated luciferase expression. Cells were transfected in a 96-well format for 48 hours and subsequently lysed. The ratio of Renilla to Firefly luciferase was calculated and the values obtained from the mock condition was set at '1'. NCM was a negative control miRNA.

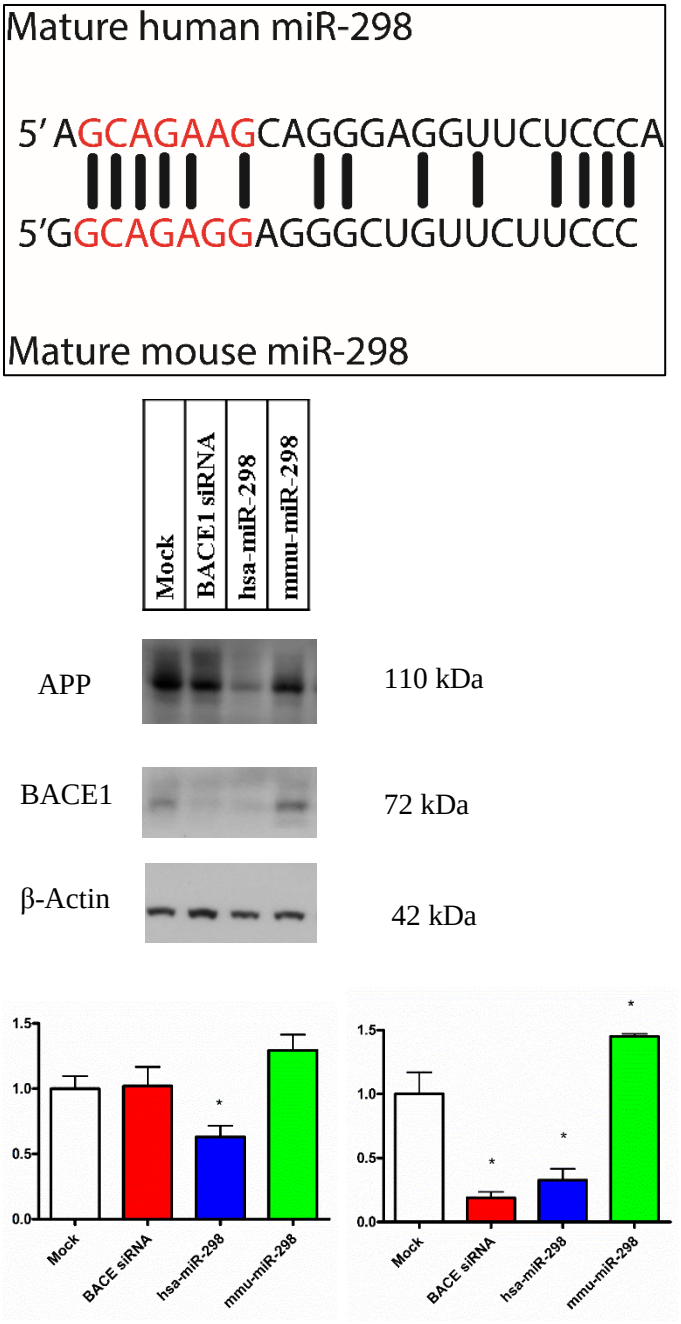

Figure 17: miR-298 is not conserved across human and rodent species. One of the non-conserved sites of the mature miRNA is within the seed sequence (red). Overexpression of mouse-miR-298 does not change levels of APP or BACE1 protein, whereas human-miR-298 reduces expression of both proteins.

MiR-298 reduces APP expression in a mixed primary human cell culture

Using a mixed neuronal primary human cell culture developed in our lab [293], we tested the effect of miR-298 overexpression on levels of endogenous APP. miR-298 overexpression reduced levels of APP by 50% (Figure 18). The co-transfection of an antagomir to miR-298 with miR-298 returned levels of APP to that observed in mock-transfected cells (Figure 14). The transfection of inhibitor or NCM alone did not change expression of APP significantly *vs*. mock-transfected cells. APP siRNA-transfected cells were used as a positive control. APP siRNA reduced APP reduction by 70% compared to mock-transfected cells. Levels of β-actin protein served as a loading control and remained consistent across conditions, as it was not the target of any miRNA or siRNA tested herein (Figure 18).

MiR-298 reduces BACE1 levels in a mixed primary human cell culture

Using the same mixed neuronal primary human cell culture developed in our lab [293], we tested the effect of miR-298 overexpression on levels of endogenous BACE1. We found that miR-298 overexpression reduced levels of BACE1 by 65% (Figure 19). The co-transfection of an antagomir to miR-298 with miR-298 returned levels of APP to that observed in mock-transfected cells (Figure 19). The transfection of inhibitor or NCM alone did not change APP significantly *vs.* mock-transfected cells. BACE1 siRNA-transfected cells were used as a positive control. APP siRNA reduced APP reduction by 50% compared to mock-transfected cells (Figure 19). β-actin served as a loading control and remained consistent across conditions.

A

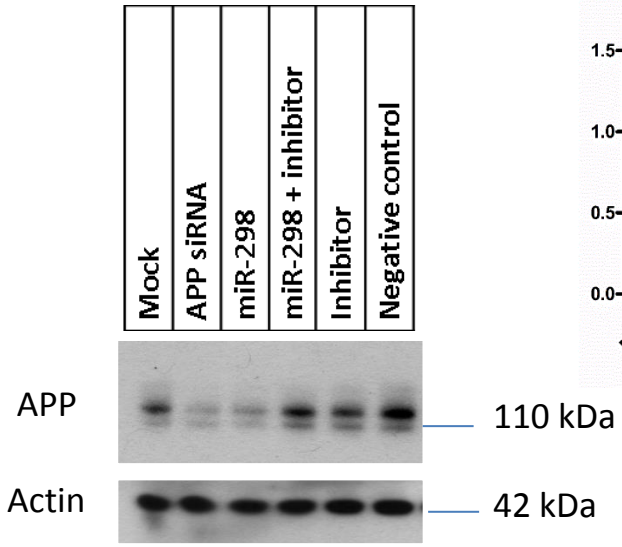

B

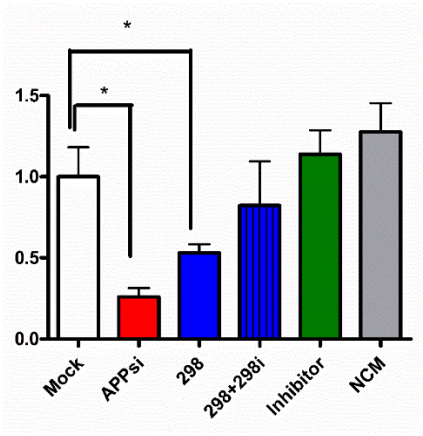

Figure 18: MiR-298 reduces APP in a primary human mixed brain culture.

Transfection of miR-298 reduces APP levels, while the co-transfection of an antagomir to miR-298 reverses miR-298-mediated reduction of APP protein. (n=4, $p<0.05$). Cells were transfected for 72 hours and subsequently lysed using M-Per buffer. Lysates were boiled and separated by SDS-PAGE. Image is a representative set of 4.

MiR-298 reduces levels of soluble Aβ peptides and soluble APP in a mixed primary human cell culture

Using cell-culture supernatants obtained from Figure 14, we tested whether miR-298 could reduce levels of soluble Aβ (1-40) and Aβ (1-42) by sensitive and specfic ELISA. Indeed, miR-298 overexpression reduced levels of Aβ (1-40) by 60% compared to mock-transfected cells, while co-transfection of the inhibitor reversed the miR-298-mediated reduction of Aβ (1-40) (Figure 20A). APP siRNA also reduced Aβ (1-40) while NCM didnot (Figure 20A).

Congruently, miR-298 reduced levels of Aβ (1-42) by 60% compared to mock-transfected cells and the co-transfection of the inhibitor reversed this reduction. APP siRNA reduced levels of Aβ (1-42) by 50%, whereas transfection of the 298 antagomir alone or NCM alone had no effect on Aβ (1-42) levels (Figure 20B).

While we observed a reduction of miR-298 in APP levels obtained from cell lysates, we were interested in whether miR-298 could modulate levels of the truncated soluble APP (sAPP) obtained from cell culture supernatants. We transfected miR-298 and collected cell culture supernatants at 24-hour time intervals upto 4 days. Interestingly, miR-298 reduced levels of sAPP at 48 and 72 hours post-transfection, compared to mock-transfected cells harvested at the same time points (Figure 20D). While time points of 24 and 96 hours showed a slight reduction in sAPP levels, this reduction was not statistically significant in both the cases (Figure 20D).

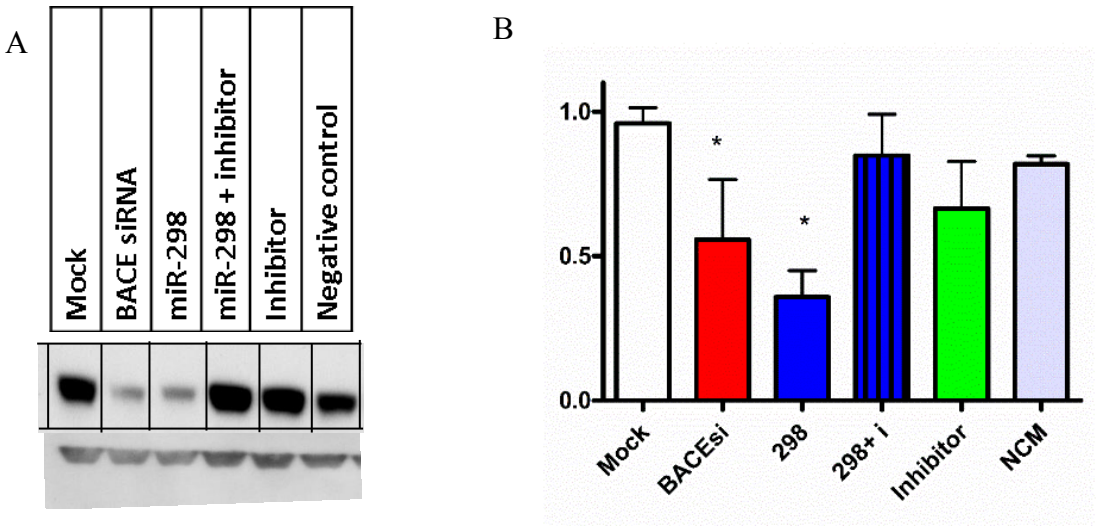

Figure 19: MiR-298 reduces BACE1 in a primary human mixed brain culture.

MiR-298 reduces BACE1 levels , while co-transfection of an antagomir to miR-298 reverses miR-298-mediated reduction of BACE1 protein. ($n=4$, $p<0.05$). Cells were transfected for 72 hours and subsequently lysed using M-Per buffer. Lysates were boiled and separated by SDS-PAGE. Image is a representative set of 4.

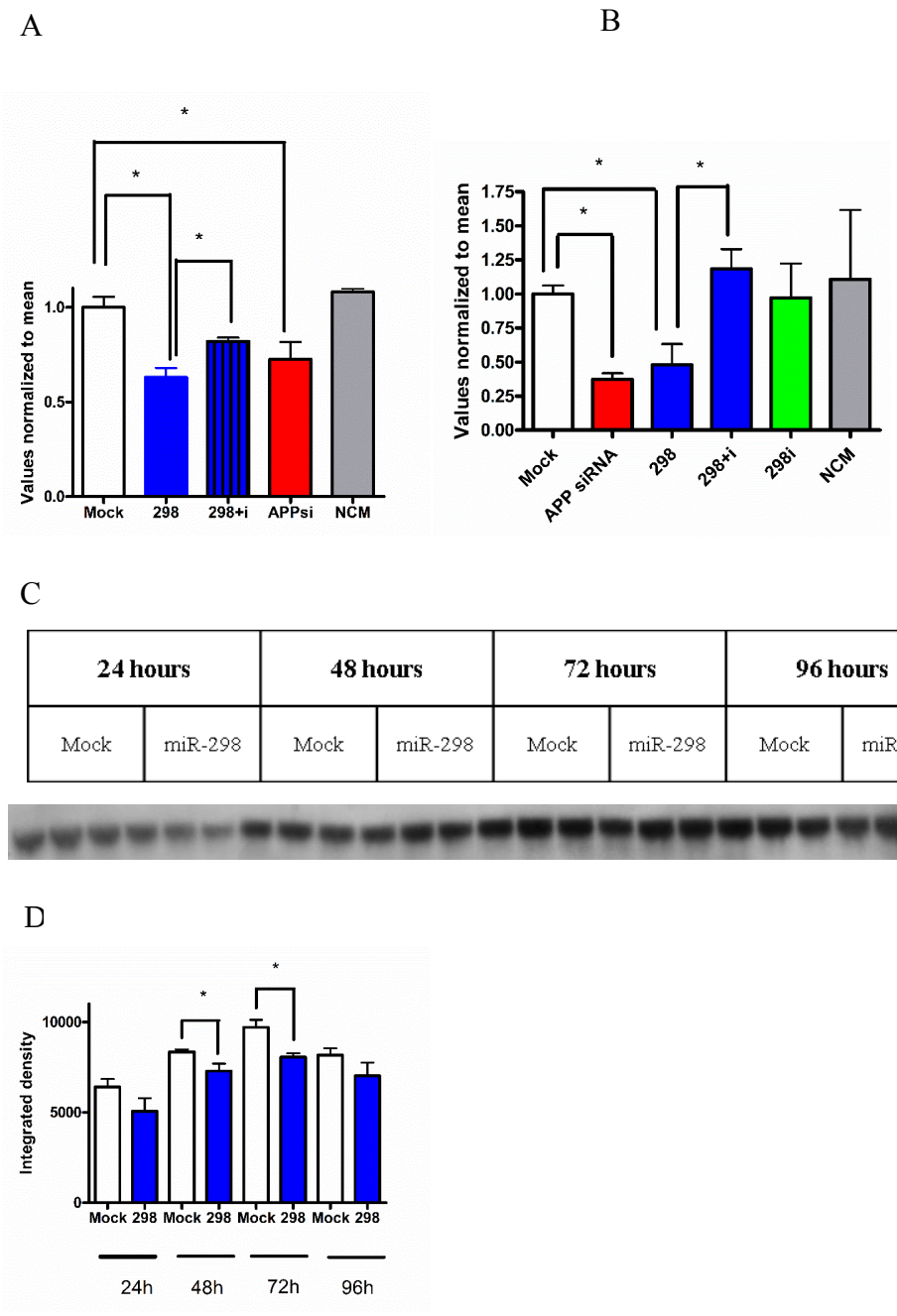

Figure 20: In a primary human mixed brain culture, miR-298 reduces levels of soluble beta-amyloid (1-40) and (1-42). Transfection of miR-298 reduces levels of both Aβ (1-40, A) and Aβ (1-42, B) as measured by sensitive ELISA (IBL). Optical density for both ELISA was compared against a standard curve of known amount of peptide to obtain concentration. Values obtained from mock-transfected cells were normalized as

'1' and used to generate graphs obtained. Congruently, co-transfection of an antagomir to miR-298 reverses miR-298-reduction of both soluble beta-amyloid peptides. ($n=4$, $p<0.05$). Using conditioned media, we also show that miR-298 reduces levels of soluble APP. ($n=3$, $p<0.05$) at 48h and 72 hr significantly. All time points showed a slight reduction, but 24h and 96h did not produce statistically significant effects. For the soluble APP experiment, equal volumes of conditioned media were separated by SDS-PAGE and probed with anti-APP (22C11).

SNPs in the MIR298 gene boundary in a large cohort of human AD patients

Using plasma expression data available from the ADNI cohort, we identified SNPs present within a +/- 5kb boundary of the MIR298 gene. We found 6 families of SNPs in this region (Figure 17). We also found that one of these SNPs rs6070629 was significantly associated with CSF phosphorylated tau, whereas, another SNP rs79259988 was significantly associated with CSF Aβ (1-42) (Figure 21). This is an important finding, which connects our mechanistic and functional work directly to the patients.

MiR-298 reduces expression of specific isoforms of tau

In order to test whether miR-298 may target tau, we further examined the protein cellextracts from two separate experiments conducted in human primary mixed brain culture. Notably, tau protein expression of the 55kDa band was reduced significantly in miR-298-transfected cells compared to mock-transfected cells ($p<0.05$) (Figure 22), whereas NCM-transfected cells showed no reduction in 55 kDa tau protein (Figure 22A,B). We also observed a doublet at 48 kDa, but the expression of this tau isoform was not changed significantly in miR-298 transfected cells (Figure 22A,C).

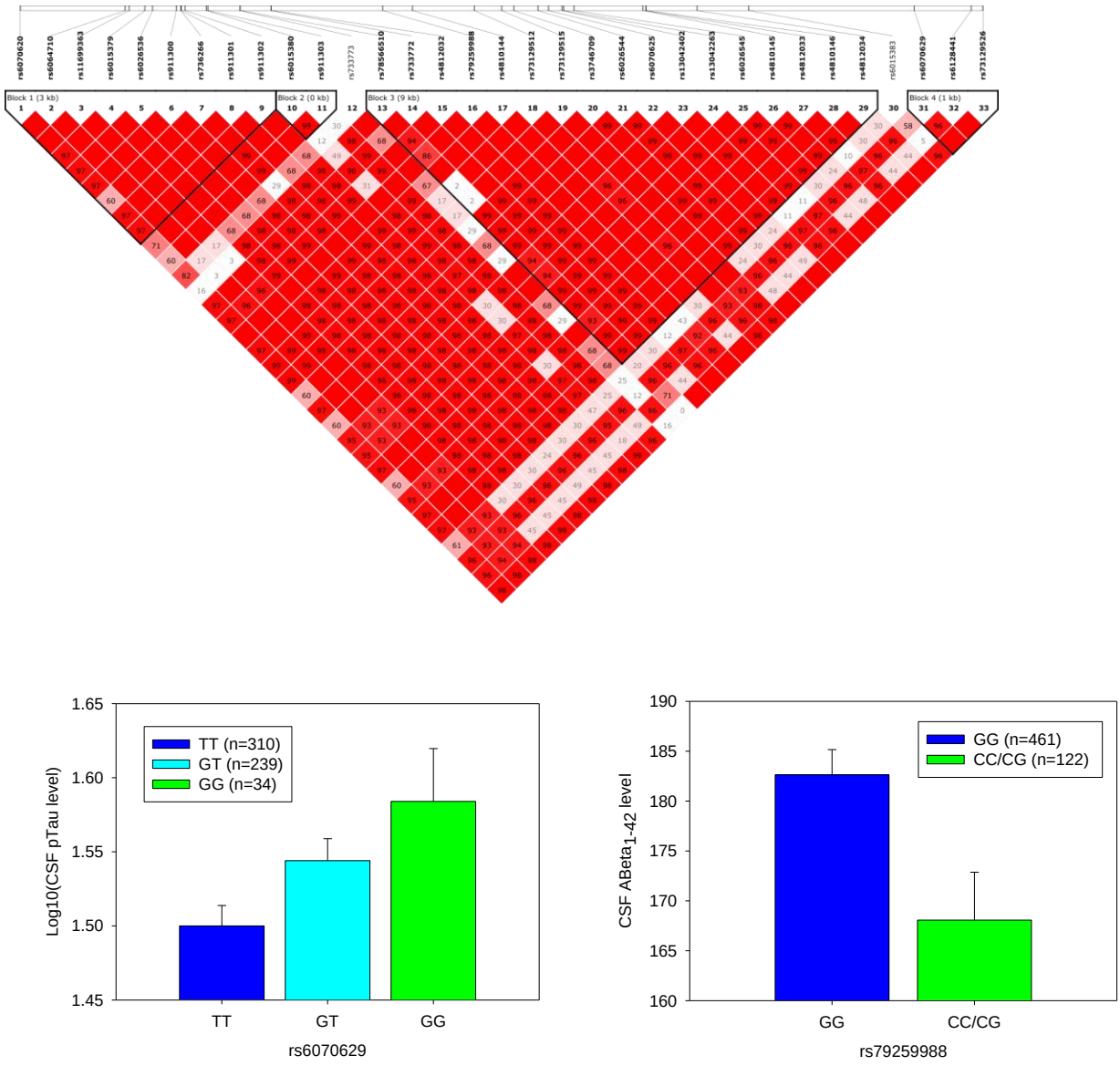

Figure 21: Two SNPs in proximity of MIR298 gene are significant associated with AD CSF biomarkers. Two SNPs in the proximity of the MIR298 gene boundary are significantly associated with CSF p-tau, and CSF beta-amyloid (1-42). This data was generated by Dr. Kwangsik Nho using patient samples available from the ADNI cohort (see methods).

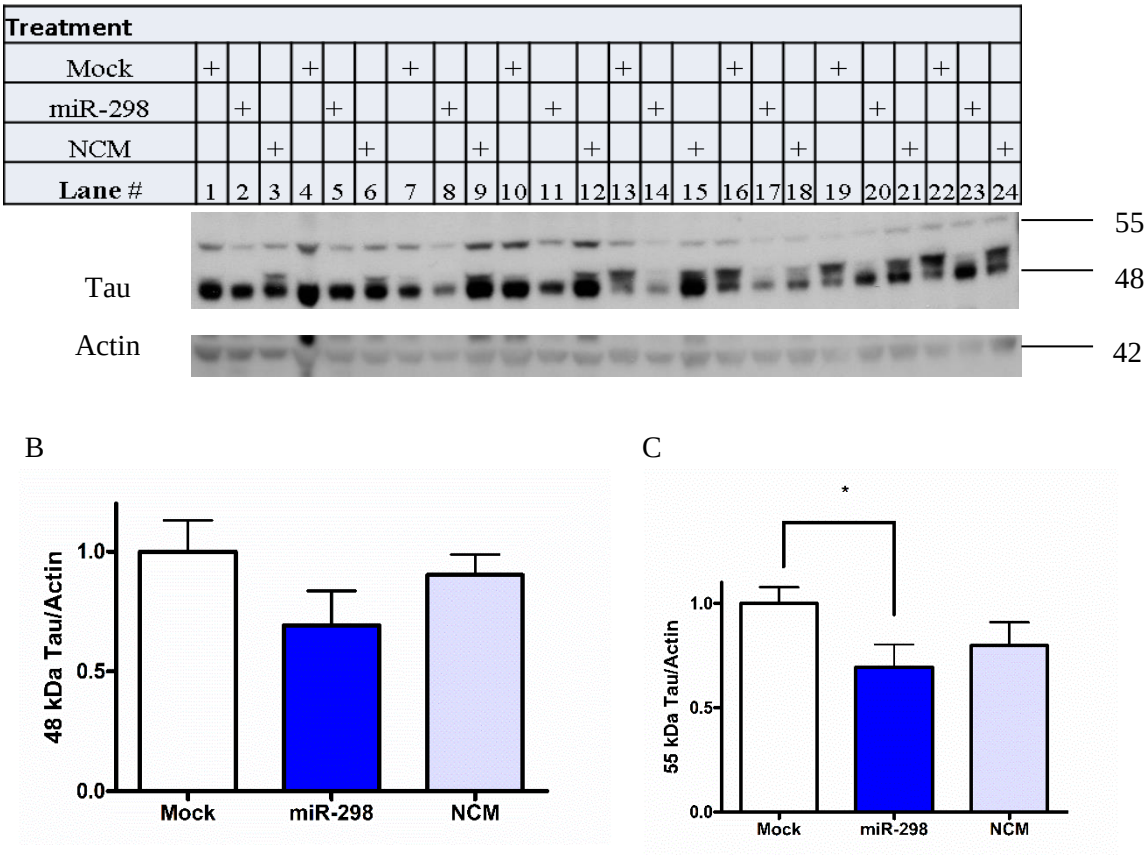

Figure 22: MiR-298 reduces total-tau expression selectively. In a primary human mixed brain culture, transfection of miR-298 significantly reduced levels of the 55 kDa form of total tau, but not the 48 kDa isoform. N=8, $p<0.05$.

Discussion

MiR-298 reduces APP and BACE1 by targeting the 3'UTR mRNA

We identified miR-298 as a negative regulator of APP levels in mammalian, including human cell cultures. Using a luciferase reporter construct containing the full-length APP or BACE1 3'UTR, we showed in separate experiments that co-transfecting miR-298 with the reporter reduced luciferase reporter activity markedly, which suggests that miR-298 targeted both the APP and BACE1 3'UTRs. Multiple bioinformatic tools predicted that miR-298 might have two target sites on the APP 3'UTR and one on the BACE1 3'UTR. We separately mutagenized both sites on the APP 3'UTR, and observed that mutation of the site 2 (781-787) reversed miR-298- mediated reduction of luciferase reporter activity. This result confirmed that miR-298 target the APP 3'UTR at site 2. It is possible that there are other noncanonical sites on the 3'UTR which may contribute synergistically to miR-298 's targeting of the APP 3'UTR. However, this remains conjectural, as we were unable to find predictions of noncanonical sites on the APP3'UTR. We also did not notice predictive algorithms that would suggest miR-298's binding sites on the 5' UTR or the coding sequence of APP. Therefore, we believe that miR-298's function as an APP regulator is a consequence of its action on site-2 of the APP 3'UTR.

While we showed that miR-298 targeted the BACE1 3'UTR, we were unable to successfully mutagenize the single predicted site for miR-298's binding on the BACE1 3'UTR. Therefore, we cannot conclusively state that miR-298's action on BACE1 is mediated via the predicted site. Like APP, we did not find predicted sites for miR-298 on the BACE15'UTR or the coding region. Noncanonical binding of miR-298 on the 3'UTR

was also not predicted. Therefore, we believe that miR-298 regulates BACE1 expression by targeting the 3'UTR, most likely at the predicted site.

We conclusively showed that miR-298 targets APP and BACE1 protein expression in mammalian cultures. First, we showed that miR-298 reduced levels of APP and BACE1 protein in U373 – a commonly used glial cell line. Using our human primary mixed brain culture developed in our lab, we were able to test the effect of miR-298 on endogenous protein expression in primary cultures containing neurons, glia and neuroprogenitors, which, to some extent mimick the brain cellular composition. We showed that miR-298 significantly reduced expression of both proteins in this tissue culture model, which is highly relevant to the CNS context. Given that we showed miR-298's reduction of APP and BACE1 proteins in human glial cells, it is interesting to speculate the reduction we observe in our primary brain culture involves reduction of neuronal APP and BACE1 as well. We were unable to successfully transfect miR-298 into differentiated human NB cells and therefore cannot ascertain the specific ability of miR-298 to regulate neuronal APP. The specific reduction of proteins by miR-298 remains a future experiment that can be performed by improving transfection efficiency in differentiated NB cells, by possibly using lentiviral delivery of miR-298. In summary, miR-298 regulates glial APP and BACE1 expression *and* possibly neuronal APP and BACE1.

We also conclusively showed that overexpression of miR-298 reduced both soluble Aβ (1-40) and Aβ (1-42) peptides. In accordance with the amyloid hypothesis [38,89,309], reduction of these two peptides is relevant to understand neuropathogenesis of AD. It is important to consider testing the reduction of the two peptides by miR-298 o in

relevant in vivo models. This is due to the fact that individual levels of miR-298, APP and BACE1 are important to regulating whether Aβ (1-40) and Aβ (1-42) can be reduced sufficiently. In other words, miR-298 levels have to be high enough to produce a subsequent enough reduction of APP, BACE1, Aβ (1-40) and Aβ (1-42), and which depend on a particular cell type or brain region involved. A future direction of work remains to measure levels of miR-298, APP and BACE1 in different regions of human brain. This would allow us to estimate the ratio of the the miRNA required to produce a subsequent change in protein expression (and by extension, Aβ (1-40) and Aβ (1-42)).

After showing the regulation of APP and BACE1 by miR-298, we investigated the possible regulation of MIR298 gene itself in a large cohort from Alzheimer's patients at different stages. Scanning a region downstream 5kb upstream/downstream of the short ~100 nucleotide region, on chromosome 20, corresponding to the precursor miRNA, we found a linkage disequilibrium (LD) block of SNPs expressed in the ADNI cohort. Interestingly, two of these SNPs significantly associated with two known markers of AD pathology – CSF Aβ (1-42) as well as CSF phosphorylated tau. It is important to note that both SNPs are outside the MIR298 boundary. Therefore, it may be possible that the associations of these SNPs is independent of miR-298's putative role in AD. However, it is also possible that these two SNPs are involved in the regulation of miR-298 expression, and, by extension, the CSF biomarker hallmarks observed in the ADNI cohort, through an yet unknown mechanism.

Another puzzling observation is that while we could explain possibly the MIR298-associated SNP in relation to CSF Aβ (1-42) changes, we could not how miR-298 targeted phospho-tau. Although we did not test phospho-tau directly, we showed that

miR-298 negatively regulated total tau levels. Even though we were able to show miR-298's regulation of tau protein, commonly used bioinformatics algorithms, such as TargetScan, did not predict miR-298 as having a canonical binding site on the tau 3'UTR. We did, however, find a non-canonical site, which predicted that miR-298 targeted the 3' UTR in a manner inclusive of it's first nucleotide as a part of the seed sequence.

As a future direction, we would like to confirm whether the SNPs we identified play a role in the expression of miR-298. One way would be to insert the full length immediate to and including the MIR298 gene into two overexpression vectors – each having one version of the SNP we identified. We would then transfect these vectors and measure miR-298 levels in neuronal cultures. We could also co-transfect each mutated plasmid along with APP 3'UTR to test if the putative difference in miR-298 results in differences in abrogation of miR-298's reduction of APP and BACE1.

We have shown that miR-298 regulates three proteins involved in the pathogenesis of AD: APP, BACE1 and tau. It is important to test these effects by miRNAs translatable into the regulation of AD in humans. It would be interesting to posit miR-298 as an evolutionary tool to repressing the aforementioned proteins for natural selection. A small bit of evidence for this idea is that the sequence of mouse-miR-298 is different from human-miR-298 – one of those differences being within the seed sequence of the miRNA. We were able to show that mmu-miR-298 was incapable of regulating human APP and BACE1, thereby suggesting that the sequence specificity of hsa-miR-298 is required for the regulation of those two proteins. Fascinatingly, using the DBSNP site on pubmed, we observed a SNP within the coding region of the MIR298 gene – specifically located within the region corresponding to the seed sequence. Unfortunately,

the expression of this allele was very low, and we were unable to find out any information about the individuals (s) expressing this SNP. The phenotypic data of individuals expressing this SNP would be an important data to understand the role of miR-298 in AD.

Chapter 7: Specific Aim 3 – To study levels of NEP protein in various cell types and tissues and identify putative miRNA that target its 3'UTR

Rationale

There is data emerging implicating Aβ deposition in early childhood that may later contribute to Alzheimer-like pathogenesis [310,311]. Therefore, it seems Aβ-degradation may be important across a person's life time. In accordance with this, measuring NEP levels from human samples across development and at various ages would help understand the disease progression. To date, while levels of different AD-related protein have been studied in autopsied human brain tissue specimens [142,312-314], the protein levels in human fetal tissues have been unexplored. Moreover, gene expression of NEP in the plasma of AD patients is unknown. Finally, while extensive work has looked at the promoter region and SNPs associated with it [155,156,315,316], identification of possible regulatory regions in the 5' and 3' regions proximal to the NEP gene remains unclear. It is unknown whether the long 3.2 kb of NEP mRNA 3'UTR may have cis- or trans-lements that may target this region and perturb protein expression. Our work herein attempts to address these gaps in the field.

Results

Detection of NEP protein

Using western blotting probing with antibodies raised against various epitopes across the NEP protein (Table 2), we attempted to detect NEP protein in lysates obtained from adult human brain (lane 1) and the positive control of rat kidney (lane 2) (Figure 23). We found that the among seven antibodies tested, we were unable to detect NEP succesfully at the expected molecular weight (Mw) using any of the antibodies. Three of the antibodies (112AP, 131AP and RnD MAB1126) showed immunoreactivity at lower Mws of 60 kDa or 50 kDa (Figure 23) than ~100 kDa. Three antibodies (131AP, 141AP and RnD) showed a distinct NEP band at the expected Mw of ~100 kDa (Figure 23). Based on the appropriate band at the right Mw, as well as the immunoreactivity observed in the adult brain lane, we selected to use the RnD antibody for further examinations.

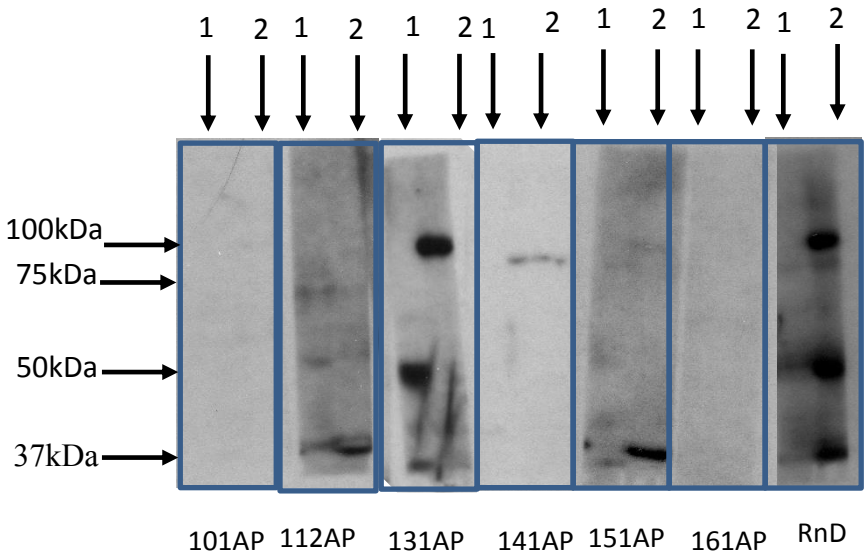

Figure 23: Western blotting to detect NEP in human adult brain. Three antibodies detect NEP at the right Mw in rat kidney samples, but no antibody detects NEP at the right Mw in adult brain. Six different commercially available antibodies were used to detect NEP Three antibodies (131AP, 141AP and RnD) showed a band in the positive control rat kidney (lane 2) sample.

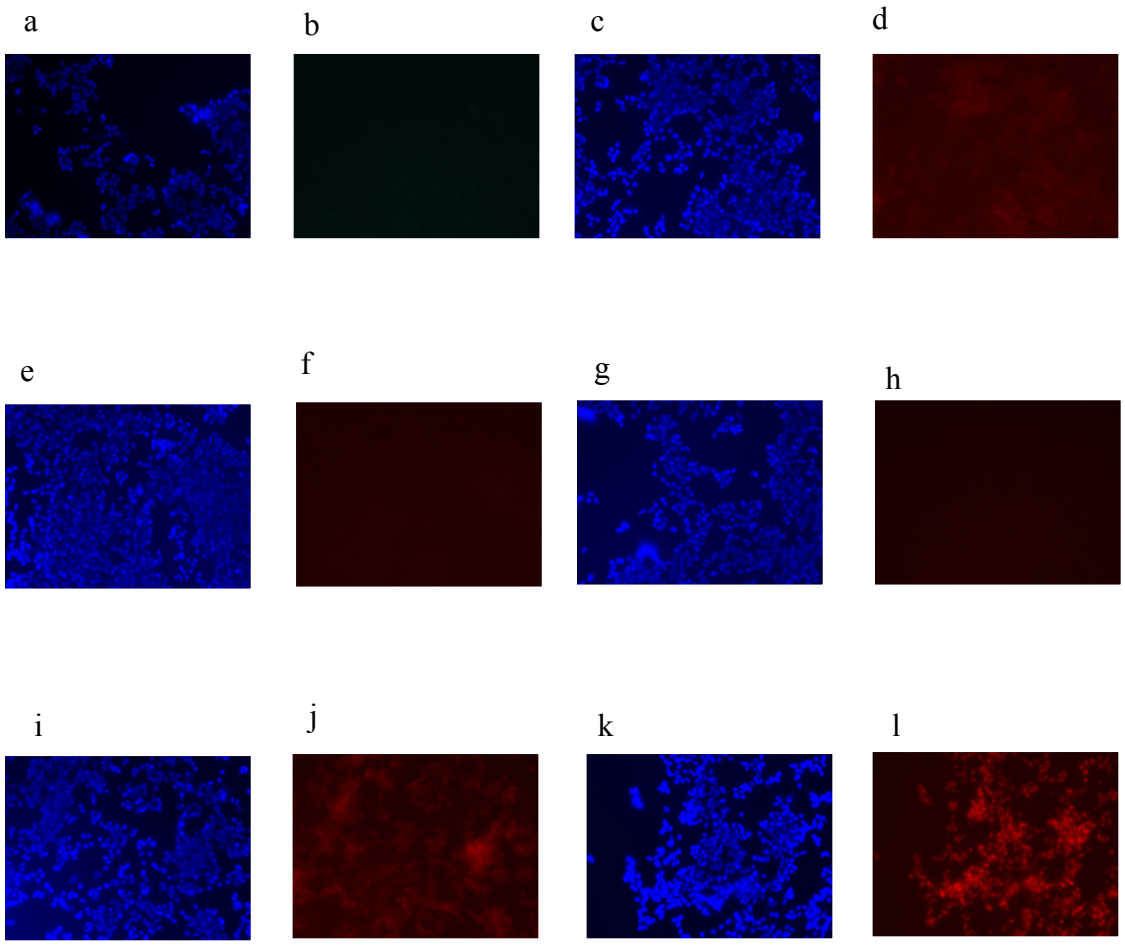

Figure 24: Detection of NEP in differentiated human neuroblastoma cells using various antibodies. Hoechst stain (a,c,e,g,h,j) and NEP immunoreactivity was tested with NEP antibodies 101AP (b),112AP (d), 131AP (f), 141AP (h), 151AP (j), 161AP (l). NEP was successfully detected by ICC using antibodies 161 AP and possibly 151AP.

Detection of NEP in neuronal cells

Using immunocytochemical (ICC) analysis probing with the same antibodies used for western blotting, we tested differentiated human neuroblastoma cells (NB) for NEP expression. Hoechst staining was used to visualize nuclei, whereas cy3-conjugated antibodies were used to visualize NEP protein expression. We observed that antibodies 151AP and 161AP showed the strongest immunoreactivity with NEP protein (Figure 24 j, l). Separately we observed that the secondary antibody (goat anti-rat) alone showed no immunoreactivty, nor did the RnD antibody used earlier (Data not shown).

Cellular detection of NEP protein using western blotting

NEP protein has been very difficult to detect in cell cultulre models. We tested various commonly used human and rodent cell lines to detect NEP. Using the RnD antibody we selected from the results shown in Figure 23, we found that no cell line expresses NEP at the expected molecular weight. We observed distinct bands at ~75 kDa band in NB and HEK-293T cells (Figure 25). We observed a ~50 kDa band across all the cell lines tested, but this was later found to be a secondary-antibody-related band. NEP was detected at the right molecular weight in rat kidney lysate (Figure 25). Both beta-actin and tubulin were used as loading controls.

To address whether the lysis buffer conditions contributed to the difficulty in detecting NEP, we used different lysis buffer formulations to lyse LNCaP cells and prepare cell extracts. We detected a faint NEP band under all 5 different lysis conditions; namely M-Per buffer alone, M-per buffer enriched with protease inhibitor and/or 0.1% SDS, or RIPA buffer (Figure 26). In all formulations, faint NEP immunoreactivity was observed at the expected molecular weight (~100-110 kDa) when 15 ug of protein was

loaded, and no immunoreactivity was observed when 3 ug of protein was loaded. A lower molecular ~75 kDa band was observed in all lanes, including the human neuroblastoma and U373 cell extracts (Figure 26).

Detection of NEP in rodent tissues

Using tissue obtained from adult rats, we tested NEP immunoreactivity in protein extracts from various rodent tissues. NEP protein expression was the highest in rat kidney, intermediate in lung, low in the cortex and undetectable in the hippocampus and liver extracts (Figure 27). Interestingly, we observed an opposite trend when probing with APP and BACE1, that is the tissue extracts such as kidney, which had high levels of NEP, showed limited APP and BACE1 expression (Figure 27). Conversely, tissues such as cortex and hippocampus which showed high APP and BACE1 expression, showed very low NEP expression. β-actin was used as a loading control (Figure 27).

We tested the hypothesis whether an inhibitor to the enzyme was present in cortical and hippocampal CNS-derived samples, which could explain the lack of NEP expression in CNS. For this, we combined cortical and hippocampal samples with kidney and lung samples and subsequently boiled in Laemmli sample buffer and separated by SDS-PAGE. We did not observe quenching of NEP protein expression in lung and kidney samples (Figure 27). However, when combining cortical tissue or kidney tissue with lung tissue, we observed bands of distinct molecular weights. This result indicated that NEP in the kidney is expressed at a slightly higher Mw than NEP in the cortex or lung (Figure 27).

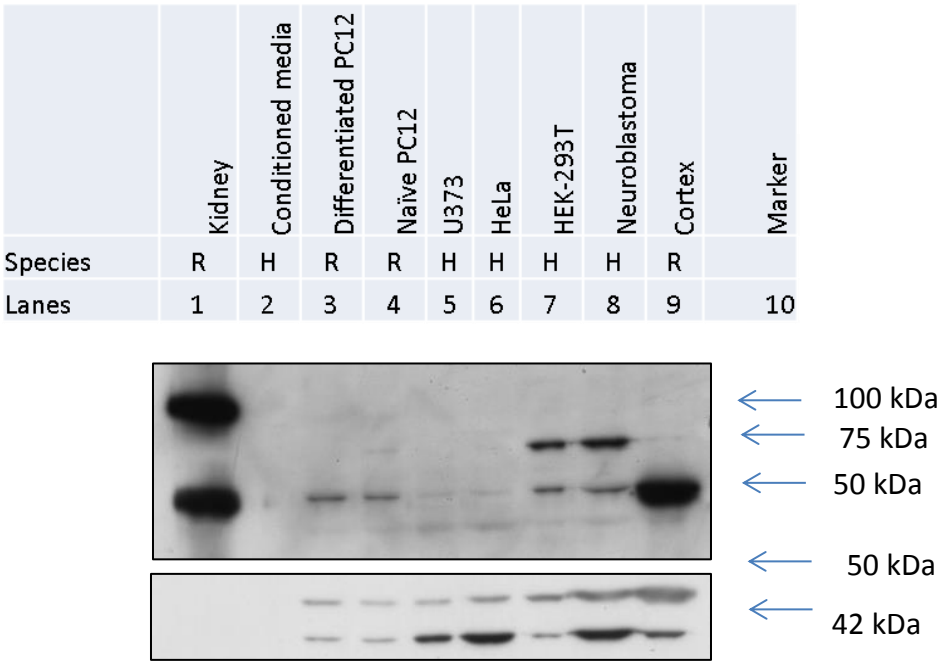

Figure 25: Different cell lines probed with anti-NEP (RnD-monoclonal) antibody). β-actin and α-tubulin serve as loading controls. R:Rat, H:Human. Lysates obtained from different cell lines were boiled and separated using SDS-PAGE and probed with anti-NEP (RnD). As can be seen, while other MW bands appeared, only the positive control (kidney, lane 1) showed a band at the right MW - ~100 kDa.

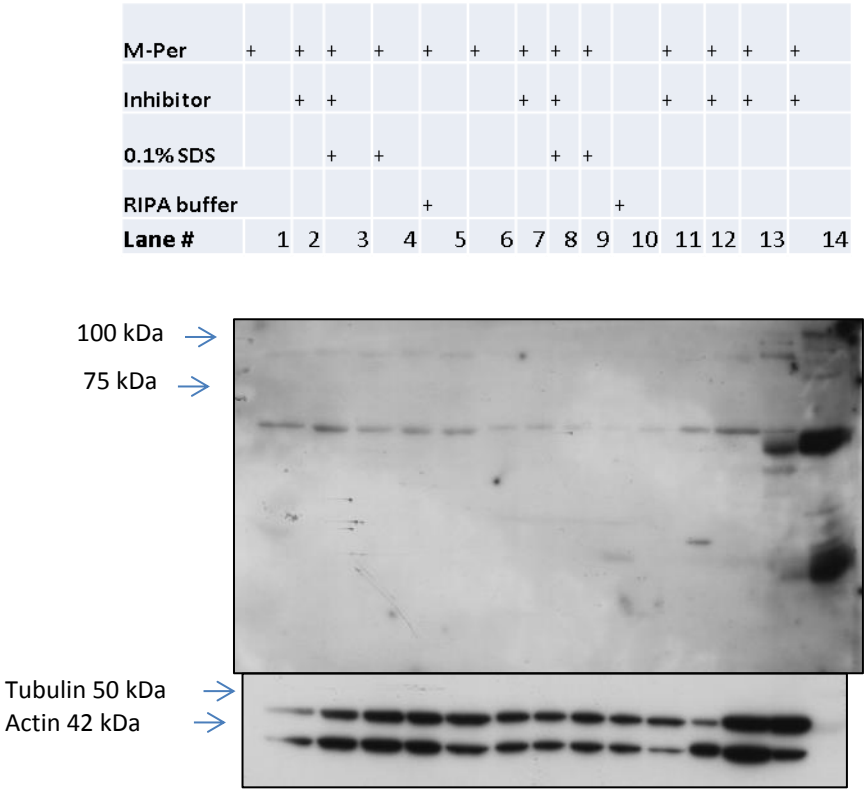

Figure 26: NEP expression using different procedures. Lanes 1-10 were loaded with LNCaP cells. Lanes 1-5 were loaded at 15ug in accordance with different extraction techniques. Lanes 6-10 were loaded with 3ug, in accordance with the appropriate technique. U373, Differentiated NB, rat cortex and rat kidney are the final lanes.

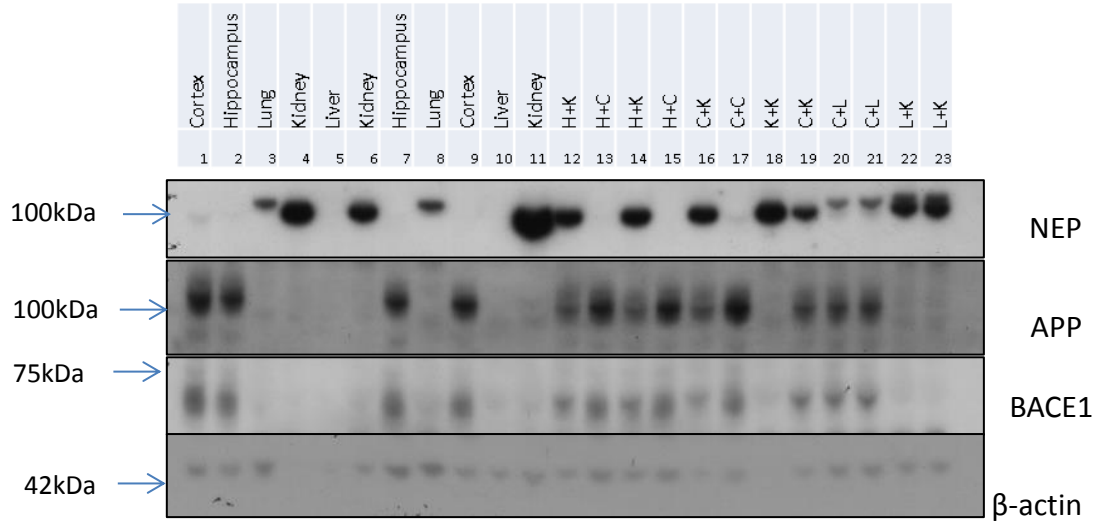

Figure 27: Tissue specific expression of NEP, APP and BACE1. Representative images after probing with antibodies targeting APP, NEP and BACE1. β-actin was used as a loading control. Clear NEP bands were observed with lung and kidney, whereas a faint NEP immunoreactivity was observed with cortex tissue. Combination of tissues confirms that NEP in lung-derived tissue is of a higher MW than that from kidney and cortical tissue.

Differential expression of NEP in fetal tissue and relationship with beta-amyloid

Using cell culture lysates obtained from legally aborted human fetal tissues, we studied the expression of NEP in various fetal organs/tissues using western blotting. NEP protein was highly expressed in the kidney, had intermediate immunoreactivity in heart, lung and thymus tissue, and low expression in adrenal cortex, brain and spleen/pancreas (Figure 28A).

In order to confirm our result further, we also used sensitive sandwich ELISA (RnD) for NEP protein and found that the pattern of expression was consistent with results obtained from western blotting (Figure 28B).

To corroborate results observed with the rodent tissues, we probed the blot sequentially with antibodies targeting APP and BACE1. APP was expressed high in the brain and kidney, intermediate in the heart, lowl in the thymus and lung, but undetectable in the adrenal cortex and spleen/pancreas (Figure 28A). BACE1 was expressed high in the brain, intermediate in the kidney and adrenal cortex, and low to negligible in the other tissues under the conditions employed herein (Figure 28A).

Given the differences in APP, BACE1 and NEP expression, we measured levels of Aβ (1-40) and Aβ (1-42) peptides in the tissue protein extracts. We found the highest levels of Aβ (1-40) in the brain (1808 pg/ug of protein), intermediate levels in the kidney (25.04 pg/ug of protein) and lower levels in other tissues (Figure 28B). Aβ (1-42) was only detectable in the brain (Figure 28B).

Finally, we ran a correlation study between NEP expression and Aβ (1-40) levels as shown by ELISA, and found that while tissues tended to have a direct correaltion

between the two proteins, the brain data did not fit a direct correlation and remained an outlier (Figure 28C).

We performed a NEP enzymatic assay using the same samples used in our western blotting and ELISAs (data not shown). Interestingly, the trend of the enzyme activity was similar to that observed by western blotting and ELISA. Specifically, the fetal kidney and lung extracts showed the highest NEP enzymatic activity among the tissue extrcats tested, with brain showing a lower, but measurable, level of activity. Absolute values were not calculated as the recombinant NEP enzyme did not produce the linearity to satisfy requirements.

A

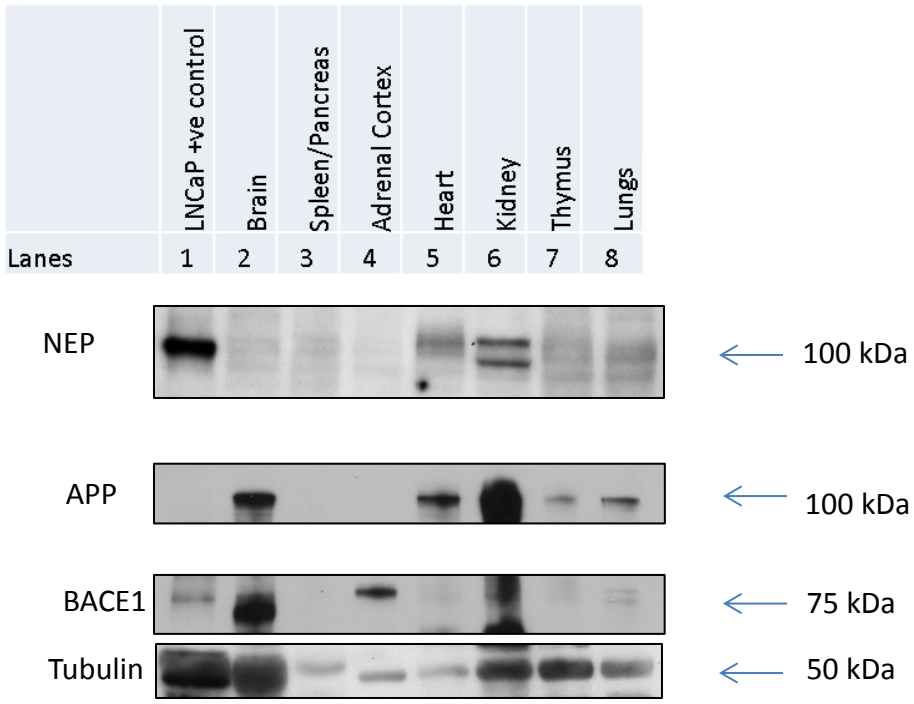

B

	Brain	Spleen/ Pancreas	Adrenal Cortex	Heart	Kidney	Thymus	Lungs
pg of Nep/ug of protein	0.84	1.91	0.16	14.34	3217	21.41	28.65
pg of Aβ40/ug of protein	1808	0.060	0.005	0.131	25.04	0.253	0.082
pg of Aβ42/ug of protein	15.77	ND	ND	ND	ND	ND	ND

C

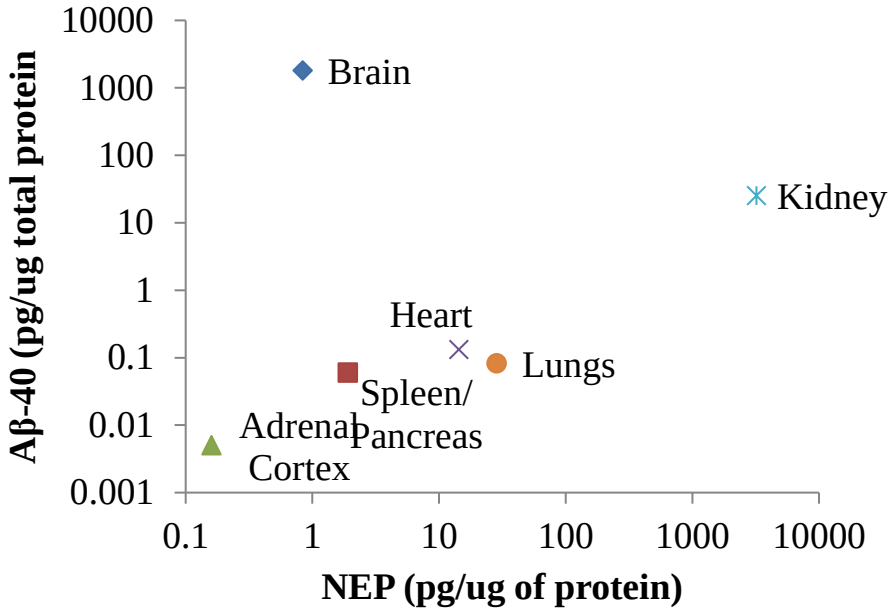

Figure 28: Differential expression of NEP in human fetal tissue. Brain, spleen/pancreas, adrenal cortex, heart, kidney, thymus and lung were loaded along with LNCaP positive control. NEP immunoreactivity was highest in kidney (A). The pattern of tissue-specific expression was confirmed by an ELISA measuring NEP expression (B). Using ELISA, we also measured levels of beta-amyloid in these tissues and found the highest levels of both peptides in fetal brain. We plotted levels of NEP measured as a function of the amount of protein in the assay (C). We found that while all tissues follow a general linear trend, brain-tissue is an outlier.

NEP gene expression is increased in AD patients

Using gene expression data from a large cohort of human patients, which was stratified by disease progression, we measured NEP gene expression. We found that the expression of 2 out of 4 NEP transcripts increased between control and AD samples (Figure 29A, B). There was no difference between the control group against early or late MCI. Expression of other Aβ-degrading enzymes such as IDE and MMPs were also measured, but found to be either unchanged or at levels below threshold of detection for analysis. As a proof of principle, we successfully detected NEP protein in human plasma samples (data not shown).

NEP protein remains unchanged in a small cohort of AD brains

Using a commerically available NEP ELISA kit , we measured levels of NEP in lysates collected from homogenized autopsied brain tissue specimens. These samples were stratified by Braak stages. We found no significant difference in NEP expression across Braak stages (Figure 30). We also did not observe a difference when all AD samples were combined as one group and compared against non-AD , age-matched controls (Figure 30).

A B

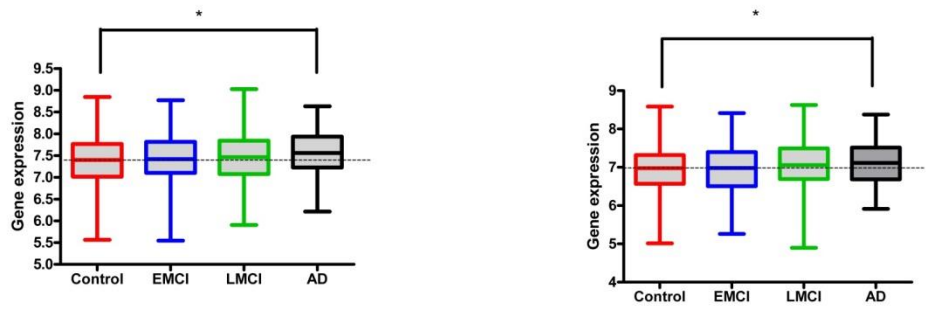

Figure 29: Peripheral gene expression of two transcript variants of MME (A,B) measured by microarray. Dashed line is used to indicate level of the mean of control for each transcript. *p<0.05 . This data was generated by Dr. Kwangsik Nho using samples available from the ADNI cohort. MME AD transcripts are significantly increased compared to the control group. Early MCI (EMCI) and late MCI (LMCI) are not significantly increased.

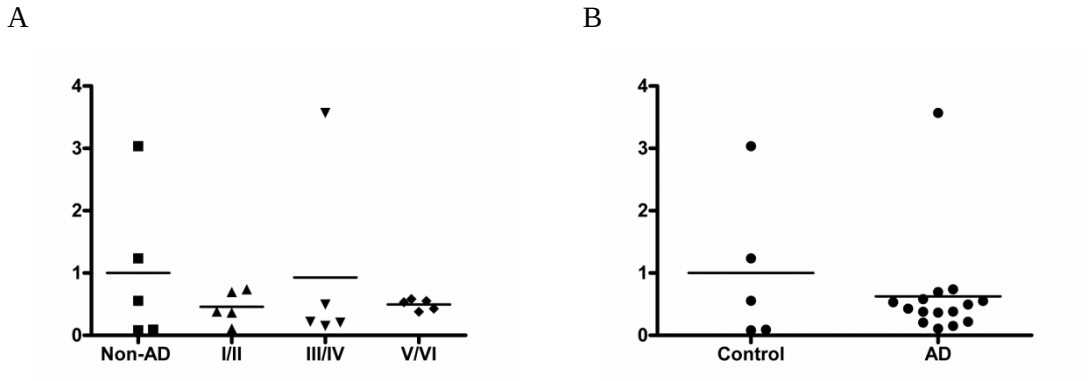

Figure 30: Level of NEP is unchanged in AD vs control brain. Samples were homogenized (see Methods), and sensitive ELISA was performed on these samples. No significant effect was seen either on comparing across Braak stages (A), or combining all AD diagnosis as one group, compared to control (B). Data were plotted by dividing each data point by the mean of the values obtained from the non-AD group.

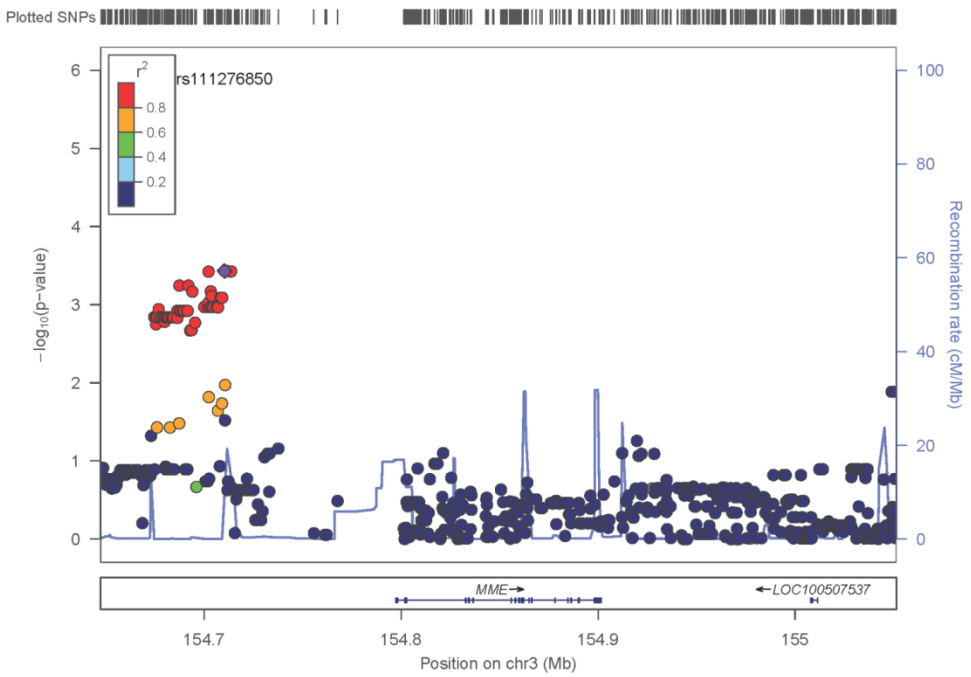

Figure 31: SNPs found in proximity to the NEP gene from a large cohort of AD patients. Using data available from the ADNI cohort, genomic region +/- 5kb of the MME gene was examined for SNPs. This data was generated by Dr. Kwangsik Nho from data available from the ADNI cohort.

Insertion of NEP 3'UTR into a reporter vector changes baseline luciferase activity in different mammalian cell lines

In order to test for the post-transcriptional regulation of NEP 3'UTR, we inserted the full-length NEP 3'UTR into a psiCheck2 reporter dual-luciferase reporter vector. We then transfected either the vector or the vector-containing the full-length 3'UTR into mammalian cell lines, such as Hela and NB cells, and measured their reporter (luciferase) activity in the corresponding cell lysates (Figure 32). An insertion of the NEP 3'UTR produced a 300% increase in reporter activity in HeLa cells ($p<0.05$), a 50% increase in U373 cells ($p<0.05$), a 300% increase in naïve NB cells ($p<0.001$) and finally a 50% increase in differentiated human NB cells ($p<0.001$) (Figure 32).

Various miRNA are predicted to target the NEP 3'UTR

In order to address if the increased NEP expression may be due to positive regulation by a specfic miRNA, we looked for predicted miRNA that may target the NEP 3'UTR. At least six miRNAs, miR-204, miR-211, miR-9, miR-128, miR-181 and miR-216, were predicted to target NEP-3'UTR, by at least 4 different miRNA prediction algorithms (Table 7). We also mapped the predicted binding sites for each miRNA on a NEP 3'UTR drawn to scale. MiR-9 and miR-128 have two possible binding sites on the NEP 3'UTR, whereas the other 4 miRNAs have one predicted site (Figure 33).

MiR-216 reduces NEP 3'UTR activity

In order to test whether the NEP 3'UTR is regulated by any of the predicted miRNA, cells were co-transfected with the luciferase reporter contianing the NEP 3'UTR with one of the abover miRNAs, at a time. We observed no miRNA postively regulating the NEP 3'UTR, and miR-216 reducing luciferase reporter expression of the NEP 3'UTR

by 25% ($p<0.05$) (Figure 34). The other miRNA tested had no effect on NEP 3'UTR-mediated luciferase activity.

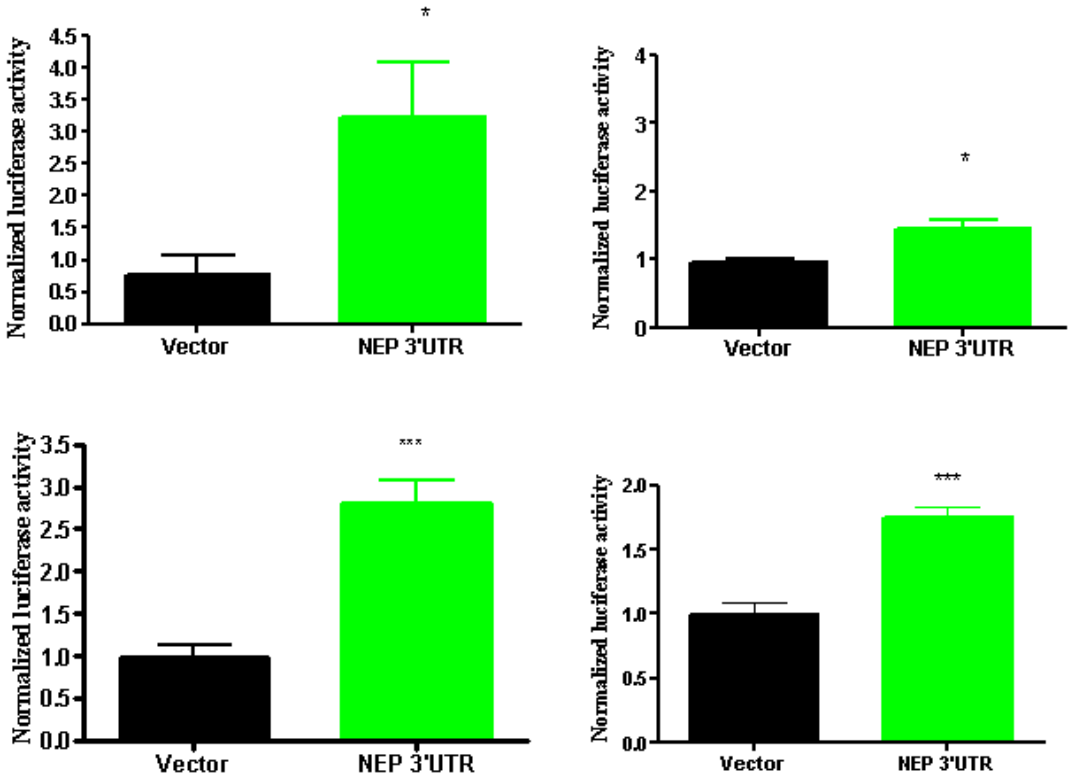

Figure 32: Effect of insertion of NEP 3'UTR on the expression of luciferase activity. The NEP 3'UTR was inserted into a PsiCheck2 vector. The control vector and UTR-containing plasmid were transfected into HeLa (a), U373 (b), SK-N-SH (c) or differentiated SK-N-SH d). Cells were lysed after 48 hours and luciferase activity was assessed. Renilla luciferase activity was normalized to Firefly luciferase activity and the mean of luciferase activity in the vector was set at 1. In glial and neuronal cells, the insertion of NEP 3'UTR significantly increased luciferase expression.

	Name of predictive algorithm							
	Targetscan		**PicTar**	**DIANA**	**PITA**		**miranda**	
	Pct	Seed match	Probability	miTG score	#sites	Score	mirSVR score	PhastCons score
Name of miRNA								
hsa-miR-204	0.16	8mer	NP	NP	5	-3.95	-0.5373	0.5108
hsa-miR-211	0.16	8mer	NP	NP	5	-5.55	-0.5408	0.5108
hsa-miR-9	0.85	7mer	0.88	0.9	7	-11.01	-0.5487	0.5573
hsa-miR-128 (a,b)	<0.1	7mer	0.9	NP	7	-12.98	-0.6741	0.5785
hsa-miR-181 (a-d)	0.34	7mer	NP	0.971	7	-8.29	-0.4782	0.5973
hsa-miR-216	0.21	8mer	NP	NP	5	-9.84	-1.0431	0.6203
NP = not predicted								

Table 7: Identification of putative miRNA targeting the NEP 3'UTR using five different bioinformatics algorithms.

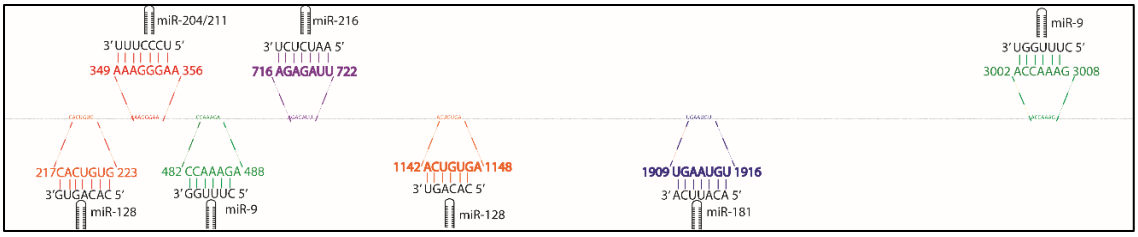

Figure 33: Various miRNA are predicted to target the NEP 3'UTR. Predicted binding sites for these miRNA are shown on a scaled NEP 3'UTR. MiR-9 and miR-128 are predicted to have two putative binding sites on the NEP 3'UTR whereas the other miRNA have a single putative binding site.

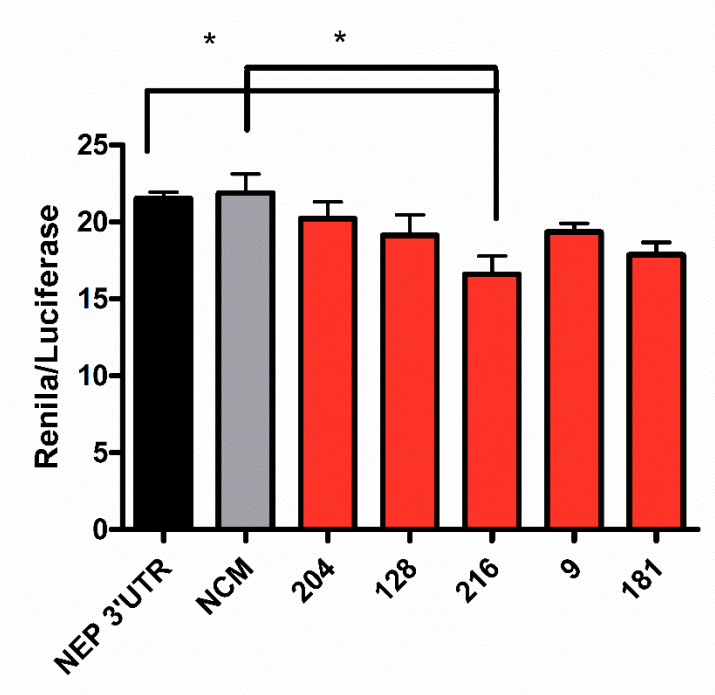

Figure 34: MiR-216 reduces NEP 3'UTR mediated luciferase expression in HeLa. cells. A reporter construct containing the full-length NEP 3'UTR co-transfected with predicted miRNAs. Compared to both negative control miRNAs, miR-216-transfected cells showed a reduction in luciferase activity ($n=5$, $p<0.05$).

Discussion

Understanding the gene and protein expression of NEP in tissues of different origins would help explain why certain tissues are more prone to Aβ insult than others. In accordance with this, we measured the adult rat and fetal human tissue-specific expression of NEP. Moreover, we explored whether NEP gene expression may differ between AD and control subjects and whether the gene may be under post-transcriptional regulation.

We observed differential NEP expression in various rat organs. We also observed NEP immunoreactivity at different molecular weights which could be due to different post-translational modifications and/or different splice variants. It has been previously show type 2b predominates in the kidney, while type 1 predominates in the brain [317]. However, given that the splice variants are independent of the coding region, we believe that our results are a consequence of post-translational modification – specifically glycosylation – of the NEP protein. Interestingly, we observed an inverse correlation between the expression of NEP and the expression of APP and BACE1. It has been previously suggested that the amyloid intracellular domain (AICD) drives the expression of the NEP promoter in a presenilin-dependent manner [318,319]. In other words, there may be a feedback loop involving the secretase enzymes, their products and the expression of NEP. This complicated feedback loop begs the question – which comes first – the increased NEP expression resulting in lower amyloid load, or does the amyloid load initially perturb NEP expression? Future work should address this question of initial causation.

NEP transcript is highly expressed in the fetal lung [320] and showed tissue-dependent transcription across various fetal tissues [315], however, it's protein expression in fetal lung had not been studied. We also observed differential expression of NEP in various human fetal tissues. In both human fetal and rat kidney, NEP is expressed at higher levels than other tissue studied (Figure 5, 6). We also observed strong NEP-immunoreactivity in the thymus, which is consistent with previous work suggesting high abundance of type 1 NEP mRNA in this region [315]. As far as levels of Aβ40 and Aβ42 in these tissues are concerned, while Aβ40 was observed at measurable levels in all tissues tested, Aβ42 levels were detected only in the brain. While the fact that all our data is from one individual is an important caveat, we can make certain interesting observations. First, the agreement between western blot and ELISA is remarkably strong; NEP is expressed high in certain peripheral tissues, such as kidney and lung, and significantly low in the brain. Second, while one might expect NEP and Aβ40 to have an inverse relationship, plotting NEP expression of peripheral tissue against that of Aβ40 measured, suggests a linear relationship between them. This may partly be due to NEP's proclivity to cleave multiple substrates, such as angiotensin, insulin and bradykinin, in peripheral tissues. The outlier to the linear relationship is fetal brain tissue samples. While NEP is measured at a level similar to adrenal cortex, the amount of Aβ40 observed in the brain is over 300,000 times more than that observed in adrenal cortex. This anecdotal observation supports the idea that perhaps Aβ40 clearance in the brain requires the concerted effort of other Aβ-degrading enzymes. A caveat to this claim would be that our results are contingent on an assumption that Aβ clearance mechanisms are the same in both fetal and adult brains, which warrants further research.

Having examined the expression of NEP in adult rodent and human fetal tissues, we examined the expression of NEP in the ADNI cohort and in the brains of a small cohort of post-mortem brains available to us. Previous work has shown that it is possible to measure NEP in the periphery in mice and non-human primates [321,322]; however, we looked at expression in a large cohort of AD patients and healthy controls. NEP was increased in AD patients vs controls. In accordance with the 'peripheral sink hypothesis' [323,324], sequestration of Aβ can help clear Aβ in the brain. Therefore, increased NEP in the periphery would be theoretically beneficial. There are reports that circulating peripheral NEP can reduce plaque burden in the brain [279,325], however, there are also conflicting reports regarding the ability of peripheral NEP to clear brain Aβ [321,322]. Therefore, while the importance of peripheral NEP expression to Aβ clearance remains controversial, we are the first to report the increased NEP expression in the plasma. It is important to note that while the effect size is not large, the result is not simply a statistical phenomenon – as other proteins involved in AD (such as APP and BACE1) did not show a change. Moreover, another Aβ-degrading enzyme, ECE1, did show an increase in AD v healthy controls (HC). This result warrants further exploration to understand the importance of the sink hypothesis to AD.

We also identified various SNPs spanning the MME gene as well as the 3' and 5' region proximal to it. Previous work has shown that rs3736187 – a SNP located on the NEP gene is associated with a decreased risk for AD[326]. In our own ADNI cohort, one SNP (rs111276850) showed a significant association with CSF Aβ (1-42) and total-tau. Given that this SNP is located at the 5' end of the gene, this SNP may act as a cis-acting regulatory element influencing NEP expression. Alternatively, it may encode a trans-

element acting on a different gene. Either way, this novel region warrants further examination.

We did not observe a change in NEP protein expression across a brain cohort stratified by Braak stage. Given the small sample size per group as well as the heterogeneity among samples, this result is not altogether surprising. We observed a marked heterogeneity in NEP levels in the control group. Given that these control subjects were age-matched to AD patients, it is interesting to speculate the reasons for this observation. Perhaps the perturbations in NEP expression reflect a dynamic turnover of the protein that is impaired in AD patients – in support of this, levels of NEP protein (except for one outlier) are very similar in AD brains. Speculatively, perhaps a dynamic turnover of NEP protein is required to prevent the onset of AD.

Along with drug therapies targeting NEP [327-331], our group (and others) has conclusively shown that it is possible to modulate the expression of proteins involved in AD by identifying specific miRNA [88,233,236]. MiRNA are short, non-coding RNA species that target the 3'UTR of associated RNA. In accordance with this, we tested whether the NEP 3'UTR was under post-transcriptional regulation by endogenous factors in various cell types. We found that induction of the NEP 3'UTR resulted in increased reporter luciferase expression in different cell lines. While other candidates, such as long non-coding RNA cannot be ruled out, it is possible that miRNA are responsible for this positive regulation of the NEP 3'UTR. Using prediction algorithms, we have identified five such potential candidates in Table 1. We identified miR-216 as a putative regulator of NEP protein.

MiR-216 has been implicated in other non-NEP modulating functions. It has been shown that miR-216 levels are modulated in a transgenic mouse models of pancreatic adenocarcinoma [332], and the knockout of a ~30 kb region on chromosome 11, which includes the MIR216 gene is embryonically lethal [332]. Additionally, the 3'UTR of GABA receptor type A was shown to have a putative target site for miR-216 [333], although the effect of miR-216 on GABA-A expression was not studied.

Another limitation is that our protein data from fetal tissue and post-mortem brain is contingent on the immunoreactivity of the NEP ELISA. Finally, we did not measure mRNA levels of NEP in the post-mortem brain to corroborate our protein data.

NEP is a protein that has been implicated in Alzheimer's disease [159,312,314,334]. Therefore, measuring NEP expression and activity in fetal and adult brain tissues as well as other periphery and CNS tissues would help in unveiling the biochemical mechanism of amyloidosis and in turn Aβ-mediated neurodegeneration seen in AD subjects.

Chapter 8: Overall discussion and future directions

We have identified structurally and characterized functionally several specific miRNA species that can modulate key proteins involved in the pathogenesis of AD. Therefore, it is important to discuss the translatability of the work, and future potential for miRNA therapy.

The first hurdle in miRNA therapy is the fact that naked RNA is rapidly degraded by ribonucleases [335]. To improve the stability of RNA moities, technologies such as 2'O-methyl RNA (2'-O-Me) [336] and locked nucleic acid (LNA) [337] were developed. While these moities improve the stability of the RNA strands, they do not facilitate delivery across the BBB [337]. By sheating the miRNA in lipid and cationic complexes, miRNA and siRNA have been successfully transported across the BBB.

Lipid-based reagents, such as lipofectamine, are successfully utilized to deliver miRNA across the cell membrane in various cell culture models, as we have shown it. However, this methodology may not be suitable for working with biologic fluids due to high salt concentration and other considerations [337]. Another difficulty is that lipid-based complexes can produce an unwanted immune response, often due to the nonspecific activation of inflammatory cytokines [338,339]. In order to circumvent these problems, neutral lipid emulsion (NLE) – cholesterol mediated cationic solid nanoparticles formulated with esterquat and stearylamine – was developed . This formulation has been shown to facilitate small molecule delivery across the BBB[340]. Alternatively, RNA complexed to a short peptide obtained from the rabies virus can be delivered into neuronal cells, by specific binding to acetylcholine receptors. This method has been shown to be capable of reducing mouse prion protein in vivo[341] .

Polyethylenimine (PEI)-based RNA delivery utilizes cationic complexes, which retain a positive charge. This positive charge provides a binding motif for the negative charge on unknown cell surface protein [342,343]. This binding, in turn, facilitates complexes to presumably undergo endocytosis and deliver RNA. As a proof of concept, PEI-conjucated-miR-124a was injected into the tail vein of mice, which was shown to increase miR-124a levels in the brain [344]. As a caveat, mannitol was used to help increase permeability of the BBB.

Other delivery systems such as exosomes, which can easily cross the BBB without eliciting a toxic immunse response [11,345,346], dendrimer-based delivery [347,348], chitosan [338,349,350] and degradable polymer-coated gold nanoparticles [351] are currently being developed for better delivery of RNA across the BBB.

Limited work has shown the viability of deliverying RNA via the intranasal route. Work in mice was successfully shown to deliver TNF-α siRNA into rodent miRNA using a nanoemulsion technique. Another method to deliver RNA would be to interfere with the BBB using compounds such as mannitol [344,352] or noninvasive ultrasound technology [353]. Injecting miRNA directly into the brain is problematic due to ethical considerations as well as the surgical difficulties associated with it. However, work has been done in mice to successfully show this as a methodology to deliver RNA into the brain ([354] and others). MiR-133 was delivered directly into the brain by injection, thereby circumventing issues such as BBB and brain region specificity [355].

In summary, we continue to discover highly specfic miRNA targeting specfic proteins or pathways involved in neurodegeneration and AD, and also to devise ways to overcoming various problems associated with miRNA delivery into the brain. Therefore,

while the delivery of miR-20b into the brain to reduce levels of APP faces many non-trivial methodological challenges, the field is advancing rapidly, and a complete characterization of novel miRNAs, such as miR-20b, would facilitate a ready “pool” of miRNA that can be used to address AD pathology leading to a successful drug discovery.

REFERENCES

1 Brookmeyer, R. *et al.* National estimates of the prevalence of Alzheimer's disease in the United States. *Alzheimer's & dementia : the journal of the Alzheimer's Association* **7**, 61-73, doi:10.1016/j.jalz.2010.11.007 (2011).

2 Tejada-Vera, B. Mortality from Alzheimer's disease in the United States: data for 2000 and 2010. *NCHS Data Brief*, 1-8 (2013).

3 Dorsey, E. R., George, B. P., Leff, B. & Willis, A. W. The coming crisis: obtaining care for the growing burden of neurodegenerative conditions. *Neurology* **80**, 1989-1996, doi:10.1212/WNL.0b013e318293e2ce (2013).

4 Steffens, D. C., Fisher, G. G., Langa, K. M., Potter, G. G. & Plassman, B. L. Prevalence of depression among older Americans: the Aging, Demographics and Memory Study. *Int Psychogeriatr* **21**, 879-888, doi:10.1017/S1041610209990044 (2009).

5 Ownby, R. L., Crocco, E., Acevedo, A., John, V. & Loewenstein, D. Depression and risk for Alzheimer disease: systematic review, meta-analysis, and metaregression analysis. *Archives of general psychiatry* **63**, 530-538, doi:10.1001/archpsyc.63.5.530 (2006).

6 Zilkens, R. R., Bruce, D. G., Duke, J., Spilsbury, K. & Semmens, J. B. Severe psychiatric disorders in mid-life and risk of dementia in late- life (age 65-84 years): a population based case-control study. *Current Alzheimer research* **11**, 681-693 (2014).

7 Nicolas, G. *et al.* Dementia in middle-aged patients with schizophrenia. *Journal of Alzheimer's disease : JAD* **39**, 809-822, doi:10.3233/JAD-131688 (2014).

8 Peter-Derex, L., Yammine, P., Bastuji, H. & Croisile, B. Sleep and Alzheimer's disease. *Sleep Med Rev* **19**, 29-38, doi:10.1016/j.smrv.2014.03.007 (2015).

9 Serafini, G. *et al.* Suicide Risk in Alzheimer's Disease: A Systematic Review. *Current Alzheimer research* (2016).

10 Fiest, K. M. *et al.* The Prevalence and Incidence of Dementia: a Systematic Review and Meta-analysis. *Can J Neurol Sci* **43 Suppl 1**, S3-S50, doi:10.1017/cjn.2016.18 (2016).

11 Alvarez-Erviti, L. *et al.* Delivery of siRNA to the mouse brain by systemic injection of targeted exosomes. *Nature biotechnology* **29**, 341-345, doi:10.1038/nbt.1807 (2011).

12 Zhao, Q., Zhou, B., Ding, D., Guo, Q. & Hong, Z. Prevalence, mortality, and predictive factors on survival of dementia in Shanghai, China. *Alzheimer Dis Assoc Disord* **24**, 151-158, doi:10.1097/WAD.0b013e3181ca0929 (2010).

13 Wada-Isoe, K. *et al.* Prevalence of dementia in the rural island town of Ama-cho, Japan. *Neuroepidemiology* **32**, 101-106, doi:10.1159/000177035 (2009).

14 de Silva, H. A., Gunatilake, S. B. & Smith, A. D. Prevalence of dementia in a semi-urban population in Sri Lanka: report from a regional survey. *Int J Geriatr Psychiatry* **18**, 711-715, doi:10.1002/gps.909 (2003).

15 Hendrie, H. C. *et al.* Incidence of dementia and Alzheimer disease in 2 communities: Yoruba residing in Ibadan, Nigeria, and African Americans residing in Indianapolis, Indiana. *JAMA* **285**, 739-747 (2001).

16 Graves, A. B. *et al.* Prevalence of dementia and its subtypes in the Japanese American population of King County, Washington state. The Kame Project. *Am J Epidemiol* **144**, 760-771 (1996).
17 Russ, T. C., Batty, G. D., Hearnshaw, G. F., Fenton, C. & Starr, J. M. Geographical variation in dementia: systematic review with meta-analysis. *Int J Epidemiol* **41**, 1012-1032, doi:10.1093/ije/dys103 (2012).
18 Alzheimer, A., Stelzmann, R. A., Schnitzlein, H. N. & Murtagh, F. R. An English translation of Alzheimer's 1907 paper, "Uber eine eigenartige Erkankung der Hirnrinde". *Clinical anatomy* **8**, 429-431, doi:10.1002/ca.980080612 (1995).
19 Braak, H. & Braak, E. Evolution of the neuropathology of Alzheimer's disease. *Acta Neurol Scand Suppl* **165**, 3-12 (1996).
20 Raskin, J., Cummings, J., Hardy, J., Schuh, K. & Dean, R. A. Neurobiology of Alzheimer's Disease: Integrated Molecular, Physiological, Anatomical, Biomarker, and Cognitive Dimensions. *Current Alzheimer research* **12**, 712-722 (2015).
21 Cacace, R., Sleegers, K. & Van Broeckhoven, C. Molecular genetics of early-onset Alzheimer's disease revisited. *Alzheimer's & dementia : the journal of the Alzheimer's Association* **12**, 733-748, doi:10.1016/j.jalz.2016.01.012 (2016).
22 Glenner, G. G. & Wong, C. W. Alzheimer's disease: initial report of the purification and characterization of a novel cerebrovascular amyloid protein. *Biochemical and biophysical research communications* **120**, 885-890 (1984).
23 Cruts, M. *et al.* Genetic and physical characterization of the early-onset Alzheimer's disease AD3 locus on chromosome 14q24.3. *Human molecular genetics* **4**, 1355-1364 (1995).
24 Sherrington, R. *et al.* Cloning of a gene bearing missense mutations in early-onset familial Alzheimer's disease. *Nature* **375**, 754-760, doi:10.1038/375754a0 (1995).
25 Levy-Lahad, E. *et al.* Candidate gene for the chromosome 1 familial Alzheimer's disease locus. *Science* **269**, 973-977 (1995).
26 Goate, A. *et al.* Segregation of a missense mutation in the amyloid precursor protein gene with familial Alzheimer's disease. *Nature* **349**, 704-706, doi:10.1038/349704a0 (1991).
27 Rogaev, E. I. *et al.* Familial Alzheimer's disease in kindreds with missense mutations in a gene on chromosome 1 related to the Alzheimer's disease type 3 gene. *Nature* **376**, 775-778, doi:10.1038/376775a0 (1995).
28 Saunders, A. M. *et al.* Association of apolipoprotein E allele epsilon 4 with late-onset familial and sporadic Alzheimer's disease. *Neurology* **43**, 1467-1472 (1993).
29 Paloneva, J. *et al.* Mutations in two genes encoding different subunits of a receptor signaling complex result in an identical disease phenotype. *Am J Hum Genet* **71**, 656-662, doi:10.1086/342259 (2002).
30 Guerreiro, R. *et al.* TREM2 variants in Alzheimer's disease. *The New England journal of medicine* **368**, 117-127, doi:10.1056/NEJMoa1211851 (2013).
31 Guerreiro, R., Bras, J. & Hardy, J. SnapShot: genetics of Alzheimer's disease. *Cell* **155**, 968-968 e961, doi:10.1016/j.cell.2013.10.037 (2013).
32 Naj, A. C. *et al.* Common variants at MS4A4/MS4A6E, CD2AP, CD33 and EPHA1 are associated with late-onset Alzheimer's disease. *Nature genetics* **43**, 436-441, doi:10.1038/ng.801 (2011).

33 Harold, D. *et al.* Genome-wide association study identifies variants at CLU and PICALM associated with Alzheimer's disease. *Nature genetics* **41**, 1088-1093, doi:10.1038/ng.440 (2009).
34 Logue, M. W. *et al.* A comprehensive genetic association study of Alzheimer disease in African Americans. *Arch Neurol* **68**, 1569-1579, doi:10.1001/archneurol.2011.646 (2011).
35 Lambert, J. C. *et al.* Meta-analysis of 74,046 individuals identifies 11 new susceptibility loci for Alzheimer's disease. *Nature genetics* **45**, 1452-1458, doi:10.1038/ng.2802 (2013).
36 Shaw, L. M. *et al.* Cerebrospinal fluid biomarker signature in Alzheimer's disease neuroimaging initiative subjects. *Annals of neurology* **65**, 403-413, doi:10.1002/ana.21610 (2009).
37 Hua, X. *et al.* Tensor-based morphometry as a neuroimaging biomarker for Alzheimer's disease: an MRI study of 676 AD, MCI, and normal subjects. *Neuroimage* **43**, 458-469, doi:10.1016/j.neuroimage.2008.07.013 (2008).
38 Hardy, J. A. & Higgins, G. A. Alzheimer's disease: the amyloid cascade hypothesis. *Science* **256**, 184-185 (1992).
39 Mullan, M. *et al.* A pathogenic mutation for probable Alzheimer's disease in the APP gene at the N-terminus of beta-amyloid. *Nature genetics* **1**, 345-347, doi:10.1038/ng0892-345 (1992).
40 Chartier-Harlin, M. C. *et al.* Early-onset Alzheimer's disease caused by mutations at codon 717 of the beta-amyloid precursor protein gene. *Nature* **353**, 844-846, doi:10.1038/353844a0 (1991).
41 Levy, E. *et al.* Mutation of the Alzheimer's disease amyloid gene in hereditary cerebral hemorrhage, Dutch type. *Science* **248**, 1124-1126 (1990).
42 Van Broeckhoven, C. *et al.* Amyloid beta protein precursor gene and hereditary cerebral hemorrhage with amyloidosis (Dutch). *Science* **248**, 1120-1122 (1990).
43 Tanzi, R. E. *et al.* Genetic linkage map of human chromosome 21. *Genomics* **3**, 129-136 (1988).
44 Sandbrink, R., Masters, C. L. & Beyreuther, K. APP gene family. Alternative splicing generates functionally related isoforms. *Ann N Y Acad Sci* **777**, 281-287 (1996).
45 Tang, K. *et al.* Identification of a novel alternative splicing isoform of human amyloid precursor protein gene, APP639. *The European journal of neuroscience* **18**, 102-108 (2003).
46 Sisodia, S. S., Koo, E. H., Hoffman, P. N., Perry, G. & Price, D. L. Identification and transport of full-length amyloid precursor proteins in rat peripheral nervous system. *The Journal of neuroscience : the official journal of the Society for Neuroscience* **13**, 3136-3142 (1993).
47 Siman, R., Card, J. P., Nelson, R. B. & Davis, L. G. Expression of beta-amyloid precursor protein in reactive astrocytes following neuronal damage. *Neuron* **3**, 275-285 (1989).
48 Van Den Heuvel, C. *et al.* Upregulation of amyloid precursor protein and its mRNA in an experimental model of paediatric head injury. *Journal of clinical neuroscience : official journal of the Neurosurgical Society of Australasia* **7**, 140-145, doi:10.1054/jocn.1999.0168 (2000).

49 Zheng, H. & Koo, E. H. Biology and pathophysiology of the amyloid precursor protein. *Molecular neurodegeneration* **6**, 27, doi:10.1186/1750-1326-6-27 (2011).
50 Soba, P. *et al.* Homo- and heterodimerization of APP family members promotes intercellular adhesion. *The EMBO journal* **24**, 3624-3634, doi:10.1038/sj.emboj.7600824 (2005).
51 Perez, R. G., Zheng, H., Van der Ploeg, L. H. & Koo, E. H. The beta-amyloid precursor protein of Alzheimer's disease enhances neuron viability and modulates neuronal polarity. *The Journal of neuroscience : the official journal of the Society for Neuroscience* **17**, 9407-9414 (1997).
52 Kinoshita, A., Whelan, C. M., Berezovska, O. & Hyman, B. T. The gamma secretase-generated carboxyl-terminal domain of the amyloid precursor protein induces apoptosis via Tip60 in H4 cells. *The Journal of biological chemistry* **277**, 28530-28536, doi:10.1074/jbc.M203372200 (2002).
53 Chasseigneaux, S. & Allinquant, B. Functions of Abeta, sAPPalpha and sAPPbeta : similarities and differences. *Journal of neurochemistry* **120 Suppl 1**, 99-108, doi:10.1111/j.1471-4159.2011.07584.x (2012).
54 Ring, S. *et al.* The secreted beta-amyloid precursor protein ectodomain APPs alpha is sufficient to rescue the anatomical, behavioral, and electrophysiological abnormalities of APP-deficient mice. *The Journal of neuroscience : the official journal of the Society for Neuroscience* **27**, 7817-7826, doi:10.1523/JNEUROSCI.1026-07.2007 (2007).
55 Phinney, A. L. *et al.* No hippocampal neuron or synaptic bouton loss in learning-impaired aged beta-amyloid precursor protein-null mice. *Neuroscience* **90**, 1207-1216 (1999).
56 Dawson, G. R. *et al.* Age-related cognitive deficits, impaired long-term potentiation and reduction in synaptic marker density in mice lacking the beta-amyloid precursor protein. *Neuroscience* **90**, 1-13 (1999).
57 Uhlen, M. *et al.* Proteomics. Tissue-based map of the human proteome. *Science* **347**, 1260419, doi:10.1126/science.1260419 (2015).
58 Paliga, K. *et al.* Human amyloid precursor-like protein 1--cDNA cloning, ectopic expression in COS-7 cells and identification of soluble forms in the cerebrospinal fluid. *Eur J Biochem* **250**, 354-363 (1997).
59 Sprecher, C. A. *et al.* Molecular cloning of the cDNA for a human amyloid precursor protein homolog: evidence for a multigene family. *Biochemistry* **32**, 4481-4486 (1993).
60 Wasco, W. *et al.* Isolation and characterization of APLP2 encoding a homologue of the Alzheimer's associated amyloid beta protein precursor. *Nature genetics* **5**, 95-100, doi:10.1038/ng0993-95 (1993).
61 Shariati, S. A. & De Strooper, B. Redundancy and divergence in the amyloid precursor protein family. *FEBS letters* **587**, 2036-2045, doi:10.1016/j.febslet.2013.05.026 (2013).
62 Moore, D. B. *et al.* Asynchronous evolutionary origins of Abeta and BACE1. *Mol Biol Evol* **31**, 696-702, doi:10.1093/molbev/mst262 (2014).
63 Lahiri, D. K. *et al.* A critical analysis of new molecular targets and strategies for drug developments in Alzheimer's disease. *Current drug targets* **4**, 97-112 (2003).

64 Esch, F. S. *et al.* Cleavage of amyloid beta peptide during constitutive processing of its precursor. *Science* **248**, 1122-1124 (1990).
65 Schubert, D., LaCorbiere, M., Saitoh, T. & Cole, G. Characterization of an amyloid beta precursor protein that binds heparin and contains tyrosine sulfate. *Proceedings of the National Academy of Sciences of the United States of America* **86**, 2066-2069 (1989).
66 Ohsawa, I., Takamura, C., Morimoto, T., Ishiguro, M. & Kohsaka, S. Amino-terminal region of secreted form of amyloid precursor protein stimulates proliferation of neural stem cells. *The European journal of neuroscience* **11**, 1907-1913 (1999).
67 Mattson, M. P. *et al.* Evidence for excitoprotective and intraneuronal calcium-regulating roles for secreted forms of the beta-amyloid precursor protein. *Neuron* **10**, 243-254 (1993).
68 Furukawa, K. *et al.* Increased activity-regulating and neuroprotective efficacy of alpha-secretase-derived secreted amyloid precursor protein conferred by a C-terminal heparin-binding domain. *Journal of neurochemistry* **67**, 1882-1896 (1996).
69 Chasseigneaux, S. *et al.* Secreted amyloid precursor protein beta and secreted amyloid precursor protein alpha induce axon outgrowth in vitro through Egr1 signaling pathway. *PloS one* **6**, e16301, doi:10.1371/journal.pone.0016301 (2011).
70 Nikolaev, A., McLaughlin, T., O'Leary, D. D. & Tessier-Lavigne, M. APP binds DR6 to trigger axon pruning and neuron death via distinct caspases. *Nature* **457**, 981-989, doi:10.1038/nature07767 (2009).
71 Vassar, R. *et al.* Beta-secretase cleavage of Alzheimer's amyloid precursor protein by the transmembrane aspartic protease BACE. *Science* **286**, 735-741 (1999).
72 Yan, R. *et al.* Membrane-anchored aspartyl protease with Alzheimer's disease beta-secretase activity. *Nature* **402**, 533-537, doi:10.1038/990107 (1999).
73 Sinha, S. *et al.* Purification and cloning of amyloid precursor protein beta-secretase from human brain. *Nature* **402**, 537-540, doi:10.1038/990114 (1999).
74 Hussain, I. *et al.* Identification of a novel aspartic protease (Asp 2) as beta-secretase. *Molecular and cellular neurosciences* **14**, 419-427, doi:10.1006/mcne.1999.0811 (1999).
75 Huse, J. T., Pijak, D. S., Leslie, G. J., Lee, V. M. & Doms, R. W. Maturation and endosomal targeting of beta-site amyloid precursor protein-cleaving enzyme. The Alzheimer's disease beta-secretase. *The Journal of biological chemistry* **275**, 33729-33737, doi:10.1074/jbc.M004175200 (2000).
76 Savonenko, A. V. *et al.* Alteration of BACE1-dependent NRG1/ErbB4 signaling and schizophrenia-like phenotypes in BACE1-null mice. *Proceedings of the National Academy of Sciences of the United States of America* **105**, 5585-5590, doi:10.1073/pnas.0710373105 (2008).
77 Kim, D. Y. *et al.* BACE1 regulates voltage-gated sodium channels and neuronal activity. *Nat Cell Biol* **9**, 755-764, doi:10.1038/ncb1602 (2007).
78 Kitazume, S. *et al.* In vivo cleavage of alpha2,6-sialyltransferase by Alzheimer beta-secretase. *The Journal of biological chemistry* **280**, 8589-8595, doi:10.1074/jbc.M409417200 (2005).

79 Kitazume, S. *et al.* Characterization of alpha 2,6-sialyltransferase cleavage by Alzheimer's beta -secretase (BACE1). *The Journal of biological chemistry* **278**, 14865-14871, doi:10.1074/jbc.M206262200 (2003).
80 Kuhn, P. H. *et al.* Secretome protein enrichment identifies physiological BACE1 protease substrates in neurons. *The EMBO journal* **31**, 3157-3168, doi:10.1038/emboj.2012.173 (2012).
81 Tun, H., Marlow, L., Pinnix, I., Kinsey, R. & Sambamurti, K. Lipid rafts play an important role in A beta biogenesis by regulating the beta-secretase pathway. *J Mol Neurosci* **19**, 31-35, doi:10.1007/s12031-002-0007-5 (2002).
82 Solans, A., Estivill, X. & de La Luna, S. A new aspartyl protease on 21q22.3, BACE2, is highly similar to Alzheimer's amyloid precursor protein beta-secretase. *Cytogenet Cell Genet* **89**, 177-184, doi:15608 (2000).
83 Bennett, B. D. *et al.* Expression analysis of BACE2 in brain and peripheral tissues. *The Journal of biological chemistry* **275**, 20647-20651, doi:10.1074/jbc.M002688200 (2000).
84 Farzan, M., Schnitzler, C. E., Vasilieva, N., Leung, D. & Choe, H. BACE2, a beta -secretase homolog, cleaves at the beta site and within the amyloid-beta region of the amyloid-beta precursor protein. *Proceedings of the National Academy of Sciences of the United States of America* **97**, 9712-9717, doi:10.1073/pnas.160115697 (2000).
85 Hu, X. *et al.* Bace1 modulates myelination in the central and peripheral nervous system. *Nature neuroscience* **9**, 1520-1525, doi:10.1038/nn1797 (2006).
86 Hu, X. *et al.* BACE1 deficiency causes altered neuronal activity and neurodegeneration. *The Journal of neuroscience : the official journal of the Society for Neuroscience* **30**, 8819-8829, doi:10.1523/JNEUROSCI.1334-10.2010 (2010).
87 Coulson, D. T. *et al.* BACE1 mRNA expression in Alzheimer's disease postmortem brain tissue. *Journal of Alzheimer's disease : JAD* **22**, 1111-1122, doi:10.3233/JAD-2010-101254 (2010).
88 Long, J. M., Ray, B. & Lahiri, D. K. MicroRNA-339-5p down-regulates protein expression of beta-site amyloid precursor protein-cleaving enzyme 1 (BACE1) in human primary brain cultures and is reduced in brain tissue specimens of Alzheimer disease subjects. *The Journal of biological chemistry* **289**, 5184-5198, doi:10.1074/jbc.M113.518241 (2014).
89 Hardy, J. & Allsop, D. Amyloid deposition as the central event in the aetiology of Alzheimer's disease. *Trends in pharmacological sciences* **12**, 383-388 (1991).
90 Hardy, J. & Selkoe, D. J. The amyloid hypothesis of Alzheimer's disease: progress and problems on the road to therapeutics. *Science* **297**, 353-356, doi:10.1126/science.1072994 (2002).
91 Herrup, K. The case for rejecting the amyloid cascade hypothesis. *Nature neuroscience* **18**, 794-799, doi:10.1038/nn.4017 (2015).
92 Masters, C. L. *et al.* Amyloid plaque core protein in Alzheimer disease and Down syndrome. *Proceedings of the National Academy of Sciences of the United States of America* **82**, 4245-4249 (1985).

93 Glenner, G. G. & Wong, C. W. Alzheimer's disease and Down's syndrome: sharing of a unique cerebrovascular amyloid fibril protein. *Biochemical and biophysical research communications* **122**, 1131-1135 (1984).
94 Glenner, G. G., Wong, C. W., Quaranta, V. & Eanes, E. D. The amyloid deposits in Alzheimer's disease: their nature and pathogenesis. *Appl Pathol* **2**, 357-369 (1984).
95 Devenny, D. A. *et al.* Dementia of the Alzheimer's type and accelerated aging in Down syndrome. *Sci Aging Knowledge Environ* **2005**, dn1, doi:10.1126/sageke.2005.14.dn1 (2005).
96 Dawkins, E. & Small, D. H. Insights into the physiological function of the beta-amyloid precursor protein: beyond Alzheimer's disease. *Journal of neurochemistry* **129**, 756-769, doi:10.1111/jnc.12675 (2014).
97 Selkoe, D. J. The cell biology of beta-amyloid precursor protein and presenilin in Alzheimer's disease. *Trends Cell Biol* **8**, 447-453 (1998).
98 De Strooper, B. Aph-1, Pen-2, and Nicastrin with Presenilin generate an active gamma-Secretase complex. *Neuron* **38**, 9-12 (2003).
99 De Strooper, B. & Annaert, W. Novel research horizons for presenilins and gamma-secretases in cell biology and disease. *Annual review of cell and developmental biology* **26**, 235-260, doi:10.1146/annurev-cellbio-100109-104117 (2010).
100 Morishima-Kawashima, M. Molecular mechanism of the intramembrane cleavage of the beta-carboxyl terminal fragment of amyloid precursor protein by gamma-secretase. *Front Physiol* **5**, 463, doi:10.3389/fphys.2014.00463 (2014).
101 Moghekar, A. *et al.* Large quantities of Abeta peptide are constitutively released during amyloid precursor protein metabolism in vivo and in vitro. *The Journal of biological chemistry* **286**, 15989-15997, doi:10.1074/jbc.M110.191262 (2011).
102 Busciglio, J., Gabuzda, D. H., Matsudaira, P. & Yankner, B. A. Generation of beta-amyloid in the secretory pathway in neuronal and nonneuronal cells. *Proceedings of the National Academy of Sciences of the United States of America* **90**, 2092-2096 (1993).
103 Chen, M., Inestrosa, N. C., Ross, G. S. & Fernandez, H. L. Platelets are the primary source of amyloid beta-peptide in human blood. *Biochemical and biophysical research communications* **213**, 96-103, doi:10.1006/bbrc.1995.2103 (1995).
104 Mitternacht, S., Staneva, I., Hard, T. & Irback, A. Comparing the folding free-energy landscapes of Abeta42 variants with different aggregation properties. *Proteins* **78**, 2600-2608, doi:10.1002/prot.22775 (2010).
105 Scheuner, D. *et al.* Secreted amyloid beta-protein similar to that in the senile plaques of Alzheimer's disease is increased in vivo by the presenilin 1 and 2 and APP mutations linked to familial Alzheimer's disease. *Nature medicine* **2**, 864-870 (1996).
106 Burdick, D. *et al.* Assembly and aggregation properties of synthetic Alzheimer's A4/beta amyloid peptide analogs. *The Journal of biological chemistry* **267**, 546-554 (1992).
107 Fukuma, T., Mostaert, A. S., Serpell, L. C. & Jarvis, S. P. Revealing molecular-level surface structure of amyloid fibrils in liquid by means of frequency

modulation atomic force microscopy. *Nanotechnology* **19**, 384010, doi:10.1088/0957-4484/19/38/384010 (2008).
108 Barz, B. & Urbanc, B. Dimer formation enhances structural differences between amyloid beta-protein (1-40) and (1-42): an explicit-solvent molecular dynamics study. *PloS one* **7**, e34345, doi:10.1371/journal.pone.0034345 (2012).
109 Borchelt, D. R. *et al.* Familial Alzheimer's disease-linked presenilin 1 variants elevate Abeta1-42/1-40 ratio in vitro and in vivo. *Neuron* **17**, 1005-1013 (1996).
110 McGowan, E. *et al.* Abeta42 is essential for parenchymal and vascular amyloid deposition in mice. *Neuron* **47**, 191-199, doi:10.1016/j.neuron.2005.06.030 (2005).
111 Kim, J. *et al.* Abeta40 inhibits amyloid deposition in vivo. *The Journal of neuroscience : the official journal of the Society for Neuroscience* **27**, 627-633, doi:10.1523/JNEUROSCI.4849-06.2007 (2007).
112 Bate, C. & Williams, A. Amyloid-beta(1-40) inhibits amyloid-beta(1-42) induced activation of cytoplasmic phospholipase A2 and synapse degeneration. *Journal of Alzheimer's disease : JAD* **21**, 985-993, doi:10.3233/JAD-2010-100528 (2010).
113 Puzzo, D. *et al.* Endogenous amyloid-beta is necessary for hippocampal synaptic plasticity and memory. *Annals of neurology* **69**, 819-830, doi:10.1002/ana.22313 (2011).
114 Pettit, D. L., Shao, Z. & Yakel, J. L. beta-Amyloid(1-42) peptide directly modulates nicotinic receptors in the rat hippocampal slice. *The Journal of neuroscience : the official journal of the Society for Neuroscience* **21**, RC120 (2001).
115 Finder, V. H. & Glockshuber, R. Amyloid-beta aggregation. *Neurodegener Dis* **4**, 13-27, doi:10.1159/000100355 (2007).
116 Yin, R. H., Tan, L., Jiang, T. & Yu, J. T. Prion-like Mechanisms in Alzheimer's Disease. *Current Alzheimer research* **11**, 755-764 (2014).
117 Watts, J. C. *et al.* Serial propagation of distinct strains of Abeta prions from Alzheimer's disease patients. *Proceedings of the National Academy of Sciences of the United States of America* **111**, 10323-10328, doi:10.1073/pnas.1408900111 (2014).
118 Stohr, J. *et al.* Distinct synthetic Abeta prion strains producing different amyloid deposits in bigenic mice. *Proceedings of the National Academy of Sciences of the United States of America* **111**, 10329-10334, doi:10.1073/pnas.1408968111 (2014).
119 Lahiri, D. K. Prions: a piece of the puzzle? *Science* **337**, 1172, doi:10.1126/science.337.6099.1172-a (2012).
120 Prusiner, S. B. Cell biology. A unifying role for prions in neurodegenerative diseases. *Science* **336**, 1511-1513, doi:10.1126/science.1222951 (2012).
121 Balducci, C. *et al.* Synthetic amyloid-beta oligomers impair long-term memory independently of cellular prion protein. *Proceedings of the National Academy of Sciences of the United States of America* **107**, 2295-2300, doi:10.1073/pnas.0911829107 (2010).
122 Shen, C. L., Fitzgerald, M. C. & Murphy, R. M. Effect of acid predissolution on fibril size and fibril flexibility of synthetic beta-amyloid peptide. *Biophys J* **67**, 1238-1246, doi:10.1016/S0006-3495(94)80593-4 (1994).

123 Arispe, N., Pollard, H. B. & Rojas, E. Giant multilevel cation channels formed by Alzheimer disease amyloid beta-protein [A beta P-(1-40)] in bilayer membranes. *Proceedings of the National Academy of Sciences of the United States of America* **90**, 10573-10577 (1993).
124 Arispe, N., Rojas, E. & Pollard, H. B. Alzheimer disease amyloid beta protein forms calcium channels in bilayer membranes: blockade by tromethamine and aluminum. *Proceedings of the National Academy of Sciences of the United States of America* **90**, 567-571 (1993).
125 Kawahara, M., Kuroda, Y., Arispe, N. & Rojas, E. Alzheimer's beta-amyloid, human islet amylin, and prion protein fragment evoke intracellular free calcium elevations by a common mechanism in a hypothalamic GnRH neuronal cell line. *The Journal of biological chemistry* **275**, 14077-14083 (2000).
126 Pollard, H. B., Rojas, E. & Arispe, N. A new hypothesis for the mechanism of amyloid toxicity, based on the calcium channel activity of amyloid beta protein (A beta P) in phospholipid bilayer membranes. *Ann N Y Acad Sci* **695**, 165-168 (1993).
127 Kayed, R. *et al.* Permeabilization of lipid bilayers is a common conformation-dependent activity of soluble amyloid oligomers in protein misfolding diseases. *The Journal of biological chemistry* **279**, 46363-46366, doi:10.1074/jbc.C400260200 (2004).
128 Sadigh-Eteghad, S. *et al.* Amyloid-beta: a crucial factor in Alzheimer's disease. *Med Princ Pract* **24**, 1-10, doi:10.1159/000369101 (2015).
129 Yamamoto, N. *et al.* A ganglioside-induced toxic soluble Abeta assembly. Its enhanced formation from Abeta bearing the Arctic mutation. *The Journal of biological chemistry* **282**, 2646-2655, doi:10.1074/jbc.M606202200 (2007).
130 Yamamoto, N., Fukata, Y., Fukata, M. & Yanagisawa, K. GM1-ganglioside-induced Abeta assembly on synaptic membranes of cultured neurons. *Biochim Biophys Acta* **1768**, 1128-1137, doi:10.1016/j.bbamem.2007.01.009 (2007).
131 Bailey, J. A., Maloney, B., Ge, Y. W. & Lahiri, D. K. Functional activity of the novel Alzheimer's amyloid beta-peptide interacting domain (AbetaID) in the APP and BACE1 promoter sequences and implications in activating apoptotic genes and in amyloidogenesis. *Gene* **488**, 13-22, doi:10.1016/j.gene.2011.06.017 (2011).
132 Maloney, B. & Lahiri, D. K. The Alzheimer's amyloid beta-peptide (Abeta) binds a specific DNA Abeta-interacting domain (AbetaID) in the APP, BACE1, and APOE promoters in a sequence-specific manner: characterizing a new regulatory motif. *Gene* **488**, 1-12, doi:10.1016/j.gene.2011.06.004 (2011).
133 Wildsmith, K. R., Holley, M., Savage, J. C., Skerrett, R. & Landreth, G. E. Evidence for impaired amyloid beta clearance in Alzheimer's disease. *Alzheimers Res Ther* **5**, 33, doi:10.1186/alzrt187 (2013).
134 Turner, A. J., Isaac, R. E. & Coates, D. The neprilysin (NEP) family of zinc metalloendopeptidases: genomics and function. *Bioessays* **23**, 261-269, doi:10.1002/1521-1878(200103)23:3<261::AID-BIES1036>3.0.CO;2-K [pii] 10.1002/1521-1878(200103)23:3<261::AID-BIES1036>3.0.CO;2-K (2001).
135 Selkoe, D. J. Clearing the brain's amyloid cobwebs. *Neuron* **32**, 177-180, doi:S0896-6273(01)00475-5 [pii] (2001).

136 Baranello, R. J. *et al.* Amyloid-beta protein clearance and degradation (ABCD) pathways and their role in Alzheimer's disease. *Current Alzheimer research* **12**, 32-46 (2015).
137 Funalot, B. *et al.* Endothelin-converting enzyme-1 is expressed in human cerebral cortex and protects against Alzheimer's disease. *Mol Psychiatry* **9**, 1122-1128, 1059, doi:10.1038/sj.mp.4001584 (2004).
138 Pacheco-Quinto, J. & Eckman, E. A. Endothelin-converting enzymes degrade intracellular beta-amyloid produced within the endosomal/lysosomal pathway and autophagosomes. *J Biol Chem* **288**, 5606-5615, doi:10.1074/jbc.M112.422964 (2013).
139 Pacheco-Quinto, J., Herdt, A., Eckman, C. B. & Eckman, E. A. Endothelin-converting enzymes and related metalloproteases in Alzheimer's disease. *J Alzheimers Dis* **33 Suppl 1**, S101-110, doi:10.3233/JAD-2012-129043 (2013).
140 Haouas, H. *et al.* Characterization of the 5' region of the CD10/neutral endopeptidase 24.11 gene. *Biochem Biophys Res Commun* **207**, 933-942, doi:S0006-291X(85)71275-2 [pii]
10.1006/bbrc.1995.1275 (1995).
141 Shipp, M. A. *et al.* Common acute lymphoblastic leukemia antigen (CALLA) is active neutral endopeptidase 24.11 ("enkephalinase"): direct evidence by cDNA transfection analysis. *Proceedings of the National Academy of Sciences of the United States of America* **86**, 297-301 (1989).
142 Yasojima, K., Akiyama, H., McGeer, E. G. & McGeer, P. L. Reduced neprilysin in high plaque areas of Alzheimer brain: a possible relationship to deficient degradation of beta-amyloid peptide. *Neuroscience letters* **297**, 97-100 (2001).
143 Hersh, L. B. Peptidases, proteases and amyloid beta-peptide catabolism. *Curr Pharm Des* **9**, 449-454 (2003).
144 Iwata, N. *et al.* Metabolic regulation of brain Abeta by neprilysin. *Science* **292**, 1550-1552, doi:10.1126/science.1059946 (2001).
145 Iwata, N., Higuchi, M. & Saido, T. C. Metabolism of amyloid-beta peptide and Alzheimer's disease. *Pharmacol Ther* **108**, 129-148, doi:S0163-7258(05)00099-9 [pii]
10.1016/j.pharmthera.2005.03.010 (2005).
146 Wang, D. S. *et al.* Decreased neprilysin immunoreactivity in Alzheimer disease, but not in pathological aging. *J Neuropathol Exp Neurol* **64**, 378-385 (2005).
147 Walther, T. *et al.* Improved learning and memory in aged mice deficient in amyloid beta-degrading neutral endopeptidase. *PloS one* **4**, e4590, doi:10.1371/journal.pone.0004590 (2009).
148 Hama, E., Shirotani, K., Iwata, N. & Saido, T. C. Effects of neprilysin chimeric proteins targeted to subcellular compartments on amyloid beta peptide clearance in primary neurons. *The Journal of biological chemistry* **279**, 30259-30264, doi:10.1074/jbc.M401891200 (2004).
149 Iijima-Ando, K. *et al.* Overexpression of neprilysin reduces alzheimer amyloid-beta42 (Abeta42)-induced neuron loss and intraneuronal Abeta42 deposits but causes a reduction in cAMP-responsive element-binding protein-mediated transcription, age-dependent axon pathology, and premature death in Drosophila.

The Journal of biological chemistry **283**, 19066-19076, doi:10.1074/jbc.M710509200 (2008).

150 Hong, C. S., Goins, W. F., Goss, J. R., Burton, E. A. & Glorioso, J. C. Herpes simplex virus RNAi and neprilysin gene transfer vectors reduce accumulation of Alzheimer's disease-related amyloid-beta peptide in vivo. *Gene therapy* **13**, 1068-1079, doi:10.1038/sj.gt.3302719 (2006).

151 Devi, L. & Ohno, M. A combination Alzheimer's therapy targeting BACE1 and neprilysin in 5XFAD transgenic mice. *Molecular brain* **8**, 19, doi:10.1186/s13041-015-0110-5 (2015).

152 Marr, R. A. *et al.* Neprilysin gene transfer reduces human amyloid pathology in transgenic mice. *The Journal of neuroscience : the official journal of the Society for Neuroscience* **23**, 1992-1996 (2003).

153 Mazur-Kolecka, B. & Frackowiak, J. Neprilysin protects human neuronal progenitor cells against impaired development caused by amyloid-beta peptide. *Brain research* **1124**, 10-18, doi:10.1016/j.brainres.2006.09.064 (2006).

154 Takaki, Y. *et al.* Biochemical identification of the neutral endopeptidase family member responsible for the catabolism of amyloid beta peptide in the brain. *J Biochem* **128**, 897-902 (2000).

155 Li, C. *et al.* Comparison of the structure and expression of the human and rat neprilysin (endopeptidase 24.11)-encoding genes. *Gene* **164**, 363-366 (1995).

156 Li, C. & Hersh, L. B. Characterization of the promoter region of the rat neprilysin gene. *Archives of biochemistry and biophysics* **358**, 189-195, doi:10.1006/abbi.1998.0855 (1998).

157 Shipp, M. A. *et al.* Molecular cloning of the common acute lymphoblastic leukemia antigen (CALLA) identifies a type II integral membrane protein. *Proceedings of the National Academy of Sciences of the United States of America* **85**, 4819-4823 (1988).

158 Caccamo, A., Oddo, S., Sugarman, M. C., Akbari, Y. & LaFerla, F. M. Age- and region-dependent alterations in Abeta-degrading enzymes: implications for Abeta-induced disorders. *Neurobiol Aging* **26**, 645-654, doi:S0197-4580(04)00239-8 [pii] 10.1016/j.neurobiolaging.2004.06.013 (2005).

159 Fukami, S. *et al.* Abeta-degrading endopeptidase, neprilysin, in mouse brain: synaptic and axonal localization inversely correlating with Abeta pathology. *Neurosci Res* **43**, 39-56, doi:S0168010202000159 [pii] (2002).

160 Kahn, J. *et al.* Neuronal filaments in Alzheimer's, Pick's, and Parkinson's diseases. *The New England journal of medicine* **313**, 520-521, doi:10.1056/NEJM198508223130817 (1985).

161 Iqbal, K. *et al.* Defective brain microtubule assembly in Alzheimer's disease. *Lancet* **2**, 421-426 (1986).

162 Iqbal, K. *et al.* Protein changes in senile dementia. *Brain research* **77**, 337-343 (1974).

163 Gache, Y., Ricolfi, F., Guilleminot, J., Theiss, G. & Nunez, J. Protein TAU variants present in paired helical filaments (PHFs) of Alzheimer brains. *FEBS letters* **272**, 65-68 (1990).

164 Braak, H. & Braak, E. Neuropathological stageing of Alzheimer-related changes. *Acta Neuropathol* **82**, 239-259 (1991).
165 Neve, R. L., Harris, P., Kosik, K. S., Kurnit, D. M. & Donlon, T. A. Identification of cDNA clones for the human microtubule-associated protein tau and chromosomal localization of the genes for tau and microtubule-associated protein 2. *Brain research* **387**, 271-280 (1986).
166 Cardenas-Aguayo Mdel, C., Gomez-Virgilio, L., DeRosa, S. & Meraz-Rios, M. A. The role of tau oligomers in the onset of Alzheimer's disease neuropathology. *ACS Chem Neurosci* **5**, 1178-1191, doi:10.1021/cn500148z (2014).
167 Avila, J., Lucas, J. J., Perez, M. & Hernandez, F. Role of tau protein in both physiological and pathological conditions. *Physiol Rev* **84**, 361-384, doi:10.1152/physrev.00024.2003 (2004).
168 Weingarten, M. D., Lockwood, A. H., Hwo, S. Y. & Kirschner, M. W. A protein factor essential for microtubule assembly. *Proceedings of the National Academy of Sciences of the United States of America* **72**, 1858-1862 (1975).
169 Iqbal, K., Liu, F., Gong, C. X. & Grundke-Iqbal, I. Tau in Alzheimer disease and related tauopathies. *Current Alzheimer research* **7**, 656-664 (2010).
170 Iqbal, K., Smith, A. J., Zaidi, T. & Grundke-Iqbal, I. Microtubule-associated protein tau. Identification of a novel peptide from bovine brain. *FEBS letters* **248**, 87-91 (1989).
171 Iqbal, K., Gong, C. X. & Liu, F. Hyperphosphorylation-induced tau oligomers. *Front Neurol* **4**, 112, doi:10.3389/fneur.2013.00112 (2013).
172 Kanai, Y. *et al.* Expression of multiple tau isoforms and microtubule bundle formation in fibroblasts transfected with a single tau cDNA. *The Journal of cell biology* **109**, 1173-1184 (1989).
173 Merrick, S. E., Trojanowski, J. Q. & Lee, V. M. Selective destruction of stable microtubules and axons by inhibitors of protein serine/threonine phosphatases in cultured human neurons. *The Journal of neuroscience : the official journal of the Society for Neuroscience* **17**, 5726-5737 (1997).
174 Fath, T., Eidenmuller, J. & Brandt, R. Tau-mediated cytotoxicity in a pseudohyperphosphorylation model of Alzheimer's disease. *The Journal of neuroscience : the official journal of the Society for Neuroscience* **22**, 9733-9741 (2002).
175 Gotz, J. *et al.* Somatodendritic localization and hyperphosphorylation of tau protein in transgenic mice expressing the longest human brain tau isoform. *The EMBO journal* **14**, 1304-1313 (1995).
176 Ishihara, T. *et al.* Age-dependent emergence and progression of a tauopathy in transgenic mice overexpressing the shortest human tau isoform. *Neuron* **24**, 751-762 (1999).
177 Lasagna-Reeves, C. A. *et al.* Alzheimer brain-derived tau oligomers propagate pathology from endogenous tau. *Scientific reports* **2**, 700, doi:10.1038/srep00700 (2012).
178 Sjogren, M. *et al.* Both total and phosphorylated tau are increased in Alzheimer's disease. *J Neurol Neurosurg Psychiatry* **70**, 624-630 (2001).
179 Kandimalla, R. J. *et al.* CSF p-Tau levels in the prediction of Alzheimer's disease. *Biol Open* **2**, 1119-1124, doi:10.1242/bio.20135447 (2013).

180 Harari, O. *et al.* Phosphorylated tau-Abeta42 ratio as a continuous trait for biomarker discovery for early-stage Alzheimer's disease in multiplex immunoassay panels of cerebrospinal fluid. *Biol Psychiatry* **75**, 723-731, doi:10.1016/j.biopsych.2013.11.032 (2014).
181 Pottiez, G. *et al.* Mass-Spectrometry-Based Method To Quantify in Parallel Tau and Amyloid beta 1-42 in CSF for the Diagnosis of Alzheimer's Disease. *Journal of proteome research* **16**, 1228-1238, doi:10.1021/acs.jproteome.6b00829 (2017).
182 Li, G. *et al.* CSF tau/Abeta42 ratio for increased risk of mild cognitive impairment: a follow-up study. *Neurology* **69**, 631-639, doi:10.1212/01.wnl.0000267428.62582.aa (2007).
183 Banik, A. *et al.* Translation of Pre-Clinical Studies into Successful Clinical Trials for Alzheimer's Disease: What are the Roadblocks and How Can They Be Overcome? *Journal of Alzheimer's disease : JAD* **47**, 815-843, doi:10.3233/JAD-150136 (2015).
184 Sarkar, S. *et al.* Oral Administration of Thioflavin T Prevents Beta Amyloid Plaque Formation in Double Transgenic AD Mice. *Current Alzheimer research* **12**, 837-846 (2015).
185 Wiessner, C. *et al.* The second-generation active Abeta immunotherapy CAD106 reduces amyloid accumulation in APP transgenic mice while minimizing potential side effects. *The Journal of neuroscience : the official journal of the Society for Neuroscience* **31**, 9323-9331, doi:10.1523/JNEUROSCI.0293-11.2011 (2011).
186 Farlow, M. *et al.* Safety and biomarker effects of solanezumab in patients with Alzheimer's disease. *Alzheimer's & dementia : the journal of the Alzheimer's Association* **8**, 261-271, doi:10.1016/j.jalz.2011.09.224 (2012).
187 Jindal, H., Bhatt, B., Sk, S. & Singh Malik, J. Alzheimer disease immunotherapeutics: then and now. *Hum Vaccin Immunother* **10**, 2741-2743, doi:10.4161/21645515.2014.970959 (2014).
188 Ivanoiu, A. *et al.* Long-term safety and tolerability of bapineuzumab in patients with Alzheimer's disease in two phase 3 extension studies. *Alzheimers Res Ther* **8**, 24, doi:10.1186/s13195-016-0193-y (2016).
189 Bohrmann, B. *et al.* Gantenerumab: a novel human anti-Abeta antibody demonstrates sustained cerebral amyloid-beta binding and elicits cell-mediated removal of human amyloid-beta. *Journal of Alzheimer's disease : JAD* **28**, 49-69, doi:10.3233/JAD-2011-110977 (2012).
190 Panza, F. *et al.* Efficacy and safety studies of gantenerumab in patients with Alzheimer's disease. *Expert Rev Neurother* **14**, 973-986, doi:10.1586/14737175.2014.945522 (2014).
191 Jacobsen, H. *et al.* Combined treatment with a BACE inhibitor and anti-Abeta antibody gantenerumab enhances amyloid reduction in APPLondon mice. *The Journal of neuroscience : the official journal of the Society for Neuroscience* **34**, 11621-11630, doi:10.1523/JNEUROSCI.1405-14.2014 (2014).
192 Bouter, Y. *et al.* Abeta targets of the biosimilar antibodies of Bapineuzumab, Crenezumab, Solanezumab in comparison to an antibody against Ntruncated Abeta in sporadic Alzheimer disease cases and mouse models. *Acta Neuropathol* **130**, 713-729, doi:10.1007/s00401-015-1489-x (2015).

193 Hawkes, N. Merck ends trial of potential Alzheimer's drug verubecestat. *BMJ* **356**, j845, doi:10.1136/bmj.j845 (2017).
194 May, P. C. *et al.* The potent BACE1 inhibitor LY2886721 elicits robust central Abeta pharmacodynamic responses in mice, dogs, and humans. *The Journal of neuroscience : the official journal of the Society for Neuroscience* **35**, 1199-1210, doi:10.1523/JNEUROSCI.4129-14.2015 (2015).
195 Lahiri, D. K., Maloney, B., Long, J. M. & Greig, N. H. Lessons from a BACE1 inhibitor trial: off-site but not off base. *Alzheimer's & dementia : the journal of the Alzheimer's Association* **10**, S411-419, doi:10.1016/j.jalz.2013.11.004 (2014).
196 Fleisher, A. S. *et al.* Phase 2 safety trial targeting amyloid beta production with a gamma-secretase inhibitor in Alzheimer disease. *Arch Neurol* **65**, 1031-1038, doi:10.1001/archneur.65.8.1031 (2008).
197 Doody, R. S. *et al.* A phase 3 trial of semagacestat for treatment of Alzheimer's disease. *The New England journal of medicine* **369**, 341-350, doi:10.1056/NEJMoa1210951 (2013).
198 Doody, R. S. *et al.* Peripheral and central effects of gamma-secretase inhibition by semagacestat in Alzheimer's disease. *Alzheimers Res Ther* **7**, 36, doi:10.1186/s13195-015-0121-6 (2015).
199 Schiering, N. *et al.* Structure of neprilysin in complex with the active metabolite of sacubitril. *Scientific reports* **6**, 27909, doi:10.1038/srep27909 (2016).
200 Kontsekova, E., Zilka, N., Kovacech, B., Novak, P. & Novak, M. First-in-man tau vaccine targeting structural determinants essential for pathological tau-tau interaction reduces tau oligomerisation and neurofibrillary degeneration in an Alzheimer's disease model. *Alzheimers Res Ther* **6**, 44, doi:10.1186/alzrt278 (2014).
201 Waite, L. M. Treatment for Alzheimer's disease: has anything changed? *Aust Prescr* **38**, 60-63 (2015).
202 Inden, M. *et al.* alpha4 nicotinic acetylcholine receptor modulated by galantamine on nigrostriatal terminals regulates dopamine receptor-mediated rotational behavior. *Neurochem Int* **94**, 74-81, doi:10.1016/j.neuint.2016.02.008 (2016).
203 Dysken, M. W. *et al.* Effect of vitamin E and memantine on functional decline in Alzheimer disease: the TEAM-AD VA cooperative randomized trial. *JAMA* **311**, 33-44, doi:10.1001/jama.2013.282834 (2014).
204 Lee, R. C., Feinbaum, R. L. & Ambros, V. The C. elegans heterochronic gene lin-4 encodes small RNAs with antisense complementarity to lin-14. *Cell* **75**, 843-854 (1993).
205 Reinhart, B. J. *et al.* The 21-nucleotide let-7 RNA regulates developmental timing in Caenorhabditis elegans. *Nature* **403**, 901-906, doi:10.1038/35002607 (2000).
206 Bhaskaran, M. & Mohan, M. MicroRNAs: history, biogenesis, and their evolving role in animal development and disease. *Vet Pathol* **51**, 759-774, doi:10.1177/0300985813502820 (2014).
207 Londin, E. *et al.* Analysis of 13 cell types reveals evidence for the expression of numerous novel primate- and tissue-specific microRNAs. *Proceedings of the National Academy of Sciences of the United States of America* **112**, E1106-1115, doi:10.1073/pnas.1420955112 (2015).

208 Khuu, C., Utheim, T. P. & Sehic, A. The Three Paralogous MicroRNA Clusters in Development and Disease, miR-17-92, miR-106a-363, and miR-106b-25. *Scientifica (Cairo)* **2016**, 1379643, doi:10.1155/2016/1379643 (2016).
209 Long, J. M. & Lahiri, D. K. Advances in microRNA experimental approaches to study physiological regulation of gene products implicated in CNS disorders. *Experimental neurology* **235**, 402-418, doi:10.1016/j.expneurol.2011.12.043 (2012).
210 Schwarz, D. S. *et al.* Asymmetry in the assembly of the RNAi enzyme complex. *Cell* **115**, 199-208 (2003).
211 Belter, A. *et al.* Mature miRNAs form secondary structure, which suggests their function beyond RISC. *PloS one* **9**, e113848, doi:10.1371/journal.pone.0113848 (2014).
212 Bartel, D. P. MicroRNAs: target recognition and regulatory functions. *Cell* **136**, 215-233, doi:10.1016/j.cell.2009.01.002 (2009).
213 Hausser, J. & Zavolan, M. Identification and consequences of miRNA-target interactions--beyond repression of gene expression. *Nat Rev Genet* **15**, 599-612, doi:10.1038/nrg3765 (2014).
214 Goodall, E. F., Heath, P. R., Bandmann, O., Kirby, J. & Shaw, P. J. Neuronal dark matter: the emerging role of microRNAs in neurodegeneration. *Frontiers in cellular neuroscience* **7**, 178, doi:10.3389/fncel.2013.00178 (2013).
215 Calin, G. A. *et al.* Frequent deletions and down-regulation of micro- RNA genes miR15 and miR16 at 13q14 in chronic lymphocytic leukemia. *Proceedings of the National Academy of Sciences of the United States of America* **99**, 15524-15529, doi:10.1073/pnas.242606799 (2002).
216 Iorio, M. V. & Croce, C. M. MicroRNA dysregulation in cancer: diagnostics, monitoring and therapeutics. A comprehensive review. *EMBO Mol Med* **4**, 143-159, doi:10.1002/emmm.201100209 (2012).
217 Ji, Q. *et al.* MicroRNA miR-34 inhibits human pancreatic cancer tumor-initiating cells. *PloS one* **4**, e6816, doi:10.1371/journal.pone.0006816 (2009).
218 Costinean, S. *et al.* Pre-B cell proliferation and lymphoblastic leukemia/high-grade lymphoma in E(mu)-miR155 transgenic mice. *Proceedings of the National Academy of Sciences of the United States of America* **103**, 7024-7029, doi:10.1073/pnas.0602266103 (2006).
219 Huang, J. *et al.* Cellular microRNAs contribute to HIV-1 latency in resting primary CD4+ T lymphocytes. *Nature medicine* **13**, 1241-1247, doi:10.1038/nm1639 (2007).
220 Junker, A. *et al.* MicroRNA profiling of multiple sclerosis lesions identifies modulators of the regulatory protein CD47. *Brain : a journal of neurology* **132**, 3342-3352, doi:10.1093/brain/awp300 (2009).
221 Hooper, C. *et al.* p53 is upregulated in Alzheimer's disease and induces tau phosphorylation in HEK293a cells. *Neuroscience letters* **418**, 34-37, doi:10.1016/j.neulet.2007.03.026 (2007).
222 Sethi, P. & Lukiw, W. J. Micro-RNA abundance and stability in human brain: specific alterations in Alzheimer's disease temporal lobe neocortex. *Neuroscience letters* **459**, 100-104, doi:10.1016/j.neulet.2009.04.052 (2009).

223 Nelson, P. T. & Wang, W. X. MiR-107 is reduced in Alzheimer's disease brain neocortex: validation study. *Journal of Alzheimer's disease : JAD* **21**, 75-79, doi:10.3233/JAD-2010-091603 (2010).
224 Schonrock, N., Humphreys, D. T., Preiss, T. & Gotz, J. Target gene repression mediated by miRNAs miR-181c and miR-9 both of which are down-regulated by amyloid-beta. *J Mol Neurosci* **46**, 324-335, doi:10.1007/s12031-011-9587-2 (2012).
225 Kim, J. *et al.* MiR-106b impairs cholesterol efflux and increases Abeta levels by repressing ABCA1 expression. *Experimental neurology* **235**, 476-483, doi:10.1016/j.expneurol.2011.11.010 (2012).
226 Hebert, S. S. *et al.* Loss of microRNA cluster miR-29a/b-1 in sporadic Alzheimer's disease correlates with increased BACE1/beta-secretase expression. *Proceedings of the National Academy of Sciences of the United States of America* **105**, 6415-6420, doi:10.1073/pnas.0710263105 (2008).
227 Krichevsky, A. M., King, K. S., Donahue, C. P., Khrapko, K. & Kosik, K. S. A microRNA array reveals extensive regulation of microRNAs during brain development. *RNA* **9**, 1274-1281 (2003).
228 Cogswell, J. P. *et al.* Identification of miRNA changes in Alzheimer's disease brain and CSF yields putative biomarkers and insights into disease pathways. *Journal of Alzheimer's disease : JAD* **14**, 27-41 (2008).
229 Alexandrov, P. N. *et al.* microRNA (miRNA) speciation in Alzheimer's disease (AD) cerebrospinal fluid (CSF) and extracellular fluid (ECF). *Int J Biochem Mol Biol* **3**, 365-373 (2012).
230 Galimberti, D. *et al.* Circulating miRNAs as potential biomarkers in Alzheimer's disease. *Journal of Alzheimer's disease : JAD* **42**, 1261-1267, doi:10.3233/JAD-140756 (2014).
231 Niwa, R., Zhou, F., Li, C. & Slack, F. J. The expression of the Alzheimer's amyloid precursor protein-like gene is regulated by developmental timing microRNAs and their targets in Caenorhabditis elegans. *Dev Biol* **315**, 418-425, doi:10.1016/j.ydbio.2007.12.044 (2008).
232 Vilardo, E., Barbato, C., Ciotti, M., Cogoni, C. & Ruberti, F. MicroRNA-101 regulates amyloid precursor protein expression in hippocampal neurons. *The Journal of biological chemistry* **285**, 18344-18351, doi:10.1074/jbc.M110.112664 (2010).
233 Long, J. M. & Lahiri, D. K. MicroRNA-101 downregulates Alzheimer's amyloid-beta precursor protein levels in human cell cultures and is differentially expressed. *Biochemical and biophysical research communications* **404**, 889-895, doi:10.1016/j.bbrc.2010.12.053 (2011).
234 Liu, W. *et al.* MicroRNA-16 targets amyloid precursor protein to potentially modulate Alzheimer's-associated pathogenesis in SAMP8 mice. *Neurobiology of aging* **33**, 522-534, doi:10.1016/j.neurobiolaging.2010.04.034 (2012).
235 Zhang, B., Chen, C. F., Wang, A. H. & Lin, Q. F. MiR-16 regulates cell death in Alzheimer's disease by targeting amyloid precursor protein. *Eur Rev Med Pharmacol Sci* **19**, 4020-4027 (2015).
236 Long, J. M., Ray, B. & Lahiri, D. K. MicroRNA-153 physiologically inhibits expression of amyloid-beta precursor protein in cultured human fetal brain cells

and is dysregulated in a subset of Alzheimer disease patients. *The Journal of biological chemistry* **287**, 31298-31310, doi:M112.366336 [pii] 10.1074/jbc.M112.366336 (2012).

237 Liang, C. *et al.* MicroRNA-153 negatively regulates the expression of amyloid precursor protein and amyloid precursor-like protein 2. *Brain research* **1455**, 103-113, doi:10.1016/j.brainres.2011.10.051 (2012).

238 Liu, C. G., Wang, J. L., Li, L. & Wang, P. C. MicroRNA-384 regulates both amyloid precursor protein and beta-secretase expression and is a potential biomarker for Alzheimer's disease. *Int J Mol Med* **34**, 160-166, doi:10.3892/ijmm.2014.1780 (2014).

239 Liu, C. G., Song, J., Zhang, Y. Q. & Wang, P. C. MicroRNA-193b is a regulator of amyloid precursor protein in the blood and cerebrospinal fluid derived exosomal microRNA-193b is a biomarker of Alzheimer's disease. *Mol Med Rep* **10**, 2395-2400, doi:10.3892/mmr.2014.2484 (2014).

240 Liu, C. G. *et al.* MicroRNA-135a and -200b, potential Biomarkers for Alzheimers disease, regulate beta secretase and amyloid precursor protein. *Brain research* **1583**, 55-64, doi:10.1016/j.brainres.2014.04.026 (2014).

241 Delay, C., Calon, F., Mathews, P. & Hebert, S. S. Alzheimer-specific variants in the 3'UTR of Amyloid precursor protein affect microRNA function. *Molecular neurodegeneration* **6**, 70, doi:10.1186/1750-1326-6-70 (2011).

242 Thompson, R. C., Herscovitch, M., Zhao, I., Ford, T. J. & Gilmore, T. D. NF-kappaB down-regulates expression of the B-lymphoma marker CD10 through a miR-155/PU.1 pathway. *The Journal of biological chemistry* **286**, 1675-1682, doi:10.1074/jbc.M110.177063 (2011).

243 Zhu, H. C. *et al.* MicroRNA-195 downregulates Alzheimer's disease amyloid-beta production by targeting BACE1. *Brain Res Bull* **88**, 596-601, doi:10.1016/j.brainresbull.2012.05.018 (2012).

244 Zhang, Y. *et al.* MicroRNA-135b has a neuroprotective role via targeting of beta-site APP-cleaving enzyme 1. *Exp Ther Med* **12**, 809-814, doi:10.3892/etm.2016.3366 (2016).

245 Fang, M. *et al.* The miR-124 regulates the expression of BACE1/beta-secretase correlated with cell death in Alzheimer's disease. *Toxicol Lett* **209**, 94-105, doi:10.1016/j.toxlet.2011.11.032 (2012).

246 Boissonneault, V., Plante, I., Rivest, S. & Provost, P. MicroRNA-298 and microRNA-328 regulate expression of mouse beta-amyloid precursor protein-converting enzyme 1. *The Journal of biological chemistry* **284**, 1971-1981, doi:10.1074/jbc.M807530200 (2009).

247 Hebert, S. S., Sergeant, N. & Buee, L. MicroRNAs and the Regulation of Tau Metabolism. *Int J Alzheimers Dis* **2012**, 406561, doi:10.1155/2012/406561 (2012).

248 Smith, P. Y. *et al.* MicroRNA-132 loss is associated with tau exon 10 inclusion in progressive supranuclear palsy. *Human molecular genetics* **20**, 4016-4024, doi:10.1093/hmg/ddr330 (2011).

249 Wu, H. *et al.* Regulation of microtubule-associated protein tau (MAPT) by miR-34c-5p determines the chemosensitivity of gastric cancer to paclitaxel. *Cancer Chemother Pharmacol* **71**, 1159-1171, doi:10.1007/s00280-013-2108-y (2013).

250 Wang, X. *et al.* MicroRNA-138 promotes tau phosphorylation by targeting retinoic acid receptor alpha. *FEBS letters* **589**, 726-729, doi:10.1016/j.febslet.2015.02.001 (2015).
251 Zhao, Z. B. *et al.* MicroRNA-922 promotes tau phosphorylation by downregulating ubiquitin carboxy-terminal hydrolase L1 (UCHL1) expression in the pathogenesis of Alzheimer's disease. *Neuroscience* **275**, 232-237, doi:10.1016/j.neuroscience.2014.06.013 (2014).
252 Choi, J. *et al.* Oxidative modifications and down-regulation of ubiquitin carboxyl-terminal hydrolase L1 associated with idiopathic Parkinson's and Alzheimer's diseases. *The Journal of biological chemistry* **279**, 13256-13264, doi:10.1074/jbc.M314124200 (2004).
253 Banzhaf-Strathmann, J. *et al.* MicroRNA-125b induces tau hyperphosphorylation and cognitive deficits in Alzheimer's disease. *The EMBO journal* **33**, 1667-1680, doi:10.15252/embj.201387576 (2014).
254 Santa-Maria, I. *et al.* Dysregulation of microRNA-219 promotes neurodegeneration through post-transcriptional regulation of tau. *The Journal of clinical investigation* **125**, 681-686, doi:10.1172/JCI78421 (2015).
255 Kai, Z. S. & Pasquinelli, A. E. MicroRNA assassins: factors that regulate the disappearance of miRNAs. *Nat Struct Mol Biol* **17**, 5-10, doi:10.1038/nsmb.1762 (2010).
256 Siomi, H. & Siomi, M. C. Posttranscriptional regulation of microRNA biogenesis in animals. *Mol Cell* **38**, 323-332, doi:10.1016/j.molcel.2010.03.013 (2010).
257 Sanei, M. & Chen, X. Mechanisms of microRNA turnover. *Curr Opin Plant Biol* **27**, 199-206, doi:10.1016/j.pbi.2015.07.008 (2015).
258 Van Giau, V. & An, S. S. Emergence of exosomal miRNAs as a diagnostic biomarker for Alzheimer's disease. *Journal of the neurological sciences* **360**, 141-152, doi:10.1016/j.jns.2015.12.005 (2016).
259 Johnstone, R. M., Adam, M., Hammond, J. R., Orr, L. & Turbide, C. Vesicle formation during reticulocyte maturation. Association of plasma membrane activities with released vesicles (exosomes). *The Journal of biological chemistry* **262**, 9412-9420 (1987).
260 Harding, C., Heuser, J. & Stahl, P. Receptor-mediated endocytosis of transferrin and recycling of the transferrin receptor in rat reticulocytes. *The Journal of cell biology* **97**, 329-339 (1983).
261 Faure, J. *et al.* Exosomes are released by cultured cortical neurones. *Molecular and cellular neurosciences* **31**, 642-648, doi:10.1016/j.mcn.2005.12.003 (2006).
262 Booth, A. M. *et al.* Exosomes and HIV Gag bud from endosome-like domains of the T cell plasma membrane. *The Journal of cell biology* **172**, 923-935, doi:10.1083/jcb.200508014 (2006).
263 Caby, M. P., Lankar, D., Vincendeau-Scherrer, C., Raposo, G. & Bonnerot, C. Exosomal-like vesicles are present in human blood plasma. *Int Immunol* **17**, 879-887, doi:10.1093/intimm/dxh267 (2005).
264 Pisitkun, T., Shen, R. F. & Knepper, M. A. Identification and proteomic profiling of exosomes in human urine. *Proceedings of the National Academy of Sciences of the United States of America* **101**, 13368-13373, doi:10.1073/pnas.0403453101 (2004).

265 Gui, Y., Liu, H., Zhang, L., Lv, W. & Hu, X. Altered microRNA profiles in cerebrospinal fluid exosome in Parkinson disease and Alzheimer disease. *Oncotarget* **6**, 37043-37053, doi:10.18632/oncotarget.6158 (2015).
266 Zhou, H. *et al.* Collection, storage, preservation, and normalization of human urinary exosomes for biomarker discovery. *Kidney Int* **69**, 1471-1476, doi:10.1038/sj.ki.5000273 (2006).
267 Cheng, L., Sharples, R. A., Scicluna, B. J. & Hill, A. F. Exosomes provide a protective and enriched source of miRNA for biomarker profiling compared to intracellular and cell-free blood. *J Extracell Vesicles* **3**, doi:10.3402/jev.v3.23743 (2014).
268 Lugli, G. *et al.* Plasma Exosomal miRNAs in Persons with and without Alzheimer Disease: Altered Expression and Prospects for Biomarkers. *PloS one* **10**, e0139233, doi:10.1371/journal.pone.0139233 (2015).
269 Denk, J. *et al.* MicroRNA Profiling of CSF Reveals Potential Biomarkers to Detect Alzheimer`s Disease. *PloS one* **10**, e0126423, doi:10.1371/journal.pone.0126423 (2015).
270 Lahiri, D. K., Zawia, N. H., Greig, N. H., Sambamurti, K. & Maloney, B. Early-life events may trigger biochemical pathways for Alzheimer's disease: the "LEARn" model. *Biogerontology* **9**, 375-379, doi:10.1007/s10522-008-9162-6 (2008).
271 Maloney, B. & Lahiri, D. K. Epigenetics of dementia: understanding the disease as a transformation rather than a state. *Lancet Neurol* **15**, 760-774, doi:10.1016/S1474-4422(16)00065-X (2016).
272 Bao, N., Lye, K. W. & Barton, M. K. MicroRNA binding sites in Arabidopsis class III HD-ZIP mRNAs are required for methylation of the template chromosome. *Developmental cell* **7**, 653-662, doi:10.1016/j.devcel.2004.10.003 (2004).
273 Tuddenham, L. *et al.* The cartilage specific microRNA-140 targets histone deacetylase 4 in mouse cells. *FEBS letters* **580**, 4214-4217, doi:10.1016/j.febslet.2006.06.080 (2006).
274 Asada, K. *et al.* Demonstration of the usefulness of epigenetic cancer risk prediction by a multicentre prospective cohort study. *Gut* **64**, 388-396, doi:10.1136/gutjnl-2014-307094 (2015).
275 Szulwach, K. E. *et al.* Cross talk between microRNA and epigenetic regulation in adult neurogenesis. *The Journal of cell biology* **189**, 127-141, doi:10.1083/jcb.200908151 (2010).
276 Cimmino, L., Abdel-Wahab, O., Levine, R. L. & Aifantis, I. TET family proteins and their role in stem cell differentiation and transformation. *Cell stem cell* **9**, 193-204, doi:10.1016/j.stem.2011.08.007 (2011).
277 Fabbri, M. *et al.* MicroRNA-29 family reverts aberrant methylation in lung cancer by targeting DNA methyltransferases 3A and 3B. *Proceedings of the National Academy of Sciences of the United States of America* **104**, 15805-15810, doi:10.1073/pnas.0707628104 (2007).
278 Long, L. M. *et al.* microRNA-214 functions as a tumor suppressor in human colon cancer via the suppression of ADP-ribosylation factor-like protein 2. *Oncology letters* **9**, 645-650, doi:10.3892/ol.2014.2746 (2015).

279 Liu, Y. *et al.* Circulating neprilysin clears brain amyloid. *Molecular and cellular neurosciences* **45**, 101-107, doi:10.1016/j.mcn.2010.05.014 (2010).
280 Koumangoye, R. B. *et al.* SOX4 interacts with EZH2 and HDAC3 to suppress microRNA-31 in invasive esophageal cancer cells. *Molecular cancer* **14**, 24, doi:10.1186/s12943-014-0284-y (2015).
281 Hwang, J. Y., Kaneko, N., Noh, K. M., Pontarelli, F. & Zukin, R. S. The gene silencing transcription factor REST represses miR-132 expression in hippocampal neurons destined to die. *Journal of molecular biology* **426**, 3454-3466, doi:10.1016/j.jmb.2014.07.032 (2014).
282 Lahiri, D. K. *et al.* Transgenerational latent early-life associated regulation unites environment and genetics across generations. *Epigenomics* **8**, 373-387, doi:10.2217/epi.15.117 (2016).
283 Izzotti, A. *et al.* Downregulation of microRNA expression in the lungs of rats exposed to cigarette smoke. *FASEB journal : official publication of the Federation of American Societies for Experimental Biology* **23**, 806-812, doi:10.1096/fj.08-121384 (2009).
284 Radom-Aizik, S., Zaldivar, F., Jr., Oliver, S., Galassetti, P. & Cooper, D. M. Evidence for microRNA involvement in exercise-associated neutrophil gene expression changes. *J Appl Physiol (1985)* **109**, 252-261, doi:10.1152/japplphysiol.01291.2009 (2010).
285 Bollati, V. *et al.* Exposure to metal-rich particulate matter modifies the expression of candidate microRNAs in peripheral blood leukocytes. *Environmental health perspectives* **118**, 763-768, doi:10.1289/ehp.0901300 (2010).
286 Tang, X. *et al.* Acetylation of drosha on the N-terminus inhibits its degradation by ubiquitination. *PloS one* **8**, e72503, doi:10.1371/journal.pone.0072503 (2013).
287 Lewis, B. P., Shih, I. H., Jones-Rhoades, M. W., Bartel, D. P. & Burge, C. B. Prediction of mammalian microRNA targets. *Cell* **115**, 787-798 (2003).
288 Enright, A. J. *et al.* MicroRNA targets in Drosophila. *Genome Biol* **5**, R1, doi:10.1186/gb-2003-5-1-r1 (2003).
289 Krek, A. *et al.* Combinatorial microRNA target predictions. *Nature genetics* **37**, 495-500, doi:10.1038/ng1536 (2005).
290 Kiriakidou, M. *et al.* A combined computational-experimental approach predicts human microRNA targets. *Genes Dev* **18**, 1165-1178, doi:10.1101/gad.1184704 (2004).
291 Kertesz, M., Iovino, N., Unnerstall, U., Gaul, U. & Segal, E. The role of site accessibility in microRNA target recognition. *Nature genetics* **39**, 1278-1284, doi:10.1038/ng2135 (2007).
292 Rehmsmeier, M., Steffen, P., Hochsmann, M. & Giegerich, R. Fast and effective prediction of microRNA/target duplexes. *RNA* **10**, 1507-1517, doi:10.1261/rna.5248604 (2004).
293 Ray, B., Chopra, N., Long, J. M. & Lahiri, D. K. Human primary mixed brain cultures: preparation, differentiation, characterization and application to neuroscience research. *Molecular brain* **7**, 63, doi:10.1186/s13041-014-0063-0 (2014).

294 Evans, H. M., Bowman, F. B. & Winternitz, M. C. An Experimental Study of the Histogenesis of the Miliary Tubercle in Vitally Stained Rabbits. *The Journal of experimental medicine* **19**, 283-302 (1914).
295 Fan, X. *et al.* miR-20a promotes proliferation and invasion by targeting APP in human ovarian cancer cells. *Acta Biochim Biophys Sin (Shanghai)* **42**, 318-324 (2010).
296 Dong, H. *et al.* Serum MicroRNA Profiles Serve as Novel Biomarkers for the Diagnosis of Alzheimer's Disease. *Dis Markers* **2015**, 625659, doi:10.1155/2015/625659 (2015).
297 Tan, L. *et al.* Circulating miR-125b as a biomarker of Alzheimer's disease. *Journal of the neurological sciences* **336**, 52-56, doi:10.1016/j.jns.2013.10.002 (2014).
298 Giraud-Triboult, K. *et al.* Combined mRNA and microRNA profiling reveals that miR-148a and miR-20b control human mesenchymal stem cell phenotype via EPAS1. *Physiol Genomics* **43**, 77-86, doi:10.1152/physiolgenomics.00077.2010 (2011).
299 Song, C., Ma, H., Yao, C., Tao, X. & Gan, H. Alveolar macrophage-derived vascular endothelial growth factor contributes to allergic airway inflammation in a mouse asthma model. *Scand J Immunol* **75**, 599-605, doi:10.1111/j.1365-3083.2012.02693.x (2012).
300 Wang, W. *et al.* Preeclampsia up-regulates angiogenesis-associated microRNA (i.e., miR-17, -20a, and -20b) that target ephrin-B2 and EPHB4 in human placenta. *The Journal of clinical endocrinology and metabolism* **97**, E1051-1059, doi:10.1210/jc.2011-3131 (2012).
301 Saleiban, A., Faxalv, L., Claesson, K., Jonsson, J. I. & Osman, A. miR-20b regulates expression of proteinase-activated receptor-1 (PAR-1) thrombin receptor in melanoma cells. *Pigment cell & melanoma research* **27**, 431-441, doi:10.1111/pcmr.12217 (2014).
302 Zhu, J. *et al.* MiR-20b, -21, and -130b inhibit PTEN expression resulting in B7-H1 over-expression in advanced colorectal cancer. *Human immunology* **75**, 348-353, doi:10.1016/j.humimm.2014.01.006 (2014).
303 Zhu, E. *et al.* miR-20b suppresses Th17 differentiation and the pathogenesis of experimental autoimmune encephalomyelitis by targeting RORgammat and STAT3. *J Immunol* **192**, 5599-5609, doi:10.4049/jimmunol.1303488 (2014).
304 Tomar, S., Nagarkatti, M. & Nagarkatti, P. S. 3,3'-Diindolylmethane attenuates LPS-mediated acute liver failure by regulating miRNAs to target IRAK4 and suppress Toll-like receptor signalling. *British journal of pharmacology* **172**, 2133-2147, doi:10.1111/bph.13036 (2015).
305 Liu, M., Wang, D. & Li, N. MicroRNA-20b Downregulates HIF-1alpha and Inhibits the Proliferation and Invasion of Osteosarcoma Cells. *Oncol Res* **23**, 257-266, doi:10.3727/096504016X14562725373752 (2016).
306 Qin, B., Liu, J., Liu, S., Li, B. & Ren, J. MiR-20b targets AKT3 and modulates vascular endothelial growth factor-mediated changes in diabetic retinopathy. *Acta Biochim Biophys Sin (Shanghai)*, doi:10.1093/abbs/gmw065 (2016).

307 Ingwersen, J. *et al.* Natalizumab restores aberrant miRNA expression profile in multiple sclerosis and reveals a critical role for miR-20b. *Annals of clinical and translational neurology* **2**, 43-55, doi:10.1002/acn3.152 (2015).
308 Chunjie, N., Huijuan, N., Zhao, Y., Jianzhao, W. & Xiaojian, Z. Disease-specific signature of serum miR-20b and its targets IL-8 and IL-25, in myasthenia gravis patients. *Eur Cytokine Netw* **26**, 61-66, doi:10.1684/ecn.2015.0367 (2015).
309 Hardy, J. Framing beta-amyloid. *Nature genetics* **1**, 233-234, doi:10.1038/ng0792-233 (1992).
310 Calderon-Garciduenas, L. *et al.* Early Alzheimer's and Parkinson's disease pathology in urban children: Friend versus Foe responses--it is time to face the evidence. *Biomed Res Int* **2013**, 161687, doi:10.1155/2013/161687 (2013).
311 Braak, H., Feldengut, S. & Del Tredici, K. [Pathogenesis and prevention of Alzheimer's disease: when and in what way does the pathological process begin?]. *Nervenarzt* **84**, 477-482, doi:10.1007/s00115-012-3688-1 (2013).
312 Miners, J. S., Baig, S., Tayler, H., Kehoe, P. G. & Love, S. Neprilysin and insulin-degrading enzyme levels are increased in Alzheimer disease in relation to disease severity. *Journal of neuropathology and experimental neurology* **68**, 902-914, doi:10.1097/NEN.0b013e3181afe475 (2009).
313 Miners, J. S. *et al.* Decreased expression and activity of neprilysin in Alzheimer disease are associated with cerebral amyloid angiopathy. *Journal of neuropathology and experimental neurology* **65**, 1012-1021, doi:10.1097/01.jnen.0000240463.87886.9a (2006).
314 Miners, J. S., van Helmond, Z., Kehoe, P. G. & Love, S. Changes with age in the activities of beta-secretase and the Abeta-degrading enzymes neprilysin, insulin-degrading enzyme and angiotensin-converting enzyme. *Brain Pathol* **20**, 794-802, doi:BPA375 [pii]
10.1111/j.1750-3639.2010.00375.x (2010).
315 Ishimaru, F. & Shipp, M. A. Analysis of the human CD10/neutral endopeptidase 24.11 promoter region: two separate regulatory elements. *Blood* **85**, 3199-3207 (1995).
316 Lilius, L. *et al.* No association between polymorphisms in the neprilysin promoter region and Swedish Alzheimer's disease patients. *Neuroscience letters* **337**, 111-113 (2003).
317 Li, C., Booze, R. M. & Hersh, L. B. Tissue-specific expression of rat neutral endopeptidase (neprilysin) mRNAs. *The Journal of biological chemistry* **270**, 5723-5728 (1995).
318 Pardossi-Piquard, R. *et al.* Presenilin-dependent transcriptional control of the Abeta-degrading enzyme neprilysin by intracellular domains of betaAPP and APLP. *Neuron* **46**, 541-554, doi:10.1016/j.neuron.2005.04.008 (2005).
319 Belyaev, N. D., Nalivaeva, N. N., Makova, N. Z. & Turner, A. J. Neprilysin gene expression requires binding of the amyloid precursor protein intracellular domain to its promoter: implications for Alzheimer disease. *EMBO reports* **10**, 94-100, doi:10.1038/embor.2008.222 (2009).
320 Sunday, M. E., Hua, J., Torday, J. S., Reyes, B. & Shipp, M. A. CD10/neutral endopeptidase 24.11 in developing human fetal lung. Patterns of expression and

modulation of peptide-mediated proliferation. *The Journal of clinical investigation* **90**, 2517-2525, doi:10.1172/JCI116145 (1992).
321 Walker, J. R. *et al.* Enhanced proteolytic clearance of plasma Abeta by peripherally administered neprilysin does not result in reduced levels of brain Abeta in mice. *The Journal of neuroscience : the official journal of the Society for Neuroscience* **33**, 2457-2464, doi:10.1523/JNEUROSCI.3407-12.2013 (2013).
322 Henderson, S. J. *et al.* Sustained peripheral depletion of amyloid-beta with a novel form of neprilysin does not affect central levels of amyloid-beta. *Brain : a journal of neurology* **137**, 553-564, doi:10.1093/brain/awt308 (2014).
323 DeMattos, R. B. *et al.* Peripheral anti-A beta antibody alters CNS and plasma A beta clearance and decreases brain A beta burden in a mouse model of Alzheimer's disease. *Proceedings of the National Academy of Sciences of the United States of America* **98**, 8850-8855, doi:10.1073/pnas.151261398 (2001).
324 Tanzi, R. E., Moir, R. D. & Wagner, S. L. Clearance of Alzheimer's Abeta peptide: the many roads to perdition. *Neuron* **43**, 605-608, doi:10.1016/j.neuron.2004.08.024 (2004).
325 Guan, H. *et al.* Peripherally expressed neprilysin reduces brain amyloid burden: a novel approach for treating Alzheimer's disease. *Journal of neuroscience research* **87**, 1462-1473, doi:10.1002/jnr.21944 (2009).
326 Guo, X. *et al.* Meta-analysis of the association between two neprilysin gene polymorphisms and Alzheimer's disease. *Journal of the neurological sciences* **346**, 6-10, doi:10.1016/j.jns.2014.07.064 (2014).
327 Miners, J. S., Barua, N., Kehoe, P. G., Gill, S. & Love, S. Abeta-degrading enzymes: potential for treatment of Alzheimer disease. *Journal of neuropathology and experimental neurology* **70**, 944-959, doi:10.1097/NEN.0b013e3182345e46 (2011).
328 Yang, L. L. *et al.* Enhancement of neutral endopeptidase activity in SK-N-SH cells by ginsenoside Rb1. *Neuro endocrinology letters* **29**, 924-928 (2008).
329 Li, M. *et al.* Copper downregulates neprilysin activity through modulation of neprilysin degradation. *Journal of Alzheimer's disease : JAD* **19**, 161-169, doi:10.3233/JAD-2010-1218 (2010).
330 Roques, B. P., Noble, F., Crine, P. & Fournie-Zaluski, M. C. Inhibitors of neprilysin: design, pharmacological and clinical applications. *Methods in enzymology* **248**, 263-283 (1995).
331 Melzig, M. F. & Janka, M. Enhancement of neutral endopeptidase activity in SK-N-SH cells by green tea extract. *Phytomedicine : international journal of phytotherapy and phytopharmacology* **10**, 494-498, doi:10.1078/094471103322331449 (2003).
332 Azevedo-Pouly, A. C. *et al.* miR-216 and miR-217 expression is reduced in transgenic mouse models of pancreatic adenocarcinoma, knockout of miR-216/miR-217 host gene is embryonic lethal. *Funct Integr Genomics*, doi:10.1007/s10142-016-0512-1 (2016).
333 Zhao, C. *et al.* Computational prediction of MicroRNAs targeting GABA receptors and experimental verification of miR-181, miR-216 and miR-203 targets in GABA-A receptor. *BMC Res Notes* **5**, 91, doi:10.1186/1756-0500-5-91 (2012).

334 Iwata, N., Takaki, Y., Fukami, S., Tsubuki, S. & Saido, T. C. Region-specific reduction of A beta-degrading endopeptidase, neprilysin, in mouse hippocampus upon aging. *J Neurosci Res* **70**, 493-500, doi:10.1002/jnr.10390 (2002).
335 Czauderna, F. *et al.* Structural variations and stabilising modifications of synthetic siRNAs in mammalian cells. *Nucleic acids research* **31**, 2705-2716 (2003).
336 Yoo, B. H., Bochkareva, E., Bochkarev, A., Mou, T. C. & Gray, D. M. 2'-O-methyl-modified phosphorothioate antisense oligonucleotides have reduced non-specific effects in vitro. *Nucleic acids research* **32**, 2008-2016, doi:10.1093/nar/gkh516 (2004).
337 Zhang, Y., Wang, Z. & Gemeinhart, R. A. Progress in microRNA delivery. *J Control Release* **172**, 962-974, doi:10.1016/j.jconrel.2013.09.015 (2013).
338 Lv, H., Zhang, S., Wang, B., Cui, S. & Yan, J. Toxicity of cationic lipids and cationic polymers in gene delivery. *J Control Release* **114**, 100-109, doi:10.1016/j.jconrel.2006.04.014 (2006).
339 Wu, S. Y. & McMillan, N. A. Lipidic systems for in vivo siRNA delivery. *AAPS J* **11**, 639-652, doi:10.1208/s12248-009-9140-1 (2009).
340 Kuo, C. P. & Leung, M. K. Electrofluorescence switching from a multilayer thin film by spin-assisted layer-by-layer assembly of an anionic fluorescent conjugated polyelectrolyte with poly(diallyldimethylammonium chloride). *Phys Chem Chem Phys* **16**, 79-87, doi:10.1039/c3cp53912a (2014).
341 Pulford, B. *et al.* Liposome-siRNA-peptide complexes cross the blood-brain barrier and significantly decrease PrP on neuronal cells and PrP in infected cell cultures. *PloS one* **5**, e11085, doi:10.1371/journal.pone.0011085 (2010).
342 Kim, Y. H. *et al.* Polyethylenimine with acid-labile linkages as a biodegradable gene carrier. *J Control Release* **103**, 209-219, doi:10.1016/j.jconrel.2004.11.008 (2005).
343 Boussif, O. *et al.* A versatile vector for gene and oligonucleotide transfer into cells in culture and in vivo: polyethylenimine. *Proceedings of the National Academy of Sciences of the United States of America* **92**, 7297-7301 (1995).
344 Hwang, D. W. *et al.* A brain-targeted rabies virus glycoprotein-disulfide linked PEI nanocarrier for delivery of neurogenic microRNA. *Biomaterials* **32**, 4968-4975, doi:10.1016/j.biomaterials.2011.03.047 (2011).
345 Srivastava, A. *et al.* Exosomes: a role for naturally occurring nanovesicles in cancer growth, diagnosis and treatment. *Curr Gene Ther* **15**, 182-192 (2015).
346 Kalani, A., Tyagi, A. & Tyagi, N. Exosomes: mediators of neurodegeneration, neuroprotection and therapeutics. *Molecular neurobiology* **49**, 590-600, doi:10.1007/s12035-013-8544-1 (2014).
347 Serramia, M. J. *et al.* In vivo delivery of siRNA to the brain by carbosilane dendrimer. *J Control Release* **200**, 60-70, doi:10.1016/j.jconrel.2014.12.042 (2015).
348 Kim, I. D. *et al.* Neuroprotection by biodegradable PAMAM ester (e-PAM-R)-mediated HMGB1 siRNA delivery in primary cortical cultures and in the postischemic brain. *J Control Release* **142**, 422-430, doi:10.1016/j.jconrel.2009.11.011 (2010).

349 Sarvaiya, J. & Agrawal, Y. K. Chitosan as a suitable nanocarrier material for anti-Alzheimer drug delivery. *Int J Biol Macromol* **72**, 454-465, doi:10.1016/j.ijbiomac.2014.08.052 (2015).
350 Koping-Hoggard, M., Mel'nikova, Y. S., Varum, K. M., Lindman, B. & Artursson, P. Relationship between the physical shape and the efficiency of oligomeric chitosan as a gene delivery system in vitro and in vivo. *J Gene Med* **5**, 130-141, doi:10.1002/jgm.327 (2003).
351 Bishop, C. J., Tzeng, S. Y. & Green, J. J. Degradable polymer-coated gold nanoparticles for co-delivery of DNA and siRNA. *Acta Biomater* **11**, 393-403, doi:10.1016/j.actbio.2014.09.020 (2015).
352 Park, T. E. *et al.* Enhanced BBB permeability of osmotically active poly(mannitol-co-PEI) modified with rabies virus glycoprotein via selective stimulation of caveolar endocytosis for RNAi therapeutics in Alzheimer's disease. *Biomaterials* **38**, 61-71, doi:10.1016/j.biomaterials.2014.10.068 (2015).
353 Bae, M. J., Lee, Y. M., Kim, Y. H., Han, H. S. & Lee, H. J. Utilizing Ultrasound to Transiently Increase Blood-Brain Barrier Permeability, Modulate of the Tight Junction Proteins, and Alter Cytoskeletal Structure. *Curr Neurovasc Res* **12**, 375-383 (2015).
354 Makimura, H., Mizuno, T. M., Mastaitis, J. W., Agami, R. & Mobbs, C. V. Reducing hypothalamic AGRP by RNA interference increases metabolic rate and decreases body weight without influencing food intake. *BMC Neurosci* **3**, 18 (2002).
355 Jan, A. *et al.* Direct intracerebral delivery of a miR-33 antisense oligonucleotide into mouse brain increases brain ABCA1 expression. [Corrected]. *Neuroscience letters* **598**, 66-72, doi:10.1016/j.neulet.2015.05.007 (2015).

Curriculum vitae

Nipun Chopra

Education

Indiana University, Indianapolis, IN
Ph.D. Medical Neuroscience, April 2017.

Indiana State University, Terre Haute, IN
M.S., Life Science, May 2009.

DePauw University, Greencastle, IN
B.A., Biology, May 2006.

Awards

2016	SNRI Travel award
2015	SNRI Travel award
2014	SNRI Travel award
2013	SNRI Travel award
2009	IBMG Research fellowship

Publications

Srinivasan M, Bayon B, **Chopra N**, Lahiri DK. Novel nuclear factor-kappa B targeting peptide suppresses Beta-amyloid induced inflammatory and apoptotic responses in neuronal cells. Plos One (2016): 11 (10).

Lahiri DK, Maloney B, Bayon BL, **Chopra N**, White FA, Greig NH, Nurenberger JI. Transgenerational latent early-life associated regulation unites environment and genetics across generations. Epigenomics (2016): 8 (2) 373-87.

Ray B, **Chopra N**, Long JM, Lahiri DK. Human primary mixed brain cultures: preparation, long-term maintenance, characterization and application to neuroscience research. Mol Brain (2014) Sep 16; 7(1):63.

Baranello RJ, Bharani KL, Padmaraju V, **Chopra N**, Lahiri DK, Greig NH, Pappolla MA, Sambamurti K. Amyloid-Beta Protein Clearance and Degradation (ABCD) Pathways and their Role in Alzheimer's Disease. Curr Alzheimer Res. (2015); 12(1):32-46.

Publications under preparation/Submitted

Chopra N, Nho K and Lahiri DK. MicroRNA-298 regulates expression of human APP, BACE1 and total tau.

Chopra N and Lahiri DK. Modulation of APP by microRNA-20b.

Chopra N, Nho K, Saykin AJ, Lahiri DK. Neprilysin is differentially expressed in various cell types, tissues and brain cultures.

Chopra N, Lahiri DK, Sambamurti K. The constitutive in vivo expression of miR-200b and miR-146a modulates expression of proteins involved in the amyloidogenic pathyway.

Posters and Presentations

Chopra N, Long JM, Ray B, Obukhov AG, Lahiri DK. Regulation of proteins implicated in AD by microRNAs. Society for Neuroscience, November 2013, San Diego, CA.

Chopra N, Nho K, Long JM, Maloney B, Saykin AJ, Lahiri DK. MicroRNA-298: a dual regulator of proteins involved in Alzheimer's disease. Society for Neuroscience, November 2014, Washington, DC.

Long JM, Chopra N, Rogers JT, Ray B, Greig NH, Sambamurti K, Maloney B, Lahiri DK. Neurobiological role of a novel microRNA regulation APP expression via interaction with IRP1: implications for AD. Society for Neuroscience, November 2014, Washington, DC.

Lahiri DK, Long JM, Huang X, Greig NH, Sambamurti K, Rogers, JT, Song W, Maloney B. Seeing a road from the CAR: Could effective microRNA "brakes" slow down the trip to AD? Drug discovery and therapy world congress, July 2015, Boston MA.

Chopra N, Nho K, Bhartur A, Long, JM, Sambamurti K, Greig NH, Saykin AJ, Lahiri DK. Role of Neprilysin in Alzheimer's disease. Drug discovery and therapy world congress, July 2015, Boston MA.

Bayon BL, Nho K, Maloney B, Chopra N, Lahiri DK. Transcription factor mediated modulation of amyloid-beta precursor protein (APP) and beta-site APP cleaving enzyme (BACE1) expression as a novel drug target in Alzheimer's disease (AD). 65th Annual Meeting of the American Society of Human Genetics, Baltimore, MA.

Chopra N, Long JM, Nelson PT, Reddy P, Vassar R, Greig NH, Obukhov AG, Lahiri DK. Novel microRNAs regulate specific genes important for AD. Society for Neuroscience, October 2015, Chicago, IL.

Bayon BL, Nho K, Maloney B, Chopra N, Lahiri,DK. Transcription factor mediated modulation of amyloid-beta precursor protein (APP) and beta-site APP cleaving enzyme (BACE1) expression as a novel drug target in Alzheimer's disease (AD). Society for Neuroscience Annual Meeting, October 2015, Chicago, IL.

Lahiri DK, Maloney B, Long JM, Chopra N, Sambamurti K, Bayon BL. Understanding the neurobiology of AD by correlating AD-associated miRNA and the MMSE cognitive scale. Society for Neuroscience, October 2015, Chicago, IL.

Bayon BL, Nho K, Maloney B, Chopra N, Lahiri DK. Differential regulation of amyloid-β precursor protein (APP) and β-secretase 1 (BACE1) by transcription factor (TF) modulating drugs in human cells. 66th Annual Meeting of the American Society of Human Genetics, July 2016, Vancouver, British Columbia, Canada.

Chopra N, Nho K, Long JM, Maloney B, Saykin AJ, Lahiri DK. MicoRNA-298: a dual regulator of proteins involved in AD. Indianapolis Society for Neuroscience, October 2016, Indianapolis, IN.

Chopra N, Nho K., Bayon BL, Lahiri DK. MicroRNA-20b reduces levels of APP and Aβ in human cells. Society for Neuroscience, November 2016, San Diego, CA.

Lahiri DK, Chopra N, Maloney B, Feng B, Chakrabarti S. Endothelium derived miR-200b may correct AD precursors in diabetes: potential role for miR-200b as a prophylactic or early treatment. Society for Neuroscience, November 2016, San Diego, CA.

Bayon BL, Nho K, Maloney B, Chopra, N, Lahiri DK. Regulation of amyloid-beta precursor protein (APP) and beta-secretase 1 (BACE1) expression by transcription factor modulating compounds mithramycin A and tolfenamic acid in human cells. Society for Neuroscience Annual Meeting, November 2016, San Diego, CA.

Lahiri DK, Bayon BL, Maloney B, Chopra N. Epigenetic role in AD: LEARning from environment, lifestyle and different cultures to prevent dementia. 7th international conference on Alzheimer's disease and related disorders in the Middle East. February 2017, Abu Dhabi, United Arab Emirates.